

UNPRECEDENTED DAYLIGHT DISPLAY OF KREUTZ SUNGRAZERS IN AD 363?

ZDENEK SEKANINA

Jet Propulsion Laboratory, California Institute of Technology, 4800 Oak Grove Drive, Pasadena, CA 91109, U.S.A.
Version February 3, 2022

ABSTRACT

In the context of the recently proposed contact-binary model (Sekanina 2021), I investigate the circumstances of the first perihelion passage of the Kreutz sungrazers in orbits with barycentric periods near 735 yr, following the initial near-aphelion splitting of the presumed progenitor, Aristotle’s comet of 372 BC. Given favorable conditions at this breakup and at episodes of secondary fragmentation in its aftermath, the fragments should have arrived at their first perihelion nearly simultaneously, reminiscent of the anticipated outcome for the two-superfragment model’s perihelion return of AD 356 (Sekanina & Chodas 2004). The relevant case of a swarm of Kreutz sungrazers is examined to appraise possible scientific ramifications of the brief remark by Ammianus Marcellinus, a Roman historian, that “*in broad daylight comets were seen*” in late AD 363, only seven years later. The tested scenario, which does not contradict Ammianus’ narrative and is consistent with the contact-binary model, involves a set of ten sungrazers visible in the daytime, all reaching perihelion over a period of 4.6 days. As part of this work, I comment on the role of the rapidly developing, brilliant post-perihelion tail; revise the apparent magnitude typical for the first and last naked-eye sightings; compare the visibility conditions in full daylight, in twilight, and at night; and, for the first time, present circumstantial evidence that favors comet X/1106 C1 as the parent to C/1843 D1 rather than to C/1882 R1 and C/1965 S1.

Subject headings: comets general: Kreutz sungrazers; comets individual: 372 BC, 943, X/1106 C1, 1232, 1381, 1588, 1663, 1666, C/1695 U1, C/1843 D1, C/1882 R1, C/1963 R1, C/1965 S1, C/2011 W3, 1P/Halley; methods: data analysis

1. INTRODUCTION

For a short period of time after the discovery of the sungrazer C/1882 R1, the Great September Comet of 1882, its possible identity with C/1843 D1, the Great March Comet of 1843, was a point of contention. The winning argument against the identity relied entirely on their long orbital periods (e.g., Tebbutt 1882, Plummer 1889, Lynn 1903). I find it puzzling that the major, nearly 20° difference in the longitude of the ascending node (and equivalent differences in the other angular elements) as well as the discrepancy of 0.5 R_{\odot} , or nearly 50 percent, in the perihelion distance were never employed in the arguments against the identity. An answer to the question of why not was later offered by Lynn (1903), when he said in his remarks on the two spectacular comets that “what events may have been occasioned in their past history by their close approaches to the Sun when in perihelion can only be matter of speculation.” Thus, as late as the beginning of the 20th century, major changes in the orbit orientation and perihelion arc (but apparently not the period) were believed possible as a result of the sungrazers’ interaction with the Sun’s corona, even though Kreutz (1888, 1891) and others were able to successfully link preperihelion and post-perihelion astrometric observations of C/1882 R1 by a gravitational orbit in compliance with the Newtonian theory.

The nature of the sources causing the significant orbital differences between C/1843 D1 and C/1882 R1 (and other Kreutz sungrazers), especially in the nodal longitude and perihelion distance, was first seriously confronted by Öpik (1966) and, in particular, Marsden

(1967). In these independent efforts the observed discrepancies in the orbital elements were interpreted as cumulative effects of the indirect planetary perturbations over a large number of revolutions about the Sun. Marsden did not appear to be very happy about the explanation (his sophisticated approach to the problem notwithstanding), but he realized that there was no alternative, insofar as all Kreutz comets were products of the process of tidal breakup at perihelion, in close proximity of the Sun. In the 1960s, this still was an overwhelmingly prevailing view, reinforced eight decades earlier by the extensive fragmentation of C/1882 R1, thoroughly documented by the observed post-perihelion multiplicity of the comet’s nucleus (Kreutz 1888, 1891), and further strengthened by evidence of fragmentation of C/1965 S1, which was investigated, among others, by Marsden (1967) himself.

2. CASCADING NATURE OF FRAGMENTATION

Two decades ago I demonstrated that a fragment separating from its parent in a Kreutz sungrazer orbit at aphelion, presumed to be at a heliocentric distance of ~170 AU (equivalent to an orbital period of 784 yr), with a velocity of 5 m s⁻¹ in the direction normal to the orbital plane is perturbed by 27° in its nodal longitude, while a separation velocity of the same magnitude in the transverse direction exerts a perturbation of 0.7 R_{\odot} in the fragment’s perihelion distance (Sekanina 2002). In that study I also argued that the process of *nontidal* fragmentation at large heliocentric distance — first proposed for dwarf sungrazers (Sekanina 2000) imaged by the coronagraphs on board the Solar and Heliospheric Observatory (SOHO) — has obviously been affecting the entire Kreutz sungrazer system, including the progenitor.

It is well-known that no perceptible perturbations of any fragment’s angular elements and perihelion distance can be achieved as a result of the parent’s breakup close to the Sun. A separation velocity of 5 m s^{-1} at perihelion does, however, change the fragment’s orbital period by ~ 400 years or more. In general, the orbital distribution of Kreutz sungrazers shows evidence of significant perturbations of all elements, thereby suggesting that nuclear fragmentation has cascading nature, occurring throughout the orbit. This conclusion is important, because it implies a *much higher number of fragmentation events per unit time* than if they were confined to close proximity of perihelion. Higher fragmentation rates lead in turn to a *shorter lifespan* of the Kreutz system, especially restricting survival of objects as intrinsically bright and massive as C/1843 D1 and C/1882 R1.¹

3. TWO-SUPERFRAGMENT MODEL AND SIMULTANEOUS ARRIVALS OF FRAGMENTS AT FIRST PERIHELION

Marsden’s (1967) description of the Kreutz group (which at the time consisted of no more than a dozen known sungrazers, including six questionable ones) in terms of two subgroups had major influence on the further evolution of ideas on the subject. Equally impressive was Marsden’s result of integration of the orbits of comets C/1965 S1 and C/1882 R1 back in time to the early 12th century, prompting his suggestion that the spectacular comet X/1106 C1 was the most promising candidate for their common parent.

A version of the two-superfragment model for the Kreutz system, proposed in Sekanina (2002), was implemented in a follow-up study (Sekanina & Chodas 2004), which adopted Marsden’s suggested relationship among X/1106 C1, C/1882 R1, and C/1965 S1. The sizable gaps between the longitudes of the ascending node and perihelion distances of C/1843 D1 and C/1882 R1 were consistent with their birth as two superfragments in the progenitor’s initial breakup at 50 AU from the Sun early in the 4th century AD. The observed evolution of the naked-eye members of the Kreutz system was then modeled as a result of progressive fragmentation of the two superfragments over a period of time a little longer than two revolutions about the Sun, with C/1843 D1 and C/1882 R1 as their respective largest surviving masses.

The two-superfragment model has been an extremely useful tool in pursuit of getting insight into the evolution of the Kreutz system. However, because of new developments since 2004, the model has become in some ways obsolete, as I recently argued (Sekanina 2021; referred to hereafter as Paper 1). Yet, two of the model’s features continue to be valid: (1) the **progenitor fragmented at a very large heliocentric distance**; and (2) the **fragments — whether two or more — arrived at their first perihelion (in the 4th century AD) nearly simultaneously**. In fact, the *modeled* superfragments arrived at their first perihelion, in AD 356 or 30 years after the progenitor’s breakup at 50 AU from the Sun, merely seven days apart.

¹ Predicated on my own study of their light curves, I referred to C/1882 R1 as the brightest Kreutz sungrazer and to C/1843 D1 as the second brightest (Sekanina 2002). The fact is that opinions differ widely on which of the two comets was more spectacular (and, presumably, more massive), with no strong preference either way (Section 5.5).

Accordingly, a promising historical account of the Kreutz system’s first appearance should include a reference to *multiple comets arriving at nearly the same time*.

4. WEAKNESSES OF TWO-SUPERFRAGMENT MODEL AND PARADIGM OF A CONTACT BINARY

Evidence on C/1843 D1 and C/1882 R1 suggests that the two superfragments may have been of approximately equal mass. If the progenitor were a solid body of quasi-spherical shape, its fracture through the center into two halves appears a priori to be an unlikely scenario. On the other hand, if, in line with Paper 1, the progenitor was a **contact binary**, consisting of two about equally large lobes that eons ago coalesced into a single body at a very low relative velocity, its splitting along the bridge linking the two lobes at a fairly recent time sounds as a plausible event.

Developing the two-superfragment model, Sekanina & Chodas (2004) had to tolerate separation velocities in a general range of $6\text{--}10 \text{ m s}^{-1}$. Compared to the separation velocities of fragments of most known split comets (e.g., Sekanina 1982), these numbers are too high by a factor of three or more. To avoid such high separation velocities, one should accept that the progenitor fragmented in the general proximity of aphelion rather than at 50 AU.

The focus of another controversy linked to the two-superfragment model was the already mentioned role of the brilliant comet (and a very probable sungrazer) X/1106 C1. Its relationship to C/1882 R1 and C/1965 S1 is an open question; in Section 5.6 I present the first circumstantial evidence that X/1106 C1 was the parent to C/1843 D1 rather than to C/1965 S1 and C/1882 R1.

Most difficulties that the two-superfragment model encounters have been removed by the introduction of a contact-binary model. Only two problems remain. One is the missing second spectacular sungrazer in the early 12th century that served as the parent to C/1882 R1, if X/1106 C1 was the parent to C/1843 D1. Even though there is a chance that the second sungrazer was bright enough to have been visible in broad daylight, it apparently was missed, if it arrived between May and early August. Short of its future accidental discovery in a historical record, this problem will remain unsolved.

The other problem is the absence of evidence for two (or more) bright sungrazers, arriving nearly simultaneously in AD 356, one revolution about the Sun before X/1106 C1. In this context it is most encouraging to note the brief remark by **Ammianus Marcellinus**, a reputable Roman historian, conveying that towards the end of AD 363 “**in broad daylight comets were seen**” from Antioch on the Orontes (Rolfe 1940), his residence at the time. His note refers to an event of the right kind, which occurred only seven years after the time that satisfies the two-superfragment model! Besides, Seargent (2009) speculated that the daylight comets could have been “*several sungrazing fragments close together*”, given that members of the Kreutz system “*very late in the year would have had a strong southerly declination and might have been seen . . . only in the daytime close to perihelion*” from much of the northern hemisphere. Even though the account by Ammianus is brutally short, I deem it worthwhile to attempt reconstructing a scenario of daytime multiple-fragment spectacle, orchestrated by Kreutz sungrazers and consistent with the contact-binary model.

Table 1
Hasegawa & Nakano’s Potential Historical Kreutz Sungrazers First Sighted Between Mid-October and Mid-December

Comet’s year of arrival	Date of perihelion, t_π (UT)	Absolute magnitude, H_0^+	Source ^a	First sighting					Last sighting ^b	
				Date, t_{first}	$t_{\text{first}} - t_\pi$ (days)	App. mag, H_{first}	Solar elong.	Moon age (days)	Date, t_{last}	$t_{\text{last}} - t_\pi$ (days)
943	Oct 27 ± 1	6.7	C, E	Nov 5	+9	3.2	29°	5	Nov 14	+18
1232	Oct 14 ± 2	3.2	C, J	Oct 17	+3	−2.6	15	2	Dec 3	+50
1381	Nov 3 ± 2	5.6	K, J, E	Nov 7	+4	0.1	18	21	Dec 1	+28
1588	Oct 16 ± 2	5.0	C	Oct 24	+8	1.7	24	4	Nov 11	+26
1663	Oct 15 ± 4	−0.2	C	Oct 31	+16	−1.5	41	1	Jan 27	+104
1666 ^c	Nov 10 ± 5	6:	C	Nov 20	+10	3:	33	24
1695 ^d	Oct 24 ± 1	6.0	C, K	>Oct 22	>−2	−3.4	6	15	Nov 18	+25

Notes.

^a Region: C = China, E = Europe, J = Japan, K = Korea.

^b Comet assumed to be of apparent magnitude $H_{\text{last}} = 5.0$.

^c Comet probably observed over a very short period of time.

^d This is comet C/1695 U1; The date of last sighting is from Kronk (1999). Kreutz (1901) was skeptical about the object’s belonging to the system, while Marsden (1967) did not rule out its Subgroup I membership.

5. THE CASE FOR DAYTIME KREUTZ SUNGRAZERS IN AD 363: PRELIMINARIES

Details on the spectacle of daylight comets seen by Ammianus will never be known. A scenario described in Section 6 simulates a display that may or may not resemble his experience. Dictated by the documented time of Ammianus’ arrival at Antioch, the comets could not have been sighted before mid-October (e.g., Drijvers 2011, 2022). On the other hand, they were probably seen before Emperor Jovian’s departure from Antioch “on a day in the dead of winter” (Rolfe 1940). While he may have left as early as November (e.g., Drijvers 2011, 2022), I conservatively adopt that the comets could have been observed as late as mid-December. The two-months period defines the time window of interest to this study. The objective is being pursued in stages.

5.1. Potential Historical Kreutz Sungrazers Discovered Between Mid-October and Mid-December

To learn more about such members of the Kreutz system, I first examine Hasegawa & Nakano’s (2001) list of 24 potential historical Kreutz sungrazers up to AD 1702 to single out the ones discovered between mid-October and mid-December. Table 1 shows that there were seven such objects. The *post-perihelion* absolute magnitudes H_0 (i.e., reduced to unit distances from the Earth, Δ , and the Sun, r ; later called H_0^+) are modified values (extended to one decimal) introduced by Hasegawa & Nakano on the assumptions that the comets moved in an average Kreutz sungrazing orbit (similar to that of Population Ia in Paper 1) and at the time of last sighting were of apparent visual magnitude 5, obeying a $\Delta^{-2}r^{-4}$ law.

The comets in Table 1 exhibit two striking peculiarities: (i) a strongly uneven temporal distribution, with four of the seven potential sungrazers discovered in the first quarter of the two-month period, six in the first half, but none in the last three weeks, apparently an effect of gradually increasing deep southerly declinations; and (ii) at least six and quite possibly all seven were not discovered until after perihelion. The lack of preperihelion

sightings may seem strange given that five of the seven comets in Table 1 passed perihelion within a week of October 21, the perihelion date of C/1965 S1 (Ikeya-Seki), whose apparition has been deemed favorable.

In order to understand the features of Table 1, I examine (i) Hasegawa & Nakano’s (2001) assumption regarding the apparent brightness at the last naked-eye sighting; (ii) the problem of the apparent brightness of a comet at naked-eye discovery; and (iii) the expected shape of Kreutz sungrazers’ preperihelion and post-perihelion light curves. In the following sections I separately address each of these issues.

5.2. Post-Perihelion Tails of Kreutz Sungrazers and Their Last Naked-Eye Sightings

Bright Kreutz sungrazers are unique in that they display conspicuous *post-perihelion* tails,² which carry enormous amounts of microscopic dust grains ejected from the nucleus at very small heliocentric distances just after perihelion but no longer subjected to instant sublimation. The supply of this dust is so substantial that the **tail becomes much brighter than the head**.

Compelling arguments are consistently provided by observations of at least three sungrazers. Roemer (1966) reported that comet Ikeya-Seki’s “tail nearly 10° in length could still be detected with the naked eye [even though the] brightness of the head ... was about magnitude 7.4” 37 days after perihelion.³ Similarly, the tail of the more recent sungrazer C/2011 W3 (Lovejoy) was detected with the naked eye by several observers (I. Cooper, R. Kaufman, M. Mattiazzo, R. McNaught)⁴ as late as 20 or more days after perihelion, when the brightness of the disintegrating head was estimated at magnitude 6.6–8.1 (Green 2012). And back in the late 19th cen-

² This excessive brightness is by no means a property of bright sungrazers’ *preperihelion* tails, except possibly near perihelion.

³ From the comet’s light curve (Sekanina 2002) I find for this time a total visual magnitude of the head equaling 6.9 (see Table 3 below).

⁴ See <https://groups.io/g/comets-ml>, messages 19113, 19120, 19121, 19134, 19146, and 19147.

tury, Gould (1883b) reported that the Great September Comet of 1882 “*was last seen by the unaided eye on [1883] March 7, at which time it was already very faint in the telescope.*” The formula for the post-perihelion light curve of C/1882 R1 (Sekanina 2002) suggests that the comet’s head could not be brighter than magnitude 6.6 at the time, more than 170 days (!) after perihelion; it again was the tail that Gould was referring to.

The prodigious brightness of the post-perihelion tails of major Kreutz sungrazers can be documented even more convincingly. One line of argument is based on Weinberg & Beeson’s (1976) photometric investigation of comet Ikeya-Seki on four days after perihelion, examining primarily the polarization of the comet’s light. From scans of a tail image obtained at Mt. Haleakala, Maui, Hawaii, on 1965 October 29.60 UT, the authors determined the surface brightness along the tail’s axis as a function of the angular distance from the nucleus at 1° intervals. The comet’s head was $5^\circ.3$ below the horizon, so that the data refer to only the outer two thirds of the tail. Weinberg & Beeson did not compute the tail’s total magnitude, but its estimate is offered in the following.

The surface-brightness distribution, $B(b, a)$, across the tail at a given angular distance from the nucleus, b , is approximated by the Gaussian function,

$$B(b, a) = B_0(b) \exp\left[-\frac{a^2}{2\sigma_b^2}\right], \quad (1)$$

where a is an angular distance from the tail’s axis, $B_0(b)$ is the surface brightness at the point on the axis at distance b from the nucleus, and σ_b is the distance from the axis at a point of the steepest surface-brightness gradient, measuring the optically perceived half-width of the tail at distance b . The values of $B_0(b)$ were published by Weinberg & Beeson, while the values of σ_b over the range of distances b were measured by the present author from the tail’s width on an image in their paper. This image was taken with the same instrument one day earlier and shows the entire comet. The measurements of σ_b were made on the assumption that the ratio σ_b/b as a function of b did not change significantly in 24 hours. The total apparent brightness of the tail between any two distances b_1 and b_2 from the nucleus is given by

$$\begin{aligned} \mathcal{B}(b_1, b_2) &= \int_{b_1}^{b_2} B_0(b) db \int_{-\infty}^{+\infty} \exp\left[-\frac{a^2}{2\sigma_b^2}\right] da \\ &= \sqrt{2\pi} \int_{b_1}^{b_2} B_0(b) \sigma_b db. \end{aligned} \quad (2)$$

Weinberg & Beeson tabulate $B_0(b)$ in units of S_{10} , the number of visual magnitude 10 stars per square degree. The product of $B_0(b)\sigma_b$ is integrated numerically over the available range of distances to derive the visual brightness of the visible part of the tail (at distances of more than $6^\circ.8$ from the nucleus) equaling $\mathcal{B}(6^\circ.8, \infty) = 42,400$ magnitude 10 stars, or a visual magnitude of -1.6 . Furthermore, extrapolating the Weinberg & Beeson’s curve of surface brightness back to the nucleus, the tail’s total brightness is crudely estimated at about $\mathcal{B}(0, \infty) = 94,000$ magnitude 10 stars, equivalent to a total visual magnitude of

$$H = -2.4 \text{ mag}. \quad (3)$$

The comet’s head at the time had a total magnitude of $+2.5$, so its brightness was just about 1 percent of the tail’s brightness!

An independent estimate is based on a generic model of comet activity and a sizable sungrazer’s production rate of dust, in line with the results obtained by Weinberg & Beeson (1976) and by others. Let \dot{Z}_0 be the average sublimation rate from a unit surface area of a comet at a heliocentric distance of 1 AU, μ_{mol} the average mass of a molecule (assuming a number of sublimating species), and R the radius of the comet’s nucleus. If f is the fraction of the nucleus surface that is active and κ is the dust-to-gas mass production rate ratio, the comet’s mass production rate of dust at 1 AU equals

$$\dot{\mathcal{M}}_0 = 4\pi\kappa f R^2 \mu_{\text{mol}} \dot{Z}_0. \quad (4)$$

Let this mass production rate vary inversely as the square of heliocentric distance, $r(t)$,

$$\dot{\mathcal{M}}(t) = \dot{\mathcal{M}}_0 \left(\frac{r_0}{r}\right)^2, \quad (5)$$

where $r_0 = 1$ AU. The post-perihelion dust tail of a sungrazer is made up of only post-perihelion ejecta, starting at a time t_{beg} , as all preperihelion particles were sublimated at perihelion. Thus, at time t_{obs} the mass of dust in the tail amounts to

$$\begin{aligned} \mathcal{M}(t) &= \int_{t_{\text{beg}}}^{t_{\text{obs}}} \dot{\mathcal{M}}(t) dt = \dot{\mathcal{M}}_0 r_0^2 \int_{t_{\text{beg}}}^{t_{\text{obs}}} \frac{dt}{r^2} \\ &= \frac{\dot{\mathcal{M}}_0 r_0^2}{k_0} \sqrt{\frac{2}{q}} \left(\arccos \sqrt{\frac{q}{r_{\text{obs}}}} - \arccos \sqrt{\frac{q}{r_{\text{beg}}}} \right), \end{aligned} \quad (6)$$

where k_0 is the Gaussian gravitational constant, q is the perihelion distance of the sungrazer’s orbit (approximated by a parabola), $r_{\text{beg}} = r(t_{\text{beg}})$ and $r_{\text{obs}} = r(t_{\text{obs}})$. The apparent visual magnitude, H , that this mass of dust has at a given time depends on its cross-sectional area X , geometric albedo p , the function $\Phi(\psi)$ of the phase angle ψ , as well as on the distances from Earth, Δ , and the Sun, r :

$$H = 15.38 - 2.5 \log X - 2.5 \log [p \Phi(\psi) \Delta^{-2} r^{-2}], \quad (7)$$

where X is in km^2 , Δ and r in AU, and $\Phi(0^\circ) = 1$. The total cross-sectional area of the dust in the tail is related to its mass \mathcal{M} via the size and mass distributions and the bulk density. The tail’s total cross-sectional area can be written as $X = \frac{1}{4}\pi \langle s^2 \rangle \mathcal{N}$ and its total mass as $\mathcal{M} = \frac{1}{6}\pi \rho \langle s^3 \rangle \mathcal{N}$, where \mathcal{N} is the number of dust particles in the tail, $\langle s^2 \rangle^{\frac{1}{2}}$ their mean diameter determined by the cross-sectional distribution, $\langle s^3 \rangle^{\frac{1}{3}}$ their mean diameter determined by the mass distribution, and ρ their bulk density. By eliminating \mathcal{N} from the expressions for X and \mathcal{M} one obtains

$$X = \frac{3\mathcal{M} \langle s^2 \rangle}{2\rho \langle s^3 \rangle}. \quad (8)$$

Inserting first from Equation (6) into (8) and then from (8) into (7), one obtains the tail’s apparent magnitude.

Assuming next that the sublimation of water ice dominates, I take $\dot{Z}_0 = 3 \times 10^{17}$ molecules $\text{cm}^{-2} \text{s}^{-1}$ and $\mu_{\text{mol}} = 3 \times 10^{-23}$ g. Adopting further for the sungrazer

Ikeya-Seki $R = 6$ km, $f = 0.2$, and $\kappa = 3$, I get for the mass production rate of dust at 1 AU from the Sun

$$\dot{\mathcal{M}}_0 = 2.4 \times 10^7 \text{ g s}^{-1} = 2.1 \times 10^{12} \text{ g day}^{-1}. \quad (9)$$

On October 29.60 UT, the time of Weinberg & Beeson's (1976) observation, the comet was 0.447 AU from the Sun and 1.048 AU from Earth. The mass of dust in the tail then equaled (in grams)

$$\mathcal{M} = 2.0 \times 10^{15}(1.44 - U), \quad (10)$$

where U depends on the earliest post-perihelion dust ejecta surviving sublimation in the tail. The value of U varies from zero at perihelion, $r_{\text{beg}} = q = 1.67 R_{\odot}$, to 0.31 for $1.84 R_{\odot}$, to 0.42 for $2.0 R_{\odot}$, and to 0.61 for $2.5 R_{\odot}$, so that the expression in the parenthesis of Equation (10) is near unity. Adopting now in Equation (8) a grain density of 2.5 g cm^{-3} and a ratio $\langle s^3 \rangle / \langle s^2 \rangle = 4 \times 10^{-4} \text{ cm}$, describing an $s^{-2.8}$ cumulative distribution with the limits of $0.1 \mu\text{m}$ and 1 cm , I obtain

$$X = 3.0 \times 10^8 \text{ km}^2. \quad (11)$$

Moving from the cross section to the apparent magnitude, strictly one should consider the implications of the tail as an extended feature. In this very approximate exercise, I note that the linear length of the nearly 20° long tail was about 0.54 AU , extending from the comet's head at 0.45 AU from the Sun to nearly 1 AU at the outer end. The tail's median point was near 0.62 AU from the Sun and 1.16 AU from Earth and the phase angle was 54° . Assuming a geometric albedo of 0.04 and using the phase law for dust-rich comets by Marcus (2007), this generic model gives for the total apparent visual magnitude of the imaged tail of Ikeya-Seki

$$H = -2.1 \text{ mag}, \quad (12)$$

a value that agrees with the estimate based on the surface-brightness measurements to within a few tenths of a magnitude, suggesting the plausibility of the procedure and chosen parametric values. Most importantly, both approaches show that at the time the tail was brighter than the head by a factor of nearly 100.

In the light of these results, Hasegawa & Nakano's (2001) assumption that after perihelion the sungrazers were observed with the naked eye until the brightness of the head declined to apparent magnitude 5 is greatly off the mark. Instead, evidence shows that a sungrazer's **tail is last sighted with the unaided eye when the object's head has faded to about magnitude 7**, implying that both the absolute magnitudes and the magnitudes at the time of first sighting in Table 1 should be fainter by 2 mag or so. This means that with the exception of the comet of 1663 and, to a lesser degree, 1232, the tabulated comets were intrinsically rather faint, most of them fainter than comet Ikeya-Seki, although not as faint as comet Lovejoy. The brightness of the comets from Table 1 is further addressed in Section 5.7.

5.3. Apparent Magnitude of Historical Comets at First Sighting with the Naked Eye

How bright on the average were historical comets when first detected with the naked eye? The most appropriate object to use in addressing this issue is surely comet 1P,

because before E. Halley's 1705 discovery of its periodicity, the comet had been detected with the naked eye as a new object at every return to perihelion back to 12 BC (Ho 1962, Kiang 1972) and, including the probable Babylonian accounts in 87 BC and 164 BC (Stephenson et al. 1985), apparently all the way back to 240 BC. The solution to the problem of naked-eye discovery was in the past sought on the assumptions that (i) Halley's light curve does not vary from one apparition to the next, as suggested first in his investigation by Holetschek (1896); and (ii) the brightness variations with heliocentric distance are satisfactorily represented by the comet's light curve at the 1910 apparition.

The first assumption is probably valid, at least approximately, even though Ferrin & Gil (1988) argued that Halley's comet had been fading at a rate of 0.055 magnitude per revolution. Over two millennia, this rate would accumulate to a total of nearly 1.5 magnitude, an effect that is not obvious from the available data. Neither is this rate of decreasing activity supported by the invariability of the nongravitational perturbations of the comet's orbital motion established by Yeomans & Kiang (1981), even though the radial component, the driver of such secular variations, was rather poorly determined. In any case, I do not see compelling evidence for a material long-term fading or a rationale for its search in the limited data set available. Unlike the first assumption, the second one is demonstrably incorrect and leads to grossly inaccurate results, which are revised below.

Let a comet's apparent brightness vary with geocentric distance Δ and heliocentric distance r according to a $\Delta^{-2}r^{-n}$ law, so that its apparent magnitude $H(\Delta, r)$ is given by

$$H(\Delta, r) = H_0 + 5 \log \Delta + 2.5n \log r, \quad (13)$$

where H_0 is the absolute magnitude (at $\Delta = r = 1 \text{ AU}$). If the light curve is asymmetric relative to perihelion, one should distinguish between the preperihelion parameters, H_0^-, n^- , and post-perihelion parameters, H_0^+, n^+ , because they may carry different physical meanings. Once known, they allow the calculation of the comet's apparent magnitude at first sighting, H_{first} , from the respective distances Δ_{first} and r_{first} .

Broughton (1979) employed this approach by plotting the heliocentric distance against the geocentric distance at first sighting for a select subset of 19 returns of Halley's comet and determined that the best fit from seven entries referring to preperihelion discoveries was reached for a power $n^- = 4.6$, which yielded $H_{\text{first}} - H_0^- = -2.2$. He argued that when he assumed $H_{\text{first}} = 3.5$, the absolute magnitude came out to be $H_0^- = 5.7$, very close to the value obtained by Ernst (1911) in his 1910 preperihelion light-curve formula

$$H(\Delta, r) = 5.8 + 5 \log \Delta + 13.5 \log r, \quad (14)$$

even though the parameter n^- by Ernst was higher than Broughton's value by 0.8 .

The present study is limited to examining the apparent magnitudes of Halley's comet at the first naked-eye sighting before perihelion and is terminated by the 1682 apparition, the last one before the predicted returns. This condition leaves a total of 10 entries of the 19 listed by Broughton (1979). From the Δ and r data that he pro-

Table 2
Apparent Visual Magnitudes of Halley’s Comet at First Sighting Before Perihelion
(Returns 12 BC to AD 1682); Preperihelion Times Only

Year of return to perihelion	Time from perihelion (days)	Apparent magnitude at first sighting ^{a,b}				Elongation		Moon age (days)
		G&M’86	M&G’10	B’10	E’10	solar	lunar	
–11	–41	2.9	4.1	4.3	4.5	78°	141°	17
451	–15	2.8	3.4	3.6	3.3	39	35	25
760	–6	(2.4)	(2.9)	(3.0)	(2.7)	35	9	26
989	–28	2.6	3.5	3.7	3.7	57	137	8
1222	–29	(1.5)	(2.4)	(2.6)	(2.6)	54	20	26
1378	–44	1.8	3.1	3.4	3.5	98	134	4
1456	–13	3.1	3.7	3.8	3.5	35	55	23
1531	–25	2.8	3.6	3.8	3.7	51	96	18
1607	–41	3.2	4.4	4.7	4.8	77	65	24
1682	–22	1.9	2.7	2.9	2.8	47	69	21
Average	2.6	3.6	3.8	3.7
		±0.52	±0.53	±0.54	±0.64

Notes.

^a Derived from Halley’s light curve — G&M’86 ($H_0^- = 4.3$, $n^- = 3.2$): 1986 apparition (Green & Morris 1987); M&G’10 ($H_0^- = 5.47$, $n^- = 4.44$): 1910 apparition (Morris & Green 1982); B’10 ($H_0^- = 5.7$, $n^- = 4.6$): 1910 apparition (Broughton 1979); E’10 ($H_0^- = 5.8$, $n^- = 5.4$): 1910 apparition (Ernst 1911).

^b Parenthesized values excluded from the averages.

vided, I calculated the apparent magnitudes at first sighting based on four different laws. Besides the light curve by Broughton ($H_0^- = 5.7$, $n^- = 4.6$) and the preperihelion light curve by Ernst [Equation (14)], I also include another 1910 light curve, derived by Morris & Green (1982) ($H_0^- = 5.47$, $n^- = 4.44$), used by Stephenson et al. (1985), and, most importantly, the 1986 light curve by Green & Morris (1987) ($H_0^- = 4.3$, $n^- = 3.2$).

The results, summarized in Table 2, are striking in two respects. One, even after removing the two entries when the Moon was less than 30° from the comet (suggesting that the comet was brighter than at routine discovery; parenthesized in the table), the average naked-eye brightness at first sighting found from the superior 1986 light curve, is apparent magnitude of 2.6, at least 1 mag brighter than the previously used numbers based on the 1910 light curves. And two, the choice among the 1910 light-curve laws had almost no effect on the resulting magnitude. In view of what follows I also may add that in none of the listed apparitions was the comet discovered at a solar elongation of less than 35° .

The disparity between the 1986- and 1910-based results is caused by the comet’s systematically underestimated total brightness in 1910. Also, the higher values of n indicate that this bias was increasing with heliocentric distance. The new value of the apparent magnitude at the first naked-eye sighting means of course that detection with the naked eye requires a comet to be brighter than previously thought.

Yau et al. (1994) examined historical records on 109P/Swift-Tuttle, another bright periodic comet, in the manner as Broughton did in the case of 1P/Halley. Unfortunately, only a very few apparitions were found and the magnitudes at first sighting varied by nearly 3 mag, thus offering no statistically meaningful information to complement the findings from the Halley data.

Hasegawa & Nakano’s (2001) brightness overestimate at the last sighting and the underestimated average brightness needed to detect a comet with the naked eye conspired to make *preperihelion* discovery of the seven Kreutz candidates in Table 1 extremely difficult, thereby explaining the second of the two striking effects commented on in Section 5.1. The first one is linked, as already noted, to the orbital orientation of the Kreutz sungrazers, which gradually become deep southern-hemisphere objects as time advances from mid-October to mid-December. This is clearly apparent from Marsden’s (1967) perennial ephemeris.

5.4. Kreutz Sungrazer C/1965 S1 (Ikeya-Seki)

I already noted that comet Ikeya-Seki was a great spectacle thanks in part to the favorable timing of its arrival, with the perihelion point reached in the second half of October. Why then all potential historical Kreutz sungrazers coming to perihelion at about the same time of the year (Table 1) were not observed before perihelion? This issue is addressed by examining at what point in its orbit would comet Ikeya-Seki have been discovered had it arrived before the era of telescopic comet hunters.

Interestingly, comet Ikeya-Seki was discovered (almost simultaneously by the two observers) only about 50 hours after it had reached a maximum solar elongation since mid-May 1965. Its light curve was symmetric relative to perihelion (Sekanina 2002), closely following a law given by Equation (13) with $H_0^- = H_0^+ = 5.9$ and $n^- = n^+ = 4.0$. As a function of time from perihelion, $t - t_\pi$, the comet’s apparent magnitude and solar and lunar elongations are presented in Table 3. One finds somewhat unexpectedly that, upon its approach, the comet brightened to the average naked-eye first-sighting magnitude of 2.6 (Section 5.3) only nine days before perihelion at a solar elongation of 28° ! In order to be discovered with the naked

Table 3
Light Curve of Comet C/1965 S1 (Ikeya-Seki)

Time from perihelion ^a (days)	Distance (AU) from		Apparent magnitude, $H(\Delta, r)$	Elongation		Moon age (days)
	Earth	Sun		solar	lunar	
-32.4 ^b	1.549	1.109	7.3	45°6	53°	23.0
-24	1.311	0.907	6.1	43.7	68	2.0
-21	1.229	0.829	5.5	42.1	98	5.0
-18	1.150	0.747	4.9	39.9	125	8.0
-15	1.076	0.661	4.3	36.9	147	11.0
-12	1.010	0.569	3.5	32.9	153	14.0
-9	0.955	0.468	2.5	27.6	135	17.0
-6	0.917	0.356	1.2	20.9	108	20.0
-4	0.906	0.270	0.0	15.4	87	22.0
-2	0.915	0.167	-2.1	8.8	67	24.0
-1	0.933	0.103	-4.1	4.9	56	25.0
-0.5	0.950	0.0629	-6.2	2.5	51	25.5
-0.3	0.960	0.0434	-7.8	1.5	49	25.7
-0.1	0.977	0.0197	-11.2	0.5	47	25.9
0	0.996	0.00785	-15.2	0.4	45	26.0
+0.1	1.011	0.0182	-11.5	0.5	43	26.1
+0.3	1.019	0.0423	-7.8	2.0	39	26.3
+0.5	1.023	0.0619	-6.1	3.1	36	26.5
+1	1.028	0.102	-4.0	5.5	27	27.0
+2	1.033	0.167	-1.8	9.2	13	28.0
+4	1.039	0.269	0.3	15.0	23	0.6
+6	1.044	0.355	1.5	19.9	50	2.6
+9	1.048	0.468	2.7	26.3	89	5.6
+12	1.051	0.568	3.6	32.1	124	8.6
+15	1.053	0.661	4.2	37.6	152	11.6
+18	1.053	0.747	4.7	42.7	145	14.6
+21	1.053	0.829	5.2	47.7	110	17.6
+24	1.052	0.907	5.6	52.6	73	20.6
+27	1.050	0.981	5.9	57.4	42	23.6
+30	1.048	1.053	6.2	62.2	41	26.6
+37.3 ^c	1.046	1.219	6.9	73.6	109	4.3

Notes.

^a Perihelion time = 1965 October 21.18 TT.

^b Discovery.

^c One of last naked-eye sightings of the tail (Roemer 1966).

eye as a morning object before or around the beginning of the astronomical twilight (with the Sun 18° below the horizon), it would have to have been detected at an elevation of less than 10° above the horizon under conditions of severe atmospheric extinction.

The comprehensive algorithm by Schaefer (1993, 1998) for the limiting magnitude of a star to be seen with the naked eye was employed to address the issue of discovering Ikeya-Seki in the pre-telescopic era. I considered the most favorable circumstances, namely, the comet's minute, nearly-stellar head (to approximately fit the conditions to which the algorithm applies), its solar elongation equaling the difference between the elevations of the comet and the Sun (i.e., the comet and the Sun located at the same azimuth). Obviously, at the given solar elongation of 28° the observing conditions, as a function of the comet's elevation above the horizon, deteriorated from an optimum position in either direction, because of either excessive atmospheric extinction or advancing twilight. Application of Schaefer's theory suggests that the optimum conditions occurred when the comet reached an elevation of 9°; at that time the naked-eye detection

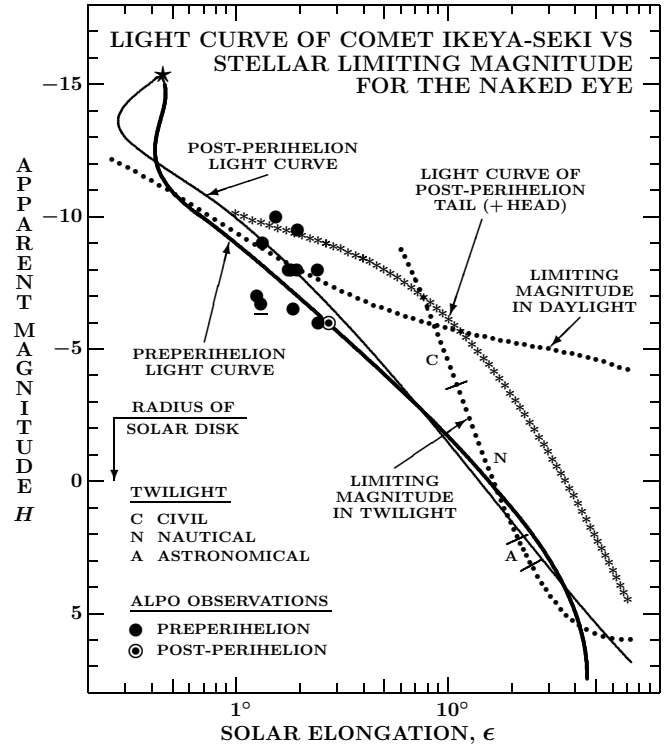


Figure 1. Comparison of the visual light curve of Comet Ikeya-Seki with Schaefer's naked-eye limiting magnitude for stellar objects in a plot of the apparent visual magnitude H as a function of the solar elongation of the comet's head. Next to its preperihelion and post-perihelion branches of the light curve (the perihelion point being marked by the star), the figure also presents an estimated light curve of the comet's post-perihelion tail (+ head) and magnitude estimates by several ALPO members; the observation by Meisel, who used a bulb photometer, is underscored. The limiting magnitude is displayed for daylight conditions (both the Sun and comet assumed at an elevation of 45°), as well as in twilight (astronomical, nautical, and civil) and at nighttime. The twilight curve fits an optimum case of the Sun and comet located at the same azimuth, as described in the text.

limit at its location was magnitude 4.1, or 1.5 magnitude fainter than the discovery magnitude 2.6. The naked-eye detection limit equaled magnitude 2.6 when the comet's elevation was 4°.6 (because of the extinction) or 13°.6 (because of advancing twilight); thus, the time available to the potential discoverer was at best about $\frac{1}{2}$ hour, more probably shorter. As for the tail at this time, it was relatively short and not bright enough to significantly improve the likelihood of detection. I conclude that the chance of naked-eye discovery of comet Ikeya-Seki in this narrow window of time about nine days preperihelion, while not nil, appears to have been relatively poor.

Next I examine the possibility of the comet's naked-eye discovery in broad daylight, whether before or after perihelion, or later after perihelion. In Figure 1 I plot the apparent visual magnitude of the head of comet Ikeya-Seki calculated from the light curve (Sekanina 2002), both preperihelion and post-perihelion, as a function of solar elongation of the comet's head. The figure also shows (i) the naked-eye magnitude estimates by members of the Association of Lunar and Planetary Observers (ALPO), summarized by Milon (1966); and (ii) an estimated apparent magnitude of the comet's dominant

post-perihelion tail, based on the approximate results of Section 5.2. These brightness data are compared with the elongation dependent limiting magnitude for stellar objects detected with the naked eye, as derived from Schaefer’s theory for daytime observation in the case of the Sun’s and comet’s elevations of 45° , as well as for twilight and nighttime observation. The daytime limiting brightness declines with increasing elevation at a rate between 0.01 and 0.03 magnitude per degree.

Figure 1 shows several interesting features. An important point to make is that the comet’s preperihelion apparent brightness increased with decreasing solar elongation less steeply than did the limiting brightness for the naked eye in twilight, but more steeply than it did in broad daylight, so that while the comet’s head was too faint to be detected at $5\text{--}15^\circ$ from the Sun, it was bright enough for detection at smaller elongations. This seemingly peculiar correlation supports the existence of the “sun-comets” reported by Strom (2002) from his inspection of historical Chinese sources and explains fairly common reports of daylight comets (not only Kreutz sungrazers) in *close* proximity to the Sun.

Another notable feature of the figure is the distribution in the plot of daytime naked-eye magnitude estimates of the comet by the ALPO observers. The scatter of some 4 mag shows the high degree of uncertainty involved in the estimates, which were not used in constructing the light curve. Yet, two effects are worth noting: (i) most estimates are decidedly not below the standard light curve, thereby showing no evidence of the r^{-4} law’s flattening out near perihelion (down to at least 0.04 AU from the Sun), unlike for numerous other comets; and (ii) some of the estimates are below Schaefer’s limiting magnitude curve, including the only one among the plotted data points that was determined with some precision (it is underscored in Figure 1).⁵ It is possible that the brighter estimates included a modest contribution from the tail, which was widely reported to be up to 3° in length between October 20.7 and 20.9 UT, that is 7–12 hr before perihelion.⁶

An unusual feature in Figure 1 is the upward trend of the twilight branch of the limiting-magnitude curve after crossing the daylight branch, indicating that daylight conditions for discovering an object of a given brightness with the naked eye may be superior to the twilight conditions. To further examine this finding, I plot in Figure 2 a limiting magnitude for the naked eye at four solar elongations between 6° and 12° as a function of the object’s elevation in the case when the object and the Sun are located at the same azimuth, the difference between their elevations then equaling the elongation. Figure 2 shows enormous changes of the limiting magnitude in the critical range of elongations: while much fainter objects could be detected in twilight than daylight at a solar elongation of 12° (displaying a deep minimum at an elevation of $5^\circ.5$), the opposite is true at 6° (where a very shallow minimum is exhibited at $4^\circ.5$), with a transition region

⁵ This brightness determination, by D. Meisel, was made with help of a simple bulb photometer, by comparing the brightness of the comet’s head with that of the Sun; this measurement is in good agreement with the standard light curve.

⁶ Interestingly, Milon (1966) reported only a single daytime detection of the comet and its tail with the naked eye the following day, about 10 hours after perihelion.

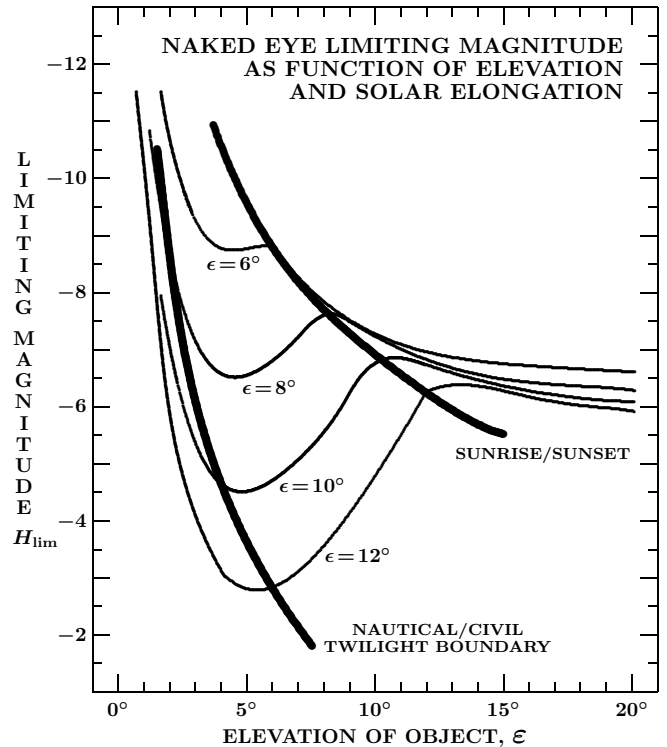


Figure 2. Schaefer’s (1998) limiting magnitude of a stellar object for the naked eye, H_{lim} , as a function of the object’s elevation, \mathcal{E} , at the solar elongations, ϵ , of 6° , 8° , 10° , and 12° . The object and the Sun are assumed to have the same azimuth, so that the elongation equals the difference between their elevations. The two heavy dotted curves show sunrise/sunset and the boundary between the civil and nautical twilight, respectively. Note the considerable depth of the minimum near elevation 5° for elongation 12° , which contrasts with the extremely shallow minimum at elevation $4^\circ.5$ for elongation 6° . Also note that the twilight minimum for elongation 12° is substantially fainter than the daylight limiting magnitude, while the opposite is true for elongation 6° .

in between. This is the effect that causes the twilight curve crossing the daylight curve near the elongation of $8\text{--}9^\circ$ in Figure 1.

If comet Ikeya-Seki were to be discovered with the naked eye in broad daylight *prior to perihelion*, this would most probably occur in immediate proximity of the Sun’s disk, as only then did its brightness exceed, *very briefly*, the detection limit by a sizable margin. However, if the comet even then remained undetected, a *rapidly developing, spectacular dust tail was about to blaze into view within days after perihelion* (Section 5.2; the asterisked curve in Figure 1).⁷ The reader will notice that this “foolproof” scenario of naked-eye discovery shortly after perihelion places comet Ikeya-Seki squarely in the category of the historical Kreutz sungrazer candidates listed in Table 1 (cf. also Table 5).

5.5. Kreutz Sungrazers C/1843 D1 and C/1882 R1

The observing conditions for the two giant members of the Kreutz system, C/1843 D1 and C/1882 R1, were relatively favorable. A major physical difference between

⁷ One has to keep in mind that thanks to its large dimensions, the tail extended to much greater solar elongations where viewing conditions were more favorable.

them was that the nucleus of the latter became multiple after perihelion as a result of extensive near-perihelion fragmentation, whereas the nucleus of the former remained single. This disparity was reflected dramatically in the post-perihelion visibility and light curves of the two objects, as discussed below.

According to Encke (1843), anonymous reports of C/1843 D1 published in New York newspapers mentioned that the comet was first detected on February 5 or 22 days before perihelion. On the other hand, in his updated “Directory of Elements of Cometary Orbits” Galle (1894) remarked that the first observations of C/1882 R1 were made on September 1, 16 days before perihelion, by unknown individuals from the Gulf of Guinea and from Cape of Good Hope; independently, Kreutz (1888) noted that the Gulf sighting was made by the crew of an Italian ship. Both comets were discovered fortuitously, with no telescopic aid; the findings from the historical discoveries of Halley’s comet therefore apply.

Until very recently, there was very little information available on the preperihelion light curve of either of the two comets. The situation changed for C/1882 R1 thanks to a comprehensive paper by Orchiston et al. (2020) on the comet’s observations in New Zealand. The authors mention that the nucleus of the comet was of magnitude 2 when observed from Wellington on the morning of September 9 and from Dunedin before sunrise on September 11, and almost equal to a star of magnitude 1 when sighted from Gisborne around 5 AM on September 11; the solar elongation of the comet’s head was then only 21°. Orchiston et al. add that an article in an Auckland newspaper stated that on September 12 the comet (not its nucleus) was as bright as Jupiter, which might be an exaggeration. The New Zealand preperihelion brightness data are complemented by W. H. Finlay’s estimate of magnitude 3 (allegedly the nucleus) on September 7.2 UT (Gill 1882) and Elkin’s (1882) magnitude estimate of 3–4 on September 8.2 UT. In addition, Eddie (1883) stated that the comet’s nucleus equaled Jupiter in brilliancy on September 13.1 UT and again on September 15.1 UT,⁸ and that it was brighter than Venus around September 17.3 UT, in full daylight and shortly before reaching perihelion. A second-hand report published by Gould (1883a) that described the comet “as being as bright as Venus” before sunrise on September 5, nearly two weeks before perihelion, is entirely outside the realm of possibility.

Most of the assembled preperihelion magnitude estimates suggest that the head of the Great September Comet of 1882 brightened as the inverse 4th power of heliocentric distance, just as did Ikeya-Seki. The r^{-4} law indicates that at the time of first sighting on September 1.2 UT the difference between the apparent and absolute brightness was $H_{\text{first}} - H_0^- = -0.8$ mag. The comet was then 30° from the Sun, an elongation only slightly greater than in the hypothetical case considered above for Ikeya-Seki. Yet, since the two independent and essentially simultaneous (although not first-hand) reports exist from widely separated locations, there are no grounds

to dispute the veracity of the sightings. Besides, additional independent accounts exist from the subsequent days. The comet apparently did display a tail. What could be questioned is the apparent magnitude, but the Halley-based value of 2.6 mag (Section 5.3) provides a conservative estimate, resulting in the absolute magnitude of $H_0^- = 3.4$ mag, or 2.5 magnitudes brighter than Ikeya-Seki. It is 2 magnitudes brighter than the absolute magnitude derived from the reported brightness estimates of the nuclear condensation mentioned above.

To address the controversy about whether the Great March Comet of 1843 was intrinsically brighter or fainter than the Great September Comet of 1882, it is appropriate to compare both objects in terms of the first naked-eye sighting. For the 1843 comet the application of the r^{-4} law gives for the discovery date of February 5.9 UT a difference of $H_{\text{first}} - H_0^- = -0.9$ mag. The comet was 54° from the Sun, but there was some interference from the Moon, which was 6 days old and less than 50° from the comet. The adopted Halley-based apparent magnitude of 2.6 implies the absolute magnitude of $H_0^- = 3.5$ mag. Given the uncertainties involved, I tentatively conclude that the two comets were intrinsically of equal brightness along the preperihelion leg of the orbit. If the inverse fourth-power law should apply all the way to perihelion (as Figure 1 suggests for Ikeya-Seki), the 1882 sungrazer would have reached a peak apparent magnitude of -17.7 , the 1843 sungrazer -19.1 on account of its slightly smaller perihelion distance.

The absolute brightness and the light curve inferred for the 1843 sungrazer can crudely be tested on three probable sightings reported from the period of time shortly before perihelion (Herrick 1843b, Peirce 1844). The first of the three allegedly occurred on February 19.9 UT from Bermuda; the comet is calculated to have been of apparent magnitude -0.3 at a solar elongation of 26°. For the second sighting, on February 24.0 UT from Philadelphia, Penn., the apparent magnitude is derived as -2.3 at an elongation of 16°. And for the third, on February 26.9 UT from Puerto Rico, the predicted apparent magnitude is -6.4 at an elongation of 6°. The comet was an evening object and the first two sightings appear to have probably taken place during twilight. For the solar elongation of 26° the Schaefer theory predicts in the best possible case the naked eye limiting magnitudes of $+2.3$ at elevation 15° (nautical twilight), $+2.9$ at elevation 10° (astronomical twilight), and $+2.7$ at elevation 5°. For the solar elongation of 16° the limiting magnitudes in the best case are -2.1 at elevation 12° (civil twilight), -0.2 at elevation 8° (nautical twilight), and -1.4 at elevation 4° (beginning of astronomical twilight). The Puerto Rico sighting appears to have been made most probably around midday; the predicted limiting magnitude is -6.1 at an elevation 60° and -6.6 at 30°. The comparisons suggest that the Bermuda sighting should have been very easy, the Philadelphia sighting fairly easy, while the Puerto Rican sighting was difficult but still doable. One of course cannot rule out that the comet was in fact intrinsically brighter than adopted.

As already hinted, the 1843 and 1882 sungrazers differed dramatically in their post-perihelion behavior. I determined a light curve of the 1882 comet from a number of visual estimates between 0.6 AU and 4.4 AU and found $H_0^+ = -0.2$ mag and $n^+ = 3.3$ (Sekamina 2002), much flat-

⁸ This could not both be correct, because it is inconceivable that the comet did not brighten over a period of 48 hours, during which its heliocentric distance dropped from 0.3 AU to 0.2 AU on its way to perihelion.

ter than the comet’s preperihelion light curve. The sungrazer was observed for the last time on 1883 June 1, or 257 days after perihelion, with a 28-cm equatorial of the Córdoba Observatory (Gould 1883b). It was then less than 40° from the Sun and its total apparent magnitude calculated from the above photometric parameters was 8.7; the nuclear condensation measured for astrometry was 2–3 mag fainter.

By contrast, the 1843 sungrazer was fading after perihelion much more rapidly. It was observed for the last time on 1843 April 19, 51 days after perihelion, with a 15-cm refractor of the Cape Observatory (Maclear 1851). A tentative post-perihelion light curve, based primarily on Warner’s (1980) published extracts from C. Piazzzi Smyth’s journal of his Cape observations and supplemented by isolated brightness estimates reported by Herick (1843a), Kendall (1843), and Simms (1845), suggests that the brightness of the comet’s condensation was declining according to an r^{-4} or a slightly steeper law. If one accepts that the power n^+ correlates with the extent to which the nucleus fragmented at perihelion, attaining a value the lower the greater the extent, the 1882 comet (six major fragments and $n^+ = 3.3$) and Ikeya-Seki (two major fragments and $n^+ = 4.0$) imply that the apparently nonfragmenting sungrazer of 1843 should indeed have had $n^+ > 4$. This is consistent with the well-known fact that sungrazers normally fade quite rapidly.

In Section 5.2 I noted that the apparent magnitude of three sungrazers — the Great Comet of 1882, Ikeya-Seki, and Lovejoy — at the time of last naked-eye sighting was always close to $H_{\text{last}} = 7$ mag. According to Kronk (2004), the Great Comet of 1843 was last time seen with the naked eye by F. W. L. Leichhardt on 1843 April 11, 43 days after perihelion. With n^+ in the range $4.0 \leq n^+ \leq 4.2$ one finds $H_{\text{last}} - H_0^+ = +2.4$ mag and therefore $H_0^+ = 4.6$ mag; the post-perihelion absolute magnitude is nominally 1.1 mag fainter than the preperihelion absolute magnitude. In order to connect with the preperihelion light curve at perihelion, it is required that $n^+ = 4.2$, in line with the condition based on the last naked-eye detection.

5.6. Probable Kreutz Sungrazer X/1106 C1

Based on the constraints to the apparent magnitudes at the first and last naked-eye sightings, a consistent picture emerges on the relationship between the two giant sungrazers, the Great Comets of 1843 and 1882. In terms of light-curve variations, the two objects appear to have behaved similarly before perihelion, but very differently after perihelion. The most profound disparity was noted in the time of last sighting of their tails with the naked eye (171 days after perihelion for 1882 vs 43 days for 1843) and their heads telescopically (257 days for 1882 vs 51 days for 1843). As noted, these enormous differences were associated with the fact that the 1882 sungrazer fragmented profusely at perihelion, whereas the nucleus of the 1843 sungrazer remained single.

There are obvious evolutionary ramifications for the Kreutz system, as the 1843 and 1882 sungrazers are considered the largest surviving masses of Lobe I and Lobe II, respectively. The propensity for *near-perihelion* fragmentation is distinctly higher for products of Lobe II than Lobe I. Although obviously implying different morphologies of the two lobes in the framework of the

contact-binary model of Paper 1, the discrepancy is of course model independent.

As a fundamental property, the susceptibility to near-perihelion fragmentation is expected to be hereditary, and this is supported (i) by the multiple nuclei of the 1882 sungrazer and Ikeya-Seki, both products of Lobe II; and (ii) by Marsden’s (1967) compelling demonstration of their common origin, that is, a breakup of their parent. Given the correlation between near-perihelion fragmentation and the duration of post-perihelion visibility,⁹ a parent sungrazer and its most massive fragment should be visible with the naked eye over comparably long post-perihelion periods of time. The continuing controversy about the population membership of comet X/1106 C1 — granted it was a Kreutz sungrazer — should be settled by the time of its last sighting: if historical sources should indicate that it was visible over 40–60 days after perihelion, it probably was a fragment of Lobe I (a member of Population I) and the parent to C/1843 D1; if it was seen for longer than ~ 150 days, it should have been a fragment of Lobe II (a member of Population II) and the parent to C/1882 R1 and C/1965 S1.

Historical records, summarized by Kronk (1999), suggest that comet X/1106 C1 was discovered shortly after perihelion. It was extensively observed in Europe, the Middle East, as well as the Far East. The comet was first seen from Belgium in broad daylight on February 2, probably just a few days after perihelion. Within the following two weeks, the comet was detected in the evening sky in a number of European countries (including England, Scotland, France, Holland, Italy, and Germany), as well as in Palestine, Armenia, Japan, Korea, and China. The tail apparently grew rapidly in length, reaching 100° on February 9. The comet was under observation throughout February and into March. Kronk (1999) writes that European chroniclers differed greatly on how long was the comet seen, the shortest period being about 15 days and the longest about 70 days, disappearing between late February and the second half of April. The Far Eastern sources indicated that the comet remained visible for more than 30 days from the time of first sighting, the estimate that was also adopted by Hasegawa & Nakano (2001). This suggests that the comet was still seen after March 10. Seargent (2009) mentions an Armenian text, which implies that the comet disappeared on April 3. And a Chinese source, quoted by Hasegawa & Nakano, noted that on April 9 a comet “changed and disappeared,” a somewhat cryptic comment on an object that may or may not have been identical with X/1106 C1.

Adopting, rather conservatively, March 17 as the date of the final sighting (according to *Historia Hierosolymitana*) and January 26 as the nominal perihelion date (Hasegawa & Nakano 2001), the comet was seen until 50 days after perihelion. Even in the extreme case it should have been seen for less than three months from perihelion. This duration is comparable to, or moderately exceeding, the 43 days from perihelion found above for C/1843 D1, but it is considerably shorter than the nearly six months, the length of time established for

⁹ Because the duration of visibility depends on the intrinsic brightness of the object, the correlation with the extent of fragmentation can meaningfully be examined only among objects of comparable pre-breakup intrinsic brightness.

Table 4
Light-Curve Parameters for Three Kreutz Sungrazers
and Probable Sungrazer X/1106 C1

Comet	Preperihelion		Post-perihelion		Popu- lation	Note
	H_0^-	n^-	H_0^+	n^+		
C/1965 S1	5.9	4.0	5.9	4.0	II	1
C/1882 R1	3.4	4.0	-0.2	3.3	II	2
C/1843 D1	3.5	4.0	4.6	4.2	I	3
X/1106 C1	2.9	4.0	4.0	4.2	I	4

Notes.

1. From the comet’s light-curve investigation by Sekanina (2002). A slope of $n^- = 4.0$ is accepted as a standard for preperihelion light curves of sungrazers whose intrinsic brightness was comparable to, or exceeded, that of C/1965 S1. A slope of $n^+ = 4.0$ is deemed typical for post-perihelion light curves of sungrazers subjected to modest near-perihelion fragmentation. One of late naked-eye sightings of tail (Roemer 1966) on 1965 November 27 ($\Delta_{\text{last}} = 1.05$ AU, $r_{\text{last}} = 1.22$ AU; solar elongation 74° ; see Table 3) implies $H_{\text{last}} = 6.9$. [Milon saw with naked eye 10° long tail of magnitude 5 on November 29 and 7° long tail on December 4, when $H_{\text{last}} = 7.3$ (Milon et al. 1967).] When extrapolated to perihelion, $H = -15.2$ mag.

2. Magnitude H_0^- is derived from the first naked-eye sighting (Galle 1894, Kreutz 1888) on 1882 September 1 ($\Delta_{\text{first}} = 1.37$ AU, $r_{\text{first}} = 0.71$ AU; solar elongation 30°) assuming apparent magnitude $H_{\text{first}} = 2.6$ (Section 5.3). Slope n^- is consistent with limited preperihelion magnitude data on nuclear condensation. The post-perihelion light-curve parameters from Sekanina (2002) imply $H_{\text{last}} = 6.6$ at the last naked-eye sighting of tail (Gould 1883b) on 1883 March 7 ($\Delta_{\text{last}} = 3.09$ AU, $r_{\text{last}} = 3.37$ AU; solar elongation 98°). Negative differences $H_0^+ - H_0^- = -3.6$ and $n^+ - n^- = -0.7$ are measures of profuse near-perihelion fragmentation. When extrapolated to perihelion, $H = -17.7$ mag.

3. Magnitude H_0^- is derived from the first sighting with naked eye (Encke 1843) on 1843 February 5 ($\Delta_{\text{first}} = 0.88$ AU, $r_{\text{first}} = 0.86$ AU; solar elongation 54° , Moon possibly interfering) assuming apparent magnitude $H_{\text{first}} = 2.6$ (Section 5.3). Adopted preperihelion light curve accommodates probable sightings (Herrick 1843b, Peirce 1844) from Bermuda on 1843 February 19 ($\Delta = 0.94$ AU, $r = 0.43$ AU; solar elongation 26°), from Philadelphia, Penn., on February 23 ($\Delta = 0.97$ AU, $r = 0.27$ AU; solar elongation 16°), and from Puerto Rico on February 26 ($\Delta = 1.00$ AU, $r = 0.10$ AU; solar elongation 6°). Post-perihelion light-curve parameters are consistent with limited magnitude data on nuclear condensation. Slope is constrained to $n^+ > 4.0$ on account of absence of evidence on near-perihelion fragmentation. Absolute magnitude H_0^+ is derived from the last naked-eye sighting of tail (Kronk 2004) on 1843 April 11 ($\Delta_{\text{last}} = 1.69$ AU, $r_{\text{last}} = 1.33$ AU; solar elongation 52°) on the assumption that $H_{\text{last}} = 7$. Positive differences $H_0^+ - H_0^- = +1.1$ and $n^+ - n^- = +0.2$ are measures of apparent absence of near-perihelion fragmentation. When extrapolated to perihelion, $H = -19.1$ mag.

4. Light-curve parameters uncertain; their approximate determination is based on the adopted last naked-eye sighting of tail (Kronk 1999; Hasegawa & Nakano 2001; Ho 1962) on 1106 March 17 ($\Delta_{\text{last}} = 1.73$ AU, $r_{\text{last}} = 1.50$ AU; solar elongation 62°), assuming $H_{\text{last}} = 7$ mag; and on perceived behavior similarity to C/1843 D1. H_0^+ was derived from H_{last} adopting equal values of n^+ for the two objects. Assumption of equal perihelion distance implied equal difference ($H_0^+ - H_0^-$), providing H_0^- . When extrapolated to perihelion, $H = -19.7$ mag.

C/1882 R1. One can therefore rather safely conclude that the post-perihelion light curve of X/1106 C1 resembled that of C/1843 D1 and that the former comet was in all probability the parent of the latter comet, both failing apparently to fragment profusely near perihelion.

Accepting that on 1106 March 17 the comet’s head was of apparent magnitude 7 and the brightness variations followed an r^{-4} or $r^{-4.2}$ law, the post-perihelion absolute magnitude of X/1106 C1 is computed to have amounted

to $H_0^+ = 4.0$. Scaling up the case of C/1843 D1, the predicted preperihelion value for X/1106 C1 becomes $H_0^- = 2.9$. The adopted light-curve parameters for C/1965 S1, C/1882 R1, C/1843 D1, and X/1106 C1, discussed in Sections 5.4–5.6, are summarized in Table 4, accompanied by extensive narrative.

In spite of uncertainties in the tabulated data, especially for X/1106 C1, the differences in the physical meaning of the light-curve parameters, H_0^- and H_0^+ in particular, are very apparent. The preperihelion brightening of these major sungrazers tends to follow a power law with $n^- = 4$ and their degree of conspicuousness is described by H_0^- .¹⁰ This parameter allows one to conclude that C/1843 D1 and C/1882 R1 were both of about equal dimensions when arriving at perihelion and X/1106 C1 may have been a little larger, while C/1965 S1 was a distinctly smaller fragment in comparison.

On the other hand, H_0^+ and especially the differences $H_0^+ - H_0^-$ and $n^+ - n^-$ describe the severity of the near-perihelion fragmentation effects on the comet’s nucleus and its activity: the more vigorous the effects are, the brighter the comet becomes after perihelion and the more negative are the differences $H_0^+ - H_0^-$ and $n^+ - n^-$.

5.7. *Potential Kreutz Sungrazers from Table 1 Revisited*

I already pointed out in Sections 5.2 and 5.3 that most of the Kreutz candidates in Table 1 are objects intrinsically fainter than the sungrazer Ikeya-Seki. Three of the seven comets do however display, at least nominally, an anomaly of a kind that deserves a comment.

In the reversed chronological order, the first of these is C/1695 U1. It is the only one of the seven for which the data nominally do not rule out the possibility of preperihelion discovery. However, closer inspection leads to a somewhat different conclusion. The Chinese source that Hasegawa & Nakano (2001) refer to says that *after* October 22, “*at the fifth watch, a comet appeared.*” Unfortunately, the report does not offer any information either on how long after the date, or how many watches were there per day. If, for example, just a single one, the message would effectively say that the comet was discovered on October 26 or 27, or a few days *after* perihelion. This guess can be compared with Kronk’s (1999) account, according to which the comet was discovered by P. Jacob, a French Jesuit living in Brazil, on October 28. Kronk writes that the comet was last seen by J. Bovet in India on November 18, which is consistent with a Korean source, quoted by Hasegawa & Nakano, that the comet “*began to disappear . . . a few days*” after November 7. The comet almost certainly was not seen before perihelion and its intrinsic brightness is estimated at $H_0^+ \simeq 7$, near an average among the seven comets.

The time of last sighting of the comet of 1663 in Table 1 immediately raises a red flag. This is the only object among the seven whose post-perihelion behavior exhibits striking similarity to that of C/1882 R1, to the extent that one could predict the former comet’s extensive near-perihelion fragmentation and Population II membership. With an estimated $n^+ \simeq 3.5$ one finds $H_0^+ \simeq 2.5$ and $H_0^- \simeq 5$, much fainter than Hasegawa & Nakano (2001) suggest, but still above average.

¹⁰ This characterization does not apply to dwarf Kreutz sungrazers, which exhibit a very different behavior (see Ye et al. 2014).

Table 5
Revised Absolute Magnitudes for Potential
Kreutz Sungrazers from Table 1

Comet	Absolute Magnitude		Preferred Population
	H_0^-	H_0^+	
943	7.5	8.5	I
1232	6.5	5.5	II
1381	7.5	7.5	II?
1588	6	7	I
1663	5	2.5	II
1666	8	9	I
C/1695 U1	6	7	I

The period of post-perihelion visibility of the comet of 1232 also appears to have been a little longer than average. It probably was another member of Population II subjected to some fragmentation near perihelion, perhaps more extensive than Ikeya-Seki.

Table 5 summarizes the revised absolute magnitudes for the seven Kreutz candidates from Table 1. While the original magnitude estimates implied that four of the objects were intrinsically brighter, two about equal, and only one fainter than Ikeya-Seki, the revised numbers reverse that trend: four were fainter, two equal, and only one brighter. Also worth noting is that all seven were substantially fainter than X/1106 C1, C/1843 D1, and C/1882 R1 before perihelion.

6. SIMULATION OF AMMIANUS' DAYTIME COMETS BY CONTACT-BINARY MODEL OF KREUTZ SYSTEM

The appearance of a comet has historically been one of the most popular portents of an impending ominous event, such as a natural disaster or the death of an influential man. One certainly could find instances of fabricating, by an unscrupulous or sloppy chronicler, the sudden appearance of a comet when none was available at the right time.

This possibility can safely be dismissed when it comes to Ammianus' remark on *comets seen in broad daylight*, which does not fit a run-of-the-mill account of a comet foretelling the death of an emperor: (i) use of the plural is unprecedented and for a good reason, as the appearance of two or more bright comets in the sky simultaneously (or nearly so) is an unrivaled event that has to be seen to believe it; (ii) the reference to broad daylight further enhances the exceptional nature of the incident, making it highly interesting astronomically but offering no obvious value to a portent; (iii) Ammianus' extensive elaboration on the nature of comets that follows the brief remark has no place in a fabricated story; and (iv) the timing is odd, several months *after* the death of Ammianus' beloved Emperor Julian; a concocted omen would have been moved by the narrator to an earlier time.

The first two points are so extraordinary that they clearly show the historian's motivation by a real event. Together with the third point, they strongly suggest that Ammianus acted like anyone else would when greatly impressed by a singular personal experience of spotting brilliant comets in full daylight, having witnessed no such spectacle ever before. The last point implies that the idea of making the story up never entered his mind.

Although it is impossible to estimate how many comets Ammianus observed and over how many days, the historian's remark does not rule out a chance of their nearly simultaneous arrival at perihelion and his sighting of more than one comet near the Sun at a time. Considering the arguments presented in Section 5.4 in relation to the limiting magnitude, it is unlikely that the comets were far from the Sun in the sky. In the following, I address the general features of the distribution of daytime comets over the sky that Ammianus should have seen, if they were products of a fragmented Kreutz progenitor and their motions and evolution were described by the contact-binary model introduced in Paper 1. Next to the primary breakup, the procedure focuses on a sequence of secondary, cascading-fragmentation events that followed over a limited period of time, all but one having taken place in the aphelion region of the orbit, at heliocentric distances of about 160 AU.

The orbital distribution of the fragments, including the times of their arrival at perihelion in AD 363, is determined by the separation velocity vectors. The ranges of angular elements, the longitudes of the ascending node in particular, are effects of the out-of-plane (normal) component V_N of the separation velocity, while the range of perihelion distances is an effect of its transverse component V_T . This component also slightly influences the times of the fragments' first perihelion passage, an effect that is declining with the fragmentation event advancing past aphelion. The radial component V_R , which is indeterminate and assumed to be nil, could potentially exert greater effects, at a rate of about 5 days per 0.1 m s^{-1} .

If the separation velocity is of rotational nature, as it appears to be the case, the direction of its vector becomes an issue of the spin-axis orientation of the parent — the progenitor sungrazer — at the time of the initial fragmentation event. A near-zero radial separation velocity implies the progenitor spinning along an axis pointing essentially at the Sun.

6.1. Contact-Binary Model and Perihelion Times of Kreutz Sungrazers in AD 363

The case of a zero radial component of the separation velocity leads effectively to the scenario of maximum orbital concentration of bright Kreutz sungrazers, the progenitor's major fragments, in a swarm that arrived at the first perihelion in late AD 363. Evidence based on observations from both the ground and aboard the Solar and Heliospheric Observatory (SOHO), as presented in Paper 1, shows the Kreutz system made up of eight populations, two having branches. The eight populations are I, Ia, II, IIa, III, IIIa, IV, and Pre-I. In addition, Population Pe is a side branch to Population I and Population IIa* a low-perihelion branch to Population IIa. As described, the swarm under consideration consists of 10 primary objects, for which the terms *sungrazer* and *fragment* are used interchangeably in this scenario's in-depth examination that follows.

The orbits of the populations were in Paper 1 approximated by the osculating orbits of the bright Kreutz sungrazers when available; for the rest (such as IIIa or IV) I used averages of the orbits of the population members among the SOHO dwarf sungrazers imaged exclusively with the C2 coronagraph, their angular elements corrected for major effects of a nongravitational accel-

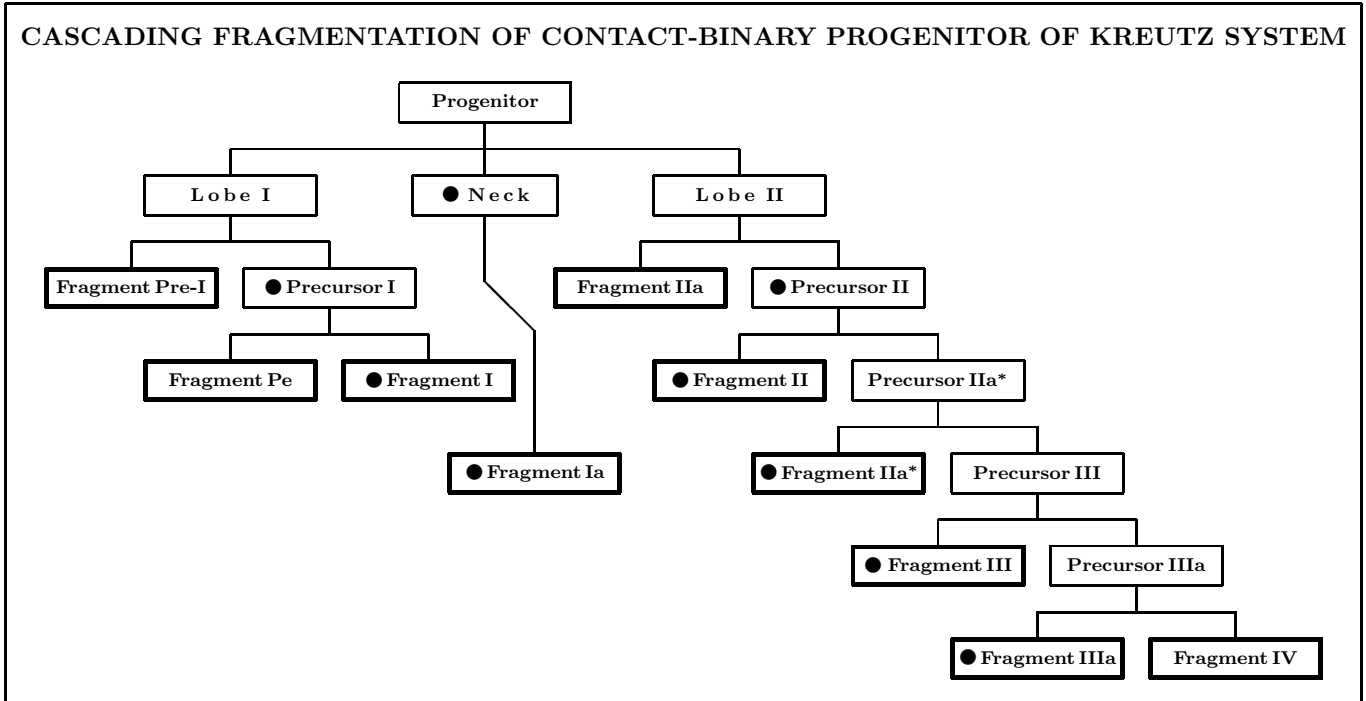


Figure 3. Chart of cascading fragmentation of the modeled contact-binary progenitor of the Kreutz system. The bullets indicate the sungrazers that move in the same orbit as their immediate parent. The sungrazers in heavily framed boxes arrived at the first perihelion in AD 363 and are used here to generate the swarm of daylight comets. Their orbits are approximated as follows: Fragment I by C/1843 D1; Fragment II by C/1882 R1; Fragment Pe by C/1963 R1; Fragment IIa by C/1970 K1; and Fragment III by C/2011 W3. The orbits for Fragments Ia, Pre-I, IIa*, IIIa, and IV were derived as described in Paper 1.

eration. Paper 1 also described a sequence of breakup events from which the primary fragments were born and in which they acquired momenta making them move in an array of fairly similar orbits and arrive at perihelion in AD 363 at only slightly differing times.

The initial fragmentation of the contact-binary progenitor is assumed to have resulted in three fragments, two lobes — the earliest precursors of Populations I and II — and the neck, the precursor of Population Ia. The model assumptions were described in detail in Paper 1. Here I only recall the requirement of perfect symmetry to simplify the computations, which dictated that the lobes be released in exactly opposite directions with separation velocities of the same magnitude. The neck was let to continue moving in the progenitor’s unperturbed orbit, arriving at perihelion in AD 363 at the time the progenitor would have, had it not broken up. To get into an orbit with a smaller perihelion distance, Lobe I had to separate from the rest of the progenitor with a transverse velocity V_T in the general direction opposite the orbital-velocity vector.¹¹ This transverse separation velocity would have caused Lobe I to arrive at perihelion more than 1 day earlier than would the progenitor (or the neck). On the other hand, Lobe II had to separate with a transverse velocity in the direction of the orbital-velocity vector, which would have caused it to arrive at perihelion about $1\frac{1}{2}$ days later than would the neck (or nearly

¹¹ It is noted that this and other separation velocities differ slightly from their values in Paper 1; the reason for these differences is a minor change of less than 10 AU in the aphelion distance of the progenitor; in this paper it equals just under 163 AU, fitting the adopted orbital period of 734.9 yr.

3 days later than Lobe I). As the lobes did not survive intact, their major fragments are assumed to have arrived at those times. This rule applies to all other fragments.

The cascading fragmentation sequence is shown in Figure 3. The events are assumed to have occurred — in the depicted order (the time increasing from the top down) — in the aphelion region of the progenitor’s orbit, with the exception of Fragment Pe, a precursor of C/1963 R1, which is suggested to have separated from Lobe I later, on the way from aphelion to perihelion, at about 70 AU.¹² The fragmentation events are favored to have occurred at aphelion because the same effect in the critical orbital elements was then achieved with a minimum separation velocity, even though this minimum was flat: the change is confined to less than 10 percent of the minimum value over an orbital arc around the aphelion point that the comet travels in nearly 300 yr, or 40 percent of the orbital period! This tolerance explains extremely wide choice for the fragmentation time.

Only the separation of Fragment Pe occurred at a location clearly different from aphelion; the time was dictated by requiring that the magnitude of the separation velocity be comparable to those of Lobes I and II from the progenitor. Table 6 demonstrates that for most fragments the total separation velocity was on the order of $2\text{--}3\text{ m s}^{-1}$ and always lower than 5 m s^{-1} . A possible slight increase in the separation velocity with time that the table might show, could — if genuine — present evidence on the fragments’ spin-up. The relationships between the components of the separation velocity and the

¹² This fragmentation time is only crudely estimated.

Table 6
Separation Velocities in Fragmentation Events and Scatter in Fragments' Perihelion Times

Fragment ^a		Separation velocity (m s ⁻¹) ^b			Time of perihelion in AD 363 (days) when breakup at ^c				
primary	secondary	V _R	V _T	V _N	aphelion	-270 yr	-170 yr	+170 yr	+270 yr
Ia	I	(0.0)	-1.86	-1.80	-1.31	-4.12	-2.46	-0.63	-0.30
Ia	II	(0.0)	+1.86	+1.80	+1.56	+4.58	+2.85	+0.73	+0.34
I	Pre-I	(0.0)	-0.55	-1.37	-0.35	-1.10	-0.65	-0.17	-0.08
I	Pe	(0.0)	-1.60	-1.82	(-1.02) ^d	-3.22	-1.92	-0.49	-0.24
II	IIa	(0.0)	+1.37	+3.19	+1.38	+3.92	+2.49	+0.64	+0.29
II	IIa*	(0.0)	-1.88	+2.75	-1.38	-4.42	-2.61	-0.67	-0.32
IIa*	III	(0.0)	-2.07	+2.89	-1.38	-4.46	-2.62	-0.67	-0.33
III	IIIa	(0.0)	-0.10	-4.40	+0.29	+0.44	+0.45	+0.11	+0.03
IIIa	IV	(0.0)	+2.25	+4.03	+2.03	+5.69	+3.65	+0.93	+0.42

Notes.

^a The first of the three sections of the table refers to the breakup of the progenitor. Second and third sections involve fragments derived, respectively, from Lobe I and II (Figure 3); time increases from the top down.

^b For fragmentation near aphelion, at 163 AU from the Sun, except for Pe (see note d). Motion of primary fragment is assumed to remain unperturbed, the secondary fragment acquiring the separation velocity (see columns 3-5). The perihelion distance and time are perturbed by the transverse component V_T , the angular elements by the normal component V_N .

^c Tabulated is difference in perihelion times, secondary minus primary fragment, in AD 363, when fragmentation occurred at previous aphelion (the nominal case considered in this paper except for fragment Pe; see note d), 270 yr and 170 yr before aphelion, and 170 yr and 270 yr after aphelion. Heliocentric distances were 163 AU at aphelion, 140 AU at 170 yr from aphelion, and 100 AU at 270 yr from aphelion.

^d Fragment Pe (precursor of C/1963 R1) is likely to have separated from the common parent with Fragment I long after aphelion; I nominally adopt that the event occurred at heliocentric distance of 70 AU, equivalent to fragmentation time of 316 yr after aphelion (or 51 yr before following perihelion); the tabulated separation velocity components refer to this time. Fragment Pe is then found to have reached AD 363 perihelion merely 0.125 day before Fragment I did.

perturbations of the orbital elements are governed by the equations presented in Appendix A.

The differences in the perihelion times of the various pairs among the 10 primary fragments, listed in Table 6, were streamlined by referring each time to that of one particular sungrazer, the obvious choice being Fragment Ia. This streamlining was readily achieved by properly adding up the tabulated differences. Designating the perihelion time of Fragment Y_0 by $t_\pi(Y_0)$, the difference between this time and the perihelion time of Fragment Ia, $t_\pi(\text{Ia})$, is given by the expression

$$t_\pi(Y_0) - t_\pi(\text{Ia}) = [t_\pi(Y_n) - t_\pi(\text{Ia})] + \sum_{k=0}^{n-1} [t_\pi(Y_k) - t_\pi(Y_{k+1})], \quad (15)$$

where Y_n is either Fragment I or Fragment II, while Y_1, \dots, Y_{n-1} are the other fragments in Table 6, all related to either Lobe I or II. For the chosen scenario, the parameters are, together with all other elements (taken from Paper 1), listed in Table 7. The middle of the time window of interest (see the beginning of Section 5), has been adopted for the reference time, equal to the perihelion time of the fragmented progenitor's center of mass. This time has been equated with the perihelion time of Fragment Ia, thus $t_\pi(\text{Ia}) = \text{Nov } 15.00$. The overall range of perihelion times of the 10 progenitor fragments is 4.6 days. Since the perturbations of both the perihelion distance and perihelion time were exerted by the transverse component of the separation velocity, one would expect a correlation between the two elements. Figure 4 confirms that this is indeed so. The correlation is perfect

for the nine sungrazers that were products of fragmentation events in the aphelion region, while Fragment Pe, separating from its parent at 70 AU from the Sun, shows a minor deviation from the fit.

In order to be able to judge the visibility of the ten sungrazers, I adopted a simple photometric model, based on the findings in Section 5, and employed it with the Schaefer (1998) algorithm for the limiting magnitude by the unaided eye. Following the conclusions from Section 5.6 I assumed that (i) all fragments on their way to the 363 perihelion were brightening in accordance with the r^{-4} law; (ii) the difference in H_0^- between two consecutive generations was 0.5 mag (as it was, approximately, between X/1106 C1 and C/1843 D1); and (iii) the absolute magnitude of the fragment of the last generation in Figure 3, Fragment IV, was comparable with those of C/1843 D1 and C/1882 R1. As a result, the progenitor was assigned $H_0^- = 1$, Fragments I and II $H_0^- = 1.5$ each, etc., except that $H_0^- = 3$ for Fragment Ia. Furthermore, to define the post-perihelion curves of the sungrazers, I assigned a number of subfragments (or "perihelion" fragments), ν , into which each arriving sungrazer is expected to have broken at the 363 perihelion passage, and subtracted 0.2 per subfragment from the value of $n^+ = 4.2$ for a sungrazer that did not break up at perihelion at all ($\nu = 1$). The post-perihelion absolute magnitude H_0^+ was then determined from

$$H_0^+ = H_0^- + 2.5(4 - n^+) \log q, \quad (16)$$

where q is the perihelion distance in AU. The adopted values of the light-curve parameters are listed on the right side of Table 7. Because the phase angle is subjected to rapid and sizable variations in close proxim-

Table 7
Adopted Orbital Elements, Number of Perihelion Fragments, and Light-Curve Parameters for the Ten Kreutz Sungrazers Modeling Daylight Comets in AD 363 (Equinox J2000)

Progenitor's fragment	Orbital elements						Number of perihelion fragments	Light-curve parameters ^a		
	t_π	ω	Ω	i	$q (R_\odot)$	e		H_0^-	H_0^+	n^+
Ia	Nov 15.00	75°.4	354°.8	143°.4	1.40	0.99992005	1	3	4.1	4.2
I	13.69	82.8	3.7	144.4	1.17	0.99993319	4	1.5	-0.8	3.6
II	16.56	69.6	347.7	142.0	1.67	0.99990464	5	1.5	-1.7	3.4
Pre-I	13.34	88.7	11.0	144.7	1.11	0.99993661	3	2	0.9	3.8
Pe	13.56	86.2	7.9	144.6	1.09	0.99993776	2	2.5	2.5	4.0
IIa	17.94	61.3	337.0	139.1	1.91	0.99989093	2	2	2.0	3.6
IIa*	15.18	61.3	337.0	139.1	1.43	0.99991834	3	2	0.9	3.8
III	13.80	53.5	326.4	134.4	1.19	0.99993205	4	2.5	0.2	3.6
IIIa	14.09	45.2	313.5	125.8	1.24	0.99992919	2	3	3.0	4.0
IV	16.12	40.7	305.1	118.2	1.59	0.99990920	1	3.5	4.6	4.2

Note.

^a Preperihelion parameter n^- always equals 4.

ity of perihelion and strong effects of forward scattering are expected to occur, the phase term was added to the light-curve formula, accounting for the phase effect by employing the method introduced by Marcus (2007).

To use the photometric model in determining under what conditions is a sungrazer visible to the naked eye, I define a simple *visibility index* \mathfrak{S} as a difference between Shaefer's limiting magnitude for the naked eye, H_{lim} , and the sungrazer's apparent magnitude, H ,

$$\mathfrak{S} = H_{\text{lim}} - H. \quad (17)$$

The sungrazer is said to be *clearly visible* with the naked eye when $\mathfrak{S} > +1.5$ mag; it is *probably visible* when $+0.5 < \mathfrak{S} \leq +1.5$ mag, and *potentially visible* when $-0.5 \leq \mathfrak{S} < +0.5$ mag. It is *probably invisible* when $-1.5 \leq \mathfrak{S} < -0.5$ mag; and *invisible* when $\mathfrak{S} < -1.5$ mag.

The final data set for the computations concerns Ammianus' observing site, Antioch on the Orontes. Overall information is in Appendix B; specifically, the geographic latitude of the location, $\phi = +36^\circ.2$.¹³ For the computation of the limiting magnitude, I assume an altitude of 70 meters above sea level, an average November temperature of 15°C (an average of a maximum 20°C and a minimum 10°C), and 55 percent humidity.

6.2. The Computations

The objective is to model a swarm of Kreutz sungrazers, fragments of a contact-binary progenitor, arriving at the first perihelion passage to find out whether the result fits Ammianus' *comets seen in broad daylight*. One needs to examine a scenario in the correct time of the year and in an approximately correct sky projection, but there is no need to actually perform the computer runs specifically in the year 363. This fits the tolerance documented by use of the osculating orbital elements, with the indirect planetary perturbations over nearly two millennia neglected, and by ignoring atmospheric refraction and the effects of the equation of time. Expressing the apparent motions of the Kreutz sungrazers relative to the Sun in the sky as a function of local solar time, the

¹³ There is no need for the geographic longitude for reasons explained in the text.

Sun culminates exactly at noon, when the local sidereal time equals the Sun's right ascension, with no need to introduce the geographic longitude. The approximations result in positional errors that are deemed acceptable.

For each of the ten sungrazers and each selected time of appearance the data file provides an ephemeris entry that contains the right ascension, α , and declination, δ , phase angle, ψ , solar elongation, ϵ , position angle of the prolonged radius vector, P_{RV} , and distances from the Earth, Δ , and the Sun, r . The Sun's right ascension, α_\odot , and declination, δ_\odot , are calculated from

$$\begin{aligned} \sin \delta_\odot &= \sin \delta \cos \epsilon - \cos \delta \sin \epsilon \cos P_{\text{RV}}, \\ \sin(\alpha - \alpha_\odot) &= \sec \delta_\odot \sin \epsilon \sin P_{\text{RV}}, \end{aligned} \quad (18)$$

where $|\alpha - \alpha_\odot| < 90^\circ$ as long as $\cos \epsilon > \sin \delta \sin \delta_\odot$.

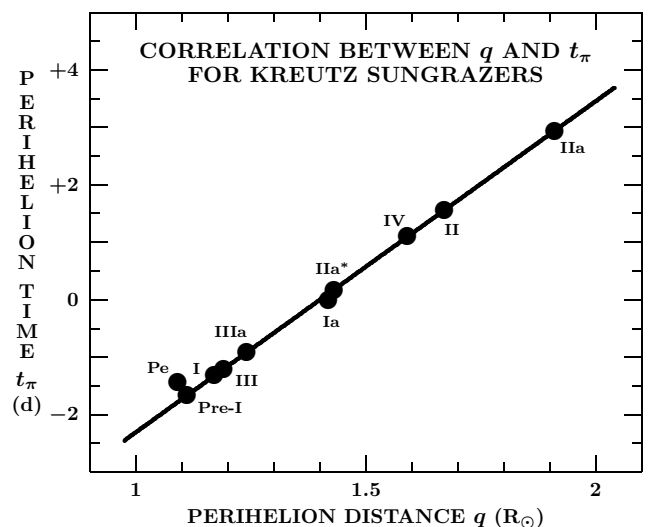


Figure 4. Correlation between the perihelion distance, q , and the perihelion time, t_π , of the Kreutz sungrazers, derived from the perturbations of their parents' orbits acquired at the breakup of the progenitor and the sequence of subsequent secondary breakups, as illustrated in Figure 3. The position of Fragment Pe is off the correlation line, because it separated from its parent at a heliocentric distance much smaller than the aphelion distance.

In order to display the positions of the Kreutz sungrazers relative to the Sun in the Antioch sky, the equatorial coordinates need to be converted to the local horizontal coordinates. The position of each fragment is then given by its azimuth, \mathcal{A} , reckoned positive from the south through the west, and by its elevation, \mathcal{E} , reckoned positive from the ideal local horizon to the zenith. The relationship between the horizontal and equatorial coordinates is given by the transformation formulas

$$\begin{aligned}\cos \mathcal{E} \sin \mathcal{A} &= \cos \delta \sin(\Theta - \alpha), \\ \cos \mathcal{E} \cos \mathcal{A} &= -\cos \phi \cos \delta + \sin \phi \cos \delta \cos(\Theta - \alpha), \\ \sin \mathcal{E} &= \sin \phi \sin \delta + \cos \phi \cos \delta \cos(\Theta - \alpha),\end{aligned}\quad (19)$$

where ϕ is the geographic latitude of Antioch, Θ is the local sidereal time, which is related to the local solar time t (in hours) by

$$\Theta(t) = \alpha_{\odot}^* + \zeta(t - 12), \quad (20)$$

α_{\odot}^* is the right ascension of the Sun at local noon, and $\zeta = 1.00273791$. Equations (19) of course equally apply to the Sun, thereby providing its azimuth \mathcal{A}_{\odot} and elevation \mathcal{E}_{\odot} . The positions of the sungrazers relative to the Sun in the sky are then given by the solar elongation ϵ (from the ephemeris) and by a zenithal position angle P_Z , which is in the local coordinate system reckoned positive from the Sun's zenithal direction clockwise through the west,

$$\sin P_Z = \csc \epsilon \cos \mathcal{E} \sin(\mathcal{A} - \mathcal{A}_{\odot}), \quad (21)$$

with the sign of $\cos P_Z$ equaling the sign of the expression $\cos \epsilon - \sin \mathcal{E} \sin \mathcal{E}_{\odot}$.

The visibility index compares a quantity that is a function of the sungrazer's photometric and orbital properties [i.e., its apparent magnitude $H = H(\Delta, r, \psi; phot)$, where *phot* stands for the light-curve law (preperihelion vs post-perihelion)] with a quantity that is a function of the observing conditions [i.e., the limiting magnitude $H_{lim} = H_{lim}(\epsilon, \mathcal{E}, \mathcal{E}_{\odot}; loc)$, where *loc* defines the observing site]. The distinction between the two quantities is that, in general, the latter varies substantially on much shorter time scales (often a small fraction of an hour) than the former. Since all scenarios involve close proximity to the Sun, the effects of the Moon are deemed insignificant and are ignored.

6.3. The Results

As noted in Table 7, a swarm of ten major sungrazers of the Kreutz progenitor is investigated for an assumed perihelion time of November 15.0, the midpoint of the two-month long period of interest, as established at the beginning of Section 5. The time frame used is the local solar time, which is adequate for the purposes of this study. The progenitor's orbit is assigned to Fragment Ia (Figure 3); the perihelion times of the other nine sungrazers range over a period of 4.6 days, from November 13.34 (Fragment Pre-I) to November 17.94 (Fragment IIa), being strongly correlated with the perihelion distance, as shown in Figure 4.

A computer code has been written that calculates, for the geographic latitude of Antioch, (a) the horizontal coordinates of the ten sungrazers and the Sun, using the objects' ephemerides; and (b) the apparent magnitudes of the sungrazers, employing the prescribed light-curve

parameters, the ephemerides, and the Marcus (2007) dust scattering law. The period of time covered by the daily ephemerides extends from November 1 to November 25, each day from 4:48 to 19:12 local solar time at a 36 minute step, thereby totaling 625 individual entries for each sungrazer.

The trajectories of the sungrazers in the sky follow the expected pattern given by the projected spatial orientation of their orbits. Relative to the Sun the comets approach from the southwest and recede to the west-southwest. They pass between the Sun and Earth on their way to perihelion; 1–2 hours before reaching it, their phase angle exceeds briefly 150° , their brightness then being strongly enhanced by forward-scattering effects. They recede from perihelion on the far side of the Sun, reckoned from the Earth. The limited, yet clearly apparent, orbital scatter is prompted by the almost 70° wide range of nodal longitudes and the associated range of nearly 30° in the inclination.

In Section 5.4 I showed for comet Ikeya-Seki that the preperihelion light curve still followed the r^{-4} law as late as 6 hours before perihelion and possibly closer. However, there is no evidence either way whether the brightness could reach magnitudes near, or in excess of, -20 mag over a period of, say, a fraction of an hour around perihelion for the most brilliant sungrazers. To a degree, this question is academic, because even if attained, these magnitudes should be highly transient. It suffices to mention that the apparent brightness of a Kreutz sungrazer that follows an inverse fourth power law varies by fully 3 magnitudes¹⁴ over an arc of 180° in true anomaly centered on the perihelion point and traveled in 1.9 to 4.4 hours (depending on the perihelion distance). While in the tables that follow I strictly adhere to the power law, the magnitudes brighter than about -15 are not to be taken literally, meaning only that the sungrazer was then surely bright enough to be seen with the naked eye even at close proximity of the Sun. Indeed, Schaefer's algorithm indicates that a stellar object in contact with the Sun's disk in the sky is visible to the naked eye when its brightness exceeds magnitude -12 to -13 .

The results are presented in three figures and a series of comprehensive tabulations in Appendix C plus a summary table. The figures are to offer views of the diverse appearances of the sungrazers' sky display relative to the Sun on particular days and to illustrate the overall evolution of the swarm. By contrast, the tables provide the in-depth positional and visibility data.

Figure 5 and Table C-1 show the development of the swarm of sungrazers on November 15. At 6:36 local solar time the Sun was still nearly 4° below the horizon (civil twilight). Of the ten sungrazers, only five were above the horizon, although all by less than 2° . None of them was visible to the naked eye because of twilight and atmospheric extinction. By 7:12, both the Sun and all ten comets moved above the horizon and Fragment IIa* became visible to the naked eye. The conditions further improved by 7:48, when three additional sungrazers joined IIa*, now more than 10° above the horizon, in becoming visible and from this time on they could be referred to as a swarm.

¹⁴ Not accounting for the effect of forward scattering.

**SWARM OF DAYLIGHT KREUTZ SUNGRAZERS AT FIRST PERIHELION IN AD 363
VIEW FROM LATITUDE OF ANTIOCH: APPEARANCE ON NOVEMBER 15**

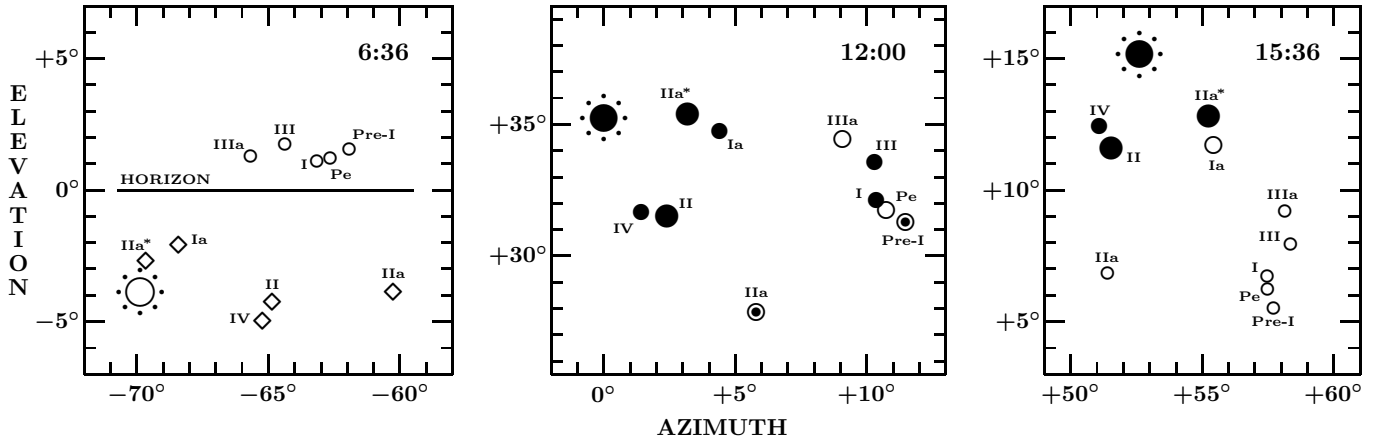


Figure 5. Simulation of the swarm of ten Kreutz sungrazers in projection onto the plane of the sky, viewed, near the Sun, from the latitude of Antioch at, respectively, 6:36, noon, and 15:36 local solar time on 363 November 15. The horizontal coordinate system has the azimuth reckoned positive from the south through the west, the elevation reckoned positive from the horizon to the zenith. The sungrazers' orbital motions and photometric properties are described by the parameters listed in Table 7. The symbols depict each sungrazer's visibility to the naked eye, defined by the index \mathfrak{S} (in magnitudes): large solid circles stand for $\mathfrak{S} > +1.5$ (clearly visible); medium solid circles for $+0.5 < \mathfrak{S} \leq +1.5$ (probably visible); circled dots for $-0.5 \leq \mathfrak{S} \leq +0.5$ (potentially visible); medium open circles for $-1.5 \leq \mathfrak{S} < -0.5$ (probably invisible); small open circles for $\mathfrak{S} < -1.5$ (invisible); and small diamonds for fragments that are below the horizon.

By noon, the number of visible comets grew to the day's peak of six. They were located from 2.6 to 10.4° from the Sun, to the west through south-southwest of it, and as bright as magnitude -11 . It is not surprising that the brightest sungrazer was IIa^* , as it passed perihelion only 8 hours earlier. The second brightest, II , still had more than 1 day to go to perihelion, but its brightness was aided a little by the effect of forward scattering. Additional two pieces were at the limit of visibility. Only IIIa and Pe remained hidden from sight, either being fainter than magnitude -6 at the time.

While in the morning of November 15 the sungrazers rose essentially with the Sun, they all set before sunset in the afternoon. Figure 5 and Table C-1 show that by 15:36 only three remained visible; by 16:48, when the Sun was still almost 3° above the horizon, all but one comet had set and none was visible. Overall, no sungrazer was seen on this date before sunrise or after sunset.

Figure 6 exhibits the noon appearance of the swarm on three days around the time of peak performance, on November 11, 14, and 17. Together with Figure 5 these data constrain the duration of the swarm to at least two days but fewer than seven days, as on November 11 and 17 only two sungrazers were visible.

Figure 7 allows one to inspect the visibility of sungrazers at times long before and/or after the peak in mid-November. It turns out that because of their greater heliocentric distances, the comets were too faint to show *after* sunrise on both November 1 (upper panels) and November 25 (lower panels). However, on both dates three sungrazers were visible over a very limited period of time (less than 1 hour) *before* sunrise very low (about 10°) above the southeastern horizon. The reader will notice that this behavior is exact opposite to the situation on November 15, when no sungrazers could be seen *before* sunrise (Figure 5) but became gradually visible *after* sunrise (Table C-1). However, one should point out that

the effect of a post-perihelion tail, whose presence could potentially increase the brightness dramatically beyond sunrise, has not been taken into consideration in the computations.

Table C-2 presents a picture of the swarm on November 13 and 14, similar to, but more compact than, that on November 15 in Table C-1. On the 13th, the appearance at 7:12 resembled the appearance 48 hr later, except that the single visible sungrazer was Pre-I (which at the time had 1 hr to go to perihelion) rather than IIa^* . By noon, six comets were visible, Pe and I extremely bright and less than 1° from the Sun. By 15:36 the number of visible sungrazers declined by only one.

A swarm of three comets was marginally visible already at 7:12 on the morning of November 14; the Sun was then merely 3° above the horizon. By noon a record seven sungrazers were seen (cf. Figure 6), five of them — Ia , I , IIa^* , III , and IIIa — about equally bright; an eighth piece, Pe , was near the visibility limit. By 15:36 the number of visible sungrazers dropped to four; again, they all had set before sunset.

Table C-3 shows the evolution of the swarm on November 16 and 17. On the 16th at 7:12 there was only one potentially visible sungrazer. By noon Fragment II was by far the brightest, reaching perihelion about 1.5 hr later; also seen were three additional comets and two more potentially. By 15:36, Fragment II was the only visible one. On the 17th, the situation further deteriorated, Fragment II clearly fading though still visible. At noon, only two sungrazers, II and IIa , were clearly visible, surviving through 15:36.

From this review of the five days, November 13–17, it is apparent that the number of visible sungrazers correlates closely with the distribution of their perihelion times. Since seven of the ten comets passed perihelion in the first half of the 4.6 day long period, the number of the visible ones was higher on November 13–14 than on

**SWARM OF DAYLIGHT KREUTZ SUNGRAZERS AT FIRST PERIHELION IN AD 363
VIEW FROM LATITUDE OF ANTIOCH: APPEARANCE AT LOCAL NOON**

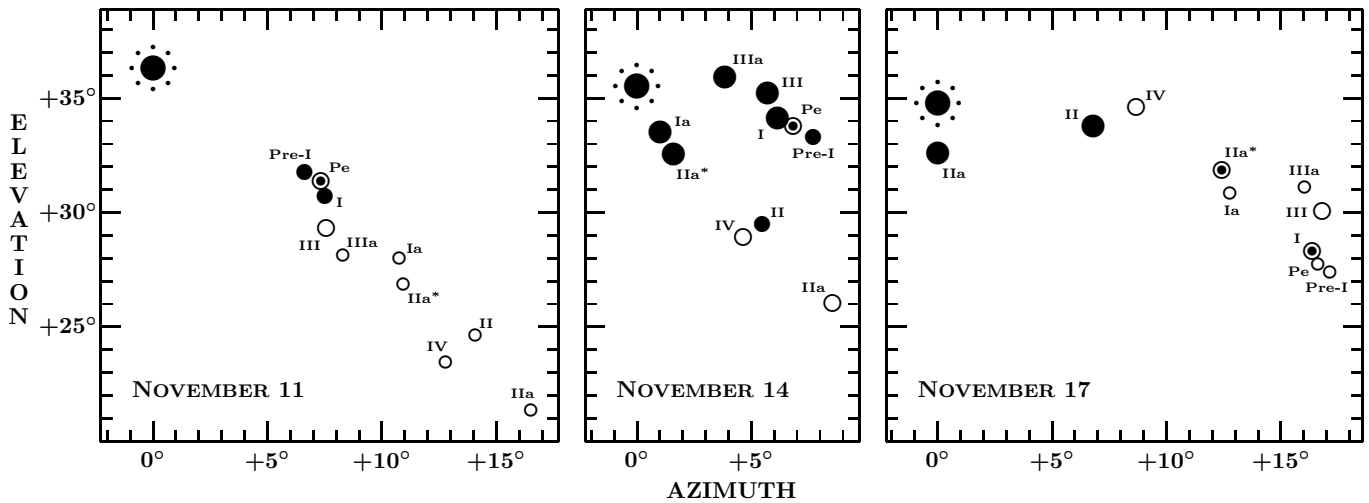


Figure 6. Simulation of the swarm of ten Kreutz sungrazers in projection onto the plane of the sky, viewed, near the Sun, from the latitude of Antioch at local noon on 363 November 11, 14, and 17. See the caption to Figure 5 for more explanation.

November 16–17. As expected, the number is also seen to correlate with the angular distance from the Sun; statistically, most visible sungrazers were very close to the Sun, mostly within 4° or so. Their largest number could be seen for several hours approximately centered on local noon, when the swarm was high enough above the horizon.

The next step was to examine the rising and setting of the swarm over a longer period of time, up to two weeks, before the sungrazers' perihelion times. It turns out that on November 1 (Table C-4 and Figure 7) the comets rose about two hours before the Sun, but their apparent magnitude was only near 0. At 5:24, when the Sun was more than 15° below the horizon, they were just a few degrees above it and the model shows that only one was about 1 mag above the limiting magnitude. The situation was not improving with time; at 6:00 the lesser effect of atmospheric extinction was compensated by advancing twilight. By 6:36, when twilight was nearly over, no sungrazer was visible any longer. By November 7 (Table C-4), the sunrise was lagging behind the sungrazers' rise by only an hour or so and they were not more than a few degrees above the horizon when civil twilight began. The comets were too faint to be seen in broad daylight and they had set long before the Sun. On November 11 (Table C-5), the noon appearance was nearly equivalent to that on November 17 (cf. Figure 6 and Table C-3), with two sungrazers then visible; none of them was visible on November 11 in the morning at 7:12 and 9:00 and in the afternoon at 15:00. Table C-5 also shows that at noon of November 19 only one of the two sungrazers seen two days earlier, Fragment II, was still visible, the brightness of the other (IIa) being marginal.

Examination of the arrangement of the swarm relative to the Sun on November 25 (Table C-6 and Figure 7), some ten days after perihelion, shows that the overall visibility of the sungrazers was comparable to that in the period of time between November 1 and 7. Fragments I and III may have been seen over a fraction of an hour at altitudes of several degrees above the horizon in the

southeast around 6:00 (when the Sun was 12° below the horizon) and Fragment II at an altitude of less than 10° around 6:36 (when the Sun was 5° below the horizon), but either was no longer seen at 7:12, after sunrise (cf. Figure 6). However, as already noted, prominent post-perihelion tails may have already been developed enough to substantially improve the visibility during the day. The sungrazers again set long before sunset, the tails then pointing to the south.

The results of this exercise are summarized in Table 8, which shows that at their first arrival at perihelion, a swarm of Kreutz sungrazers, generated in the framework of the proposed contact-binary model, is capable to produce a spectacle of several brilliant daylight comets, which lasts over a few days, each day for several hours about local noon (when high enough above the horizon). The apparent brightness of at least some of the comets is magnitude -10 or more, exceeding the limiting magnitude for the naked eye by up to about 7 magnitudes. The display could certainly be described by Ammianus' words. The number, distribution, and identities of the sungrazers vary from day to day and even from the morning to late afternoon on each day. The swarm is most impressive on November 13 to 15.

Two weeks before perihelion, at the beginning of November, up to three comets may briefly (for less than an hour) be visible before sunrise very low above the southeastern horizon; they are too faint to remain visible toward the end of twilight, when they are overwhelmed by approaching daylight. In late November the sungrazers may be visible because of the post-perihelion tail development, several of them could continue to be daytime objects, but the prime of the show would move to pre-noon hours, with the tails then pointing toward the horizon. For example, at 10:12 on November 25, five sungrazers with tails more than 5 mag brighter than the head — II, I, III, IIa, and IIa* in the order of decreasing brightness — could be visible at elevations lower than that of the Sun; by 14:30 they all would be below the horizon, their tails preceding them in the southerly direction.

**SWARM OF DAYLIGHT KREUTZ SUNGRAZERS AT FIRST PERIHELION IN AD 363
VIEW FROM LATITUDE OF ANTIOCH**

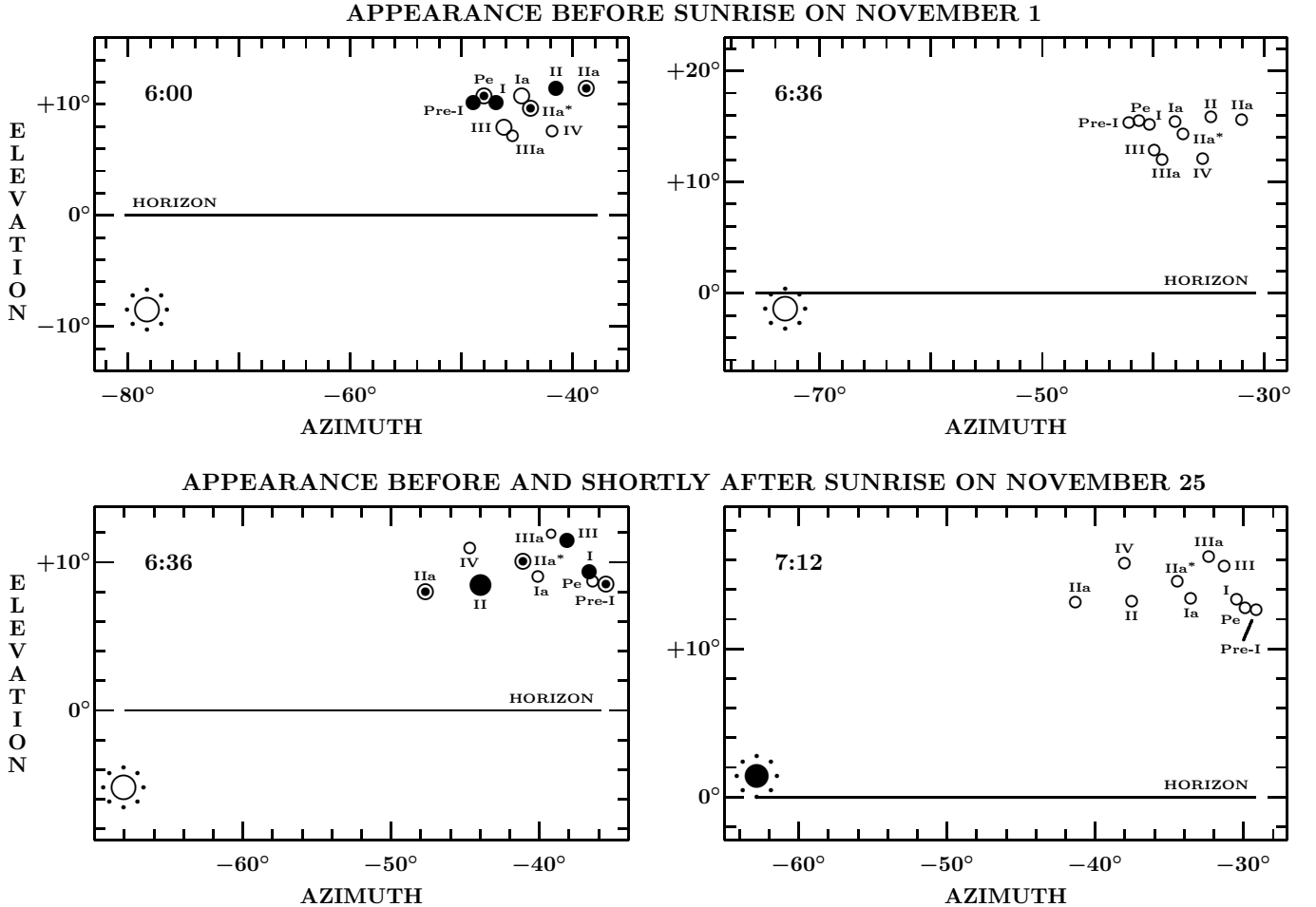


Figure 7. Simulation of the swarm of ten Kreutz sungrazers in projection onto the plane of the sky, viewed from the latitude of Antioch at, respectively, 6:00 and 6:36 local solar time on November 1 (at the top) and at 6:36 and 7:12 local solar time on November 25. See the caption to Figure 5 for more explanation.

7. CONCLUSIONS

The results of this investigation offer the following conclusions:

(1) Even though the developments in the past decade revealed weaknesses of the two-superfragment model, two of its fundamental properties — the progenitor’s fragmentation taking place at large heliocentric distance and the fragments arriving nearly simultaneously at their first perihelion in the mid-4th century AD — are still deemed absolutely essential for reaching a self-consistent solution to the problem of origin and evolution of the Kreutz system, the division into Populations I and II in particular; accordingly, they have been incorporated into the new contact-binary model in Paper 1.

(2) The cascading nature of the fragmentation process, which the Kreutz system is subjected to, is of utmost importance because the fact that a sungrazer can break up at any point of the orbit — rather than at perihelion only — does dramatically boost the fragmentation *rate*, which, in turn, severely curtails the *lifespan* of sungrazers, including the giant ones.

(3) The remark by the Roman historian Ammianus Marcellinus that “in broad daylight comets were seen” in late AD 363 is highly relevant to the problem of the Kreutz system in that (i) the time closely agrees with the perihelion time anticipated by the two-superfragment model; (ii) the plural implies an unrivaled, essentially simultaneous appearance of spectacular daylight comets, a scenario expected for the progenitor’s fragments; and (iii) the timing, halfway between the arrivals of the Aristotle’s comet of 372 BC and the probable Kreutz member X/1106 C1 — with a further link to C/1843 D1 — suggests a periodicity of about 740 years, connecting four generations of sungrazers.

(4) I argue that Ammianus’ remark must have been motivated by a lasting impression that the event left on him and that there is no chance that the spectacle was fabricated by him to serve as a portent. A simultaneous or nearly simultaneous appearance of two or more brilliant comets is historically unprecedented, in broad daylight even more so. It could never have crossed his mind that a celestial show of the kind was at all possible, until he witnessed it. Besides, if fabricating it as a portent,

Table 8
Summary of Kreutz Sungrazers' Visibility in Swarm

Time of appearance		Part of day	Number of visible sungrazers	Best visible sungrazer			List of visible sungrazers (in order of decreasing \mathfrak{S})	
Date of year	hr:min			\mathfrak{S} (mag)	$t-t_\pi$ (d)	Elong, ϵ		
Nov	14.500	12:00	daylight	7	+3.1	-0.68	3°2	IIa*, I, Ia, III, IIIa, Pre-I, II
	13.500	12:00	"	6	+7.1	-0.06	0.4	Pe, I, Pre-I, III, IIIa, IIa*
	15.500	12:00	"	6	+3.5	+0.32	2.6	IIa*, II, I, IV, Ia, III
	13.650	15:36	"	5	+7.8	-0.04	0.4	I, III, Pe, Pre-I, IIIa
	16.500	12:00	"	4	+7.3	-0.06	0.7	II, IIa, IV, IIa*
	15.325	7:48	"	4	+4.2	+0.15	1.4	IIa*, Ia, I, II
	14.650	15:36	"	4	+3.0	-0.35	1.6	Ia, IIa*, I, III
	25.275	6:36	twilight	3	+2.3	+8.72	27.6	II, I, III
	15.650	15:36	daylight	3	+2.0	+0.47	3.5	IIa*, II, IV
	25.250	6:00	twilight	3	+1.9	+11.45	34.1	III, I, II
	1.250	6:00	"	3	+1.0	-12.44	36.0	I, II, Pre-I
	14.300	7:12	daylight	3	+0.8	+0.21	2.0	IIIa, I, III
	17.650	15:36	"	2	+4.2	-0.29	1.6	IIa, II
	17.500	12:00	"	2	+4.0	-0.44	2.2	IIa, II
	1.225	5:24	twilight	2	+1.2	-15.33	41.7	II, IIa
	11.500	12:00	daylight	2	+0.8	-1.84	7.1	Pre-I, I
	16.650	15:36	"	1	+5.2	+0.09	0.8	II
	13.300	7:12	"	1	+5.1	-0.04	0.4	Pre-I
	15.300	7:12	"	1	+2.5	+1.12	1.2	IIa*
	19.375	9:00	"	1	+1.0	+2.82	12.3	II
	19.500	12:00	"	1	+1.0	+2.94	12.7	II
	17.300	7:12	"	1	+0.9	+0.74	4.8	II
	1.275	6:36	twilight	0
	7.275	6:36	"	0
	7.300	7:12	daylight	0
	7.450	10:48	"	0
	11.300	7:12	"	0
	11.375	9:00	"	0
	11.625	15:00	"	0
	15.275	6:36	twilight	0
	15.700	16:48	daylight	0
	16.300	7:12	"	0
	25.300	7:12	"	0
	25.425	10:12	"	0
	25.500	12:00	"	0

Ammianus would certainly have dated the event before the death of his beloved Emperor Julian, not months after it.

(5) Under the circumstances it is beneficial to test whether, or to what extent, could the event noted by Ammianus be broadly consistent with the appearance of a swarm of Kreutz sungrazers. In the modeled scenario, the swarm is generated by a process of cascading fragmentation of the contact-binary progenitor near aphelion of its orbit, the individual fragments arriving at perihelion over a period of a few days in late AD 363.

(6) Inspection of Hasegawa & Nakano's list of potential historical members of the Kreutz system shows a total of seven comets first sighted late in the year, between mid-October and mid-December: 943, 1232, 1381, 1588, 1663, 1666, and 1695 (C/1695 U1). The temporal distribution of their first sightings is strongly skewed toward the early part of the period, late October and early November, apparently an effect of the gradually increasing deep southerly declinations. None of the seven comets appears to have been detected before perihelion.

(7) The apparent magnitude of Halley's comet at times of its preperihelion first sightings recorded in returns before the comet's identity was recognized, starting in 12 BC, is revised. It is shown that the existing brightness limit, based on the comet's inaccurate light curve from the 1910 apparition, is underestimated. A revised calibration, employing the Green & Morris light curve from the 1986 apparition, implies that at times of the first naked-eye sighting, Halley's comet was on the average of an apparent magnitude 2.6, rather than the previously proposed magnitude 3.5 to 4.

(8) Hasegawa & Nakano's assumption that the potential historical Kreutz sungrazers had an apparent magnitude 5 when last sighted with the naked eye after perihelion is significantly off the mark. The magnitude of the head is found instead to have been near 7, because the brightest part of the comet was then its tail, consisting primarily of massive, early post-perihelion emissions of microscopic dust. A week or so after perihelion the tail could be up to 5 magnitudes brighter than the head; at the time of the last naked-eye sighting the difference

could still amount to about 2 magnitudes. The implication is that the intrinsic brightness of the head of potential historical Kreutz sungrazers in the Hasegawa & Nakano paper is significantly overestimated.

(9) Among the bright members of the Kreutz system, the best determined light curve is available for comet Ikeya-Seki. The comet was brightening and fading symmetrically relative to perihelion, following an inverse fourth power of heliocentric distance, with the absolute magnitude of 5.9. Recently published brightness estimates for the Great September Comet of 1882 from New Zealand, combined with the previously available spotty data, suggests that this comet's nuclear condensation brightened on the way to perihelion as an inverse fourth power of heliocentric distance as well. I assume in this paper that the r^{-4} variation is the universal preperihelion light-curve law for all sungrazers comparable with, or exceeding, Ikeya-Seki in intrinsic brightness, including the potential sungrazers on the Hasegawa-Nakano list and the proposed Kreutz comets in AD 363.

(10) Comparison of the light curve of comet Ikeya-Seki with Schaefer's algorithm for the limiting magnitude of a stellar object by the naked eye shows that the comet brightened with decreasing solar elongation less steeply than the limiting magnitude in advanced twilight but more steeply than the limiting magnitude in broad daylight. These findings imply that if Ikeya-Seki had arrived before the era of telescopic comet hunters, the chance of its detection with the naked eye was decreasing from early twilight (when it was modest at best) until the comet was nearing the Sun's disk when, very briefly, the detection probability was up.

(11) Comet Ikeya-Seki would certainly have been discovered with the naked eye days after perihelion when its brilliant tail was rapidly developing. Suddenly blazing into view, this massive dust feature also explains the detection times of the Kreutz candidates on Hasegawa & Nakano's (2001) list that passed perihelion in October–November, even though they were, on the average, intrinsically fainter than Ikeya-Seki. None of them was discovered before perihelion and neither would have been, quite possibly, Ikeya-Seki in the pre-telescope era.

(12) The first naked-eye sighting just days after perihelion appears to be a general rule of a thumb for most historical Kreutz sungrazers, confirming the importance of the post-perihelion tail. The brightest among the bright objects were detected in broad daylight, the rest in twilight. The brightness supremacy of the Great March Comet of 1843, the main surviving fragment of the progenitor's Lobe I (and the largest mass of Population I), and the Great September Comet of 1882, the main surviving fragment of Lobe II (and the largest mass of Population II), is demonstrated by the fact that they are the only two Kreutz sungrazers discovered — in the telescope era — with the naked eye *weeks before perihelion*.¹⁵

(13) Based on the times of their first sightings and expected compliance with the r^{-4} law, the two giant sungrazers are found to have been of equivalent intrinsic brightness when approaching perihelion. Calibrated with the Halley data, the absolute magnitudes come nominally out to be $H_0^- = 3.5$ mag for C/1843 D1 and

$H_0^- = 3.4$ mag for C/1882 R1, with uncertainty greater than the difference.

(14) The dramatically different behavior of the two giant sungrazers after perihelion is attributed to the nuclear fragmentation of the 1882 comet in close proximity of perihelion, while the nucleus of the 1843 comet appeared intact throughout its apparition. In broader terms, this distinction may imply that, as a rule, members of Population II are more susceptible to perihelion fragmentation than members of Population I, a tendency confirmed by other sungrazers, such as Ikeya-Seki and Pereyra (C/1963 R1), as well. The fragmentation of C/1882 R1 resulted in major effects on the comet's post-perihelion light curve (making it distinctly flatter and the absolute magnitude much brighter than before perihelion) as well as on the time of the last sighting (with both the naked eye and telescopically). Indeed, the head of the 1882 sungrazer is known to have been fading after perihelion according to an $r^{-3.3}$ law, its absolute magnitude having reached -0.2 (Sekanina 2002). Its tail was seen with the naked eye for nearly six months after perihelion! The post-perihelion light curve of the nuclear condensation of the 1843 sungrazer shows a rate of fading a little steeper than the inverse fourth power of heliocentric distance. I adopted for this comet an $r^{-4.2}$ law, which combined with the condition for the last sighting with the naked eye implied a post-perihelion absolute magnitude of 4.6, nominally 1.1 mag fainter than before perihelion. The last naked-eye sighting of its tail occurred $1\frac{1}{2}$ months after perihelion.

(15) Based on this limited evidence, I adopted a rule that the post-perihelion light curve of an intrinsically bright Kreutz sungrazer *not fragmenting at perihelion* followed an $r^{-4.2}$ law and that the exponent of the light-curve law got flatter by 0.2 for each additional major secondary nucleus observed. The preperihelion and post-perihelion absolute magnitudes were linked by requiring a smooth light-curve transition at perihelion. This rule was applied to the Kreutz sungrazers in the proposed AD 363 scenario to define their light curves.

(16) The enormous difference between C/1843 D1 and C/1882 R1 in the time of the last sighting with the naked eye is believed to be hereditary, transferred from the parent to its fragments, thereby offering a test of the contentious issue of whether the comet X/1106 C1 — granted it was a Kreutz sungrazer — constituted the previous appearance of the 1843 comet or the 1882 comet. Given that the 1106 comet was seen for only about 50 days, the test unequivocally suggests a close relationship between X/1106 C1 and C/1843 D1. The post-perihelion and preperihelion absolute magnitudes of the 1106 comet were determined under these circumstances to have equaled 4.0 and 2.9, respectively.

(17) The main computations in this study were to simulate a swarm of 10 daylight comets in AD 363, equated with fragments of the Kreutz progenitor modeled as a contact binary. For each fragment I adopted its orbital elements from Paper 1 and assigned it a set of light-curve parameters. November 15.00 was adopted as a reference time, defined by the perihelion passage of the fragmented progenitor's center of mass. The perihelion times of the comets, reckoned from this reference time, were determined by the perturbations produced by the transverse

¹⁵ The apparent discovery of comet C/1843 D1 in early February makes it eligible for the designation C/1843 C1.

component of the separation velocities acquired in a sequence of fragmentation events that marked the birth of each of the 10 sungrazers. The range of their perihelion times was 4.6 days.

(18) Employing approximations to simulate the AD 363 scenario, in particular the use of local solar time to eliminate the dependence on the observing site's geographic longitude and local sidereal time, I determined, for each of the 10 Kreutz sungrazers in the swarm: (i) the horizontal coordinates for the latitude of Antioch on the Orontes, Ammianus' residence at the time, and (ii) the visibility index \mathfrak{S} in terms of Schaefer's limiting magnitude for a stellar object, as a function of the sungrazer's solar elongation and elevation and the Sun's elevation. The outcome was the swarm of sungrazers projected onto the plane of the sky relative to the Sun and the discrimination between the ones that are and are not expected to be naked-eye detectable. The computations were made for every day, starting November 1 and ending November 25, for 25 instances every day, between 4:48 and 19:12 at 36 minute intervals.

(19) The results of this exercise show that, in projection onto the plane of the sky, the Kreutz sungrazers were approaching the Sun from the southwest, passing between the Sun and Earth, and were receding to the west-southwest on the far side of the Sun. Up to seven comets were simultaneously visible with the naked eye when near the Sun and high enough above the horizon. Their number, identity, and arrangement of display varied from day to day, their apparent brightness being up to more than 7 mag above the limiting magnitude for the naked eye. As expected, in most cases the brightest and best seen comets were those within a day or so of their perihelion passage; they were located mostly within a few degrees of the Sun.

(20) The impressive show continued over four or five consecutive days (essentially equaling the range of the sungrazers' perihelion times), the number of visible comets decreasing rather steeply from the peak of the seven on November 14 and six on the 13th and 15th on both earlier and later days. Except when within a few hours of perihelion, the comets always set before sunset. Around November 1 and November 25 a few sungrazers could be seen with the naked eye rather briefly very low above the southeastern horizon in morning twilight, but they disappeared by daybreak.

(21) The tested scenario certainly does not contradict Ammianus' narrative. The narrow range of the perihelion times is obviously the decisive factor in making the swarm of daylight Kreutz sungrazers look compact. To a degree this range depends on the orbital locations of the fragmentation events; if they should occur after aphelion, the degree of compactness of the swarm would still be increased; if before aphelion, the perihelion times of fragments would be spread out over a little longer interval and so would the swarm.

(22) The range of the fragments' perihelion times would grow rapidly — and the swarm of comets would tend to vanish — with increasing magnitude of the separation velocity's radial component, which was in the tested scenario assumed to be nil. A radial velocity as low as 0.1 m s^{-1} would change a perihelion time by about 5 days, so that a systematic effect of this or greater magnitude in several consecutive fragmentation

events could easily extend the range of perihelion times over months, in which case it is highly unlikely that Ammianus would use the plural in his remark. The individual sungrazers would arrive at perihelion far apart from one another and their close physical relationship would be harder to recognize.

This research was carried out at the Jet Propulsion Laboratory under contract with the National Aeronautics and Space Administration.

Appendix A

EFFECTS OF THE SEPARATION VELOCITY OF A DETACHING FRAGMENT ON ITS ORBITAL ELEMENTS

Let a Kreutz sungrazer move about the Sun unaffected by an outgassing-driven nongravitational acceleration and/or the planetary perturbations, and let its orbit be determined by the argument of perihelion ω , the longitude of the ascending node Ω , the inclination i , the perihelion distance q , and the orbital period P . Let the comet pass through perihelion at time t_0 and break up at time t_{frg} , where $t_0 \leq t_{\text{frg}} < t_\pi$ and t_π is the time of next perihelion, $t_\pi = t_0 + P$. Let the comet's heliocentric distance and true anomaly at t_{frg} be, respectively, $r(t_{\text{frg}}) = r_{\text{frg}}$ and $u(t_{\text{frg}}) = u_{\text{frg}}$. The outcome of the breakup event is the birth of a fragment that separates at a rate of V_{sep} , usually on the order of 1 m s^{-1} , from the main mass whose orbital motion is deemed unaffected by the fragmentation episode.

Next, I introduce an RTN right-handed orthogonal coordinate system, whose origin is in the center of mass of the primary, the R axis pointing radially away from the Sun, the T axis in the orbital plane, and the N axis normal to this plane. Let the components of the fragment's separation velocity vector \mathbf{V}_{sep} in the cardinal directions of the RTN system be V_R , V_T , and V_N . This velocity vector prompts the fragment to get into a new orbit, determined by the asterisk-labeled elements

$$\begin{aligned}\omega^* &= \omega + \Delta\omega(\mathbf{V}_{\text{sep}}), \\ \Omega^* &= \Omega + \Delta\Omega(\mathbf{V}_{\text{sep}}), \\ i^* &= i + \Delta i(\mathbf{V}_{\text{sep}}), \\ q^* &= q + \Delta q(\mathbf{V}_{\text{sep}}), \\ P^* &= P + \Delta P(\mathbf{V}_{\text{sep}}), \\ t_\pi^* &= t_\pi + \Delta t_\pi(\mathbf{V}_{\text{sep}}).\end{aligned}\tag{A-1}$$

The aim of this exercise is to derive $\Delta\omega, \dots, \Delta t_\pi$ as a function of the separation velocity vector \mathbf{V}_{sep} .

To undertake this task, I begin with the determination of the primary comet's position vector (\mathbf{S}_{frg}) and orbital-velocity vector (\mathbf{U}_{frg}) at the fragmentation time, t_{frg} , in the ecliptic coordinates:

$$\mathbf{S}_{\text{frg}} = (x_{\text{frg}}, y_{\text{frg}}, z_{\text{frg}}), \quad \mathbf{U}_{\text{frg}} = (\dot{x}_{\text{frg}}, \dot{y}_{\text{frg}}, \dot{z}_{\text{frg}}).\tag{A-2}$$

They are given by the expressions:

$$\begin{pmatrix} x_{\text{frg}} \\ y_{\text{frg}} \\ z_{\text{frg}} \end{pmatrix} = r_{\text{frg}} \begin{pmatrix} P_x & Q_x \\ P_y & Q_y \\ P_z & Q_z \end{pmatrix} \times \begin{pmatrix} \cos u_{\text{frg}} \\ \sin u_{\text{frg}} \end{pmatrix},\tag{A-3}$$

and

$$\begin{pmatrix} \dot{x}_{\text{frg}} \\ \dot{y}_{\text{frg}} \\ \dot{z}_{\text{frg}} \end{pmatrix} = \frac{k_0}{\sqrt{p}} \begin{pmatrix} P_x & Q_x \\ P_y & Q_y \\ P_z & Q_z \end{pmatrix} \times \begin{pmatrix} -\sin u_{\text{frg}} \\ e + \cos u_{\text{frg}} \end{pmatrix}, \quad (\text{A-4})$$

where the directional cosines P_x, \dots, Q_z , are, together with R_x, R_y , and R_z (employed below), the components of the unit vectors \mathbf{P} , \mathbf{Q} , and \mathbf{R} in the orthogonal coordinate system tied to the orbital plane and the line of apsides:

$$\begin{pmatrix} P_x & P_y & P_z \\ Q_x & Q_y & Q_z \\ R_x & R_y & R_z \end{pmatrix} = \begin{pmatrix} \cos \omega & \sin \omega & 0 \\ -\sin \omega & \cos \omega & 0 \\ 0 & 0 & 1 \end{pmatrix} \\ \times \begin{pmatrix} 1 & 0 & 0 \\ 0 & \cos i & \sin i \\ 0 & -\sin i & \cos i \end{pmatrix} \times \begin{pmatrix} \cos \Omega & \sin \Omega & 0 \\ -\sin \Omega & \cos \Omega & 0 \\ 0 & 0 & 1 \end{pmatrix}. \quad (\text{A-5})$$

At the time of separation, t_{frg} , the position vector of the fragment, $\mathbf{S}_{\text{frg}}^*$, coincides with the primary's position vector, while the fragment's orbital-velocity vector, $\mathbf{U}_{\text{frg}}^*$, is the sum of the primary's orbital-velocity vector and the fragment's separation velocity vector, whose ecliptic components are denoted by V_x, V_y , and V_z ,

$$\begin{pmatrix} x_{\text{frg}}^* \\ y_{\text{frg}}^* \\ z_{\text{frg}}^* \end{pmatrix} = \begin{pmatrix} x_{\text{frg}} \\ y_{\text{frg}} \\ z_{\text{frg}} \end{pmatrix}, \quad \begin{pmatrix} \dot{x}_{\text{frg}}^* \\ \dot{y}_{\text{frg}}^* \\ \dot{z}_{\text{frg}}^* \end{pmatrix} = \begin{pmatrix} \dot{x}_{\text{frg}} \\ \dot{y}_{\text{frg}} \\ \dot{z}_{\text{frg}} \end{pmatrix} + \begin{pmatrix} V_x \\ V_y \\ V_z \end{pmatrix}. \quad (\text{A-6})$$

The ecliptic components of the separation velocity vector are related to its components in the RTN coordinate system by

$$\begin{pmatrix} V_x \\ V_y \\ V_z \end{pmatrix} = \begin{pmatrix} P_x & Q_x & R_x \\ P_y & Q_y & R_y \\ P_z & Q_z & R_z \end{pmatrix} \times \begin{pmatrix} \cos u_{\text{frg}} & -\sin u_{\text{frg}} & 0 \\ \sin u_{\text{frg}} & \cos u_{\text{frg}} & 0 \\ 0 & 0 & 1 \end{pmatrix} \times \begin{pmatrix} V_R \\ V_T \\ V_N \end{pmatrix}. \quad (\text{A-7})$$

One is now ready to initiate the determination of the fragment's orbital elements by introducing the angular-momentum vector components:

$$\mathfrak{S}_{xy} = \begin{vmatrix} x_{\text{frg}} & y_{\text{frg}} \\ \dot{x}_{\text{frg}}^* & \dot{y}_{\text{frg}}^* \end{vmatrix}, \\ \mathfrak{S}_{yz} = \begin{vmatrix} y_{\text{frg}} & z_{\text{frg}} \\ \dot{y}_{\text{frg}}^* & \dot{z}_{\text{frg}}^* \end{vmatrix}, \\ \mathfrak{S}_{zx} = \begin{vmatrix} z_{\text{frg}} & x_{\text{frg}} \\ \dot{z}_{\text{frg}}^* & \dot{x}_{\text{frg}}^* \end{vmatrix}. \quad (\text{A-8})$$

The following computations allow to incorporate, if deemed desirable, a nongravitational acceleration into the orbital motion of the fragment on the assumptions that it points in the antisolar direction and varies inversely as the square of heliocentric distance, the constraints employed by Hamid & Whipple (1953) in their investigation and likewise integrated into the standard model for the split comets (Sekanina 1982). Let k_0 be the Gaussian gravitational constant expressed in $\text{AU}^{\frac{3}{2}} \text{day}^{-1}$ and γ_0 a dimensionless parameter that describes the fragment's nongravitational acceleration in units of 10^{-5} the Sun's gravitational acceleration. The fragment's *effective* Gaussian gravitational constant k_0^* , which replaces

k_0 below, is equal to

$$k_0^* = \sqrt{k_0^2 - 10^{-5} \gamma_0 k_0^2} = k_0 \sqrt{1 - 10^{-5} \gamma_0}. \quad (\text{A-9})$$

The fragment's longitude of the ascending node, Ω^* , inclination, i^* , and semilatus rectum, p^* , related to the perihelion distance, q^* , via the orbital eccentricity, e^* , by $p^* = q^*(1+e^*)$, follow from the relations,

$$\begin{pmatrix} \mathfrak{S}_{xy} \\ \mathfrak{S}_{yz} \\ \mathfrak{S}_{zx} \end{pmatrix} = k_0^* \sqrt{p^*} \begin{pmatrix} \cos i^* \\ \sin \Omega^* \sin i^* \\ -\cos \Omega^* \sin i^* \end{pmatrix}. \quad (\text{A-10})$$

For the longitude of the ascending node one finds

$$\tan \Omega^* = -\frac{\mathfrak{S}_{yz}}{\mathfrak{S}_{zx}}, \quad \text{sign}(\sin \Omega^*) = \text{sign}(\mathfrak{S}_{yz}); \quad (\text{A-11})$$

for the inclination

$$\tan i^* = \frac{\sqrt{\mathfrak{S}_{yz}^2 + \mathfrak{S}_{zx}^2}}{\mathfrak{S}_{xy}}, \quad (\text{A-12})$$

where the sign of the denominator determines the quadrant of the inclination; and for the semilatus rectum

$$p^* = \frac{\mathfrak{S}_{xy}^2 + \mathfrak{S}_{yz}^2 + \mathfrak{S}_{zx}^2}{(k_0^*)^2}. \quad (\text{A-13})$$

Next, the fragment's orbital eccentricity is

$$e^* = \sqrt{1 + p^* \left\{ \frac{1}{(k_0^*)^2} \left[(\dot{x}_{\text{frg}}^*)^2 + (\dot{y}_{\text{frg}}^*)^2 + (\dot{z}_{\text{frg}}^*)^2 \right] - \frac{2}{r_{\text{frg}}} \right\}}, \quad (\text{A-14})$$

so that the perihelion distance comes out from

$$q^* = \frac{p^*}{1+e^*} \quad (\text{A-15})$$

and the orbital period from

$$P^* = \frac{2\pi}{k_0^*} \left(\frac{q^*}{1-e^*} \right)^{\frac{3}{2}}. \quad (\text{A-16})$$

The fragment's true anomaly at the time of separation from the primary is given by

$$\sin u_{\text{frg}}^* = \frac{\sqrt{p^*}}{k_0^* e^* r_{\text{frg}}} (x_{\text{frg}} \dot{x}_{\text{frg}}^* + y_{\text{frg}} \dot{y}_{\text{frg}}^* + z_{\text{frg}} \dot{z}_{\text{frg}}^*) \quad (\text{A-17})$$

with $\text{sign}(\cos u_{\text{frg}}^*) = \text{sign}(p^* - r_{\text{frg}})$. The argument of perihelion is involved with the true anomaly at separation by

$$\cos(\omega^* + u_{\text{frg}}^*) = \frac{x_{\text{frg}} \cos \Omega^* + y_{\text{frg}} \sin \Omega^*}{r_{\text{frg}}} \quad (\text{A-18})$$

with $\text{sign}[\sin(\omega^* + u_{\text{frg}}^*)] = \text{sign}(z_{\text{frg}})$. Equations (A-17) and (A-18) isolate the argument of perihelion. Finally, to derive the fragment's next perihelion time, t_{π}^* , one first gets the eccentric anomaly at separation, ϵ_{frg}^* ,

$$\epsilon_{\text{frg}}^* = 2 \arctan \left(\sqrt{\frac{1-e^*}{1+e^*}} \tan \frac{1}{2} u_{\text{frg}}^* \right), \quad (\text{A-19})$$

which provides the following relation for the time of the fragment's next perihelion passage:

$$t_{\pi}^* = t_{\text{frg}} - \frac{\epsilon_{\text{frg}}^* - e^* \sin \epsilon_{\text{frg}}^*}{k_0^*} \left(\frac{q^*}{1 - e^*} \right)^{\frac{3}{2}}. \quad (\text{A-20})$$

The eccentric anomaly ϵ_{frg}^* in this equation is in radians and for fragmentation times t_{frg} between t_0 and t_{π}^* its range is $-2\pi \leq \epsilon_{\text{frg}}^* \leq 0$. Inserting ω^* , \dots , t_{π}^* into (A-1) completes the derivation of the effects of the fragment's separation velocity on its orbital elements.

Appendix B

ANCIENT ANTIOCH: THE CITY, GEOGRAPHY, AND LOCAL HORIZON

The ancient city of Antioch ($\lambda\nu\tau\iota\acute{o}\chi\epsilon\iota\alpha$) was located on the site of the modern city of Antakya, the capital of the Hatay Province, Turkey, at latitude $36^{\circ}.2\text{N}$ and longitude $36^{\circ}.2\text{E}$.

In a mountainous terrain and near the border with Syria to the east and south, the location is a fertile valley on the river Orontes, which flows through the municipality from the north-northeast to the south-southwest (albeit with numerous minor bends), eventually feeding the Levantine Sea, the easternmost part of the Mediterranean. Antioch's distance from the sea is 17 km.

The Antioch valley is surrounded, on the north side, by Mount Amanus, which is connected to the Taurus range

further north, and, on the south side, by the Mount Casius (also Kel Dağı or Jebel al-Aqra) range (peaking at 1700 meters), which terminates, just to the southeast and east of the city, by a 440-meter high triple-peaked hill, extending parallel to the valley and known in the antiquity as Mount Silpius (now Habib-i Neccar). This geography is clearly apparent from Figure B-1, a satellite image of the area. Although the valley between the mountains is about 16 km long and 8 km wide, the city of Antioch is said to have been built on the eastern side of the river, in part at the very foot of Mount Silpius, covering in the early period an area of about 4.5 km^2 , its extent apparently growing with time.

Completed in the 1st century AD was a nearly 20 km long defensive wall, encircling the entire city and climbing, on the eastern side, the slopes of Mount Silpius. Along the entire length of the wall, separated from one another by about 100–150 meters, were multi-storied bastions staffed by mercenaries and at the summit of Mount Silpius the rampart was dominated by a fortified citadel that was overlooking the city. A panorama of Antioch and the surrounding area in the early 19th century — with the commanding appearance of Mount Silpius and clear evidence of the surviving wall with the bastions, especially its southern sector, and the citadel — is displayed in Figure B-2 (Bartlett 1836), while a view of the modern city of Antakya is offered in Figure B-3.

With the city at an altitude of 70 meters and Mount Silpius summit at 440 meters, the eastern and southeastern horizon of Antioch was greatly elevated. This applied to a wide range of azimuths, as Figure B-2 shows that the ridge connecting the three peaks was not significantly depressed. For example, the city's locations that were about 3 kilometers distant from the foot of Mount Silpius, objects in the eastern and southeastern sky at elevations of up to $\arctan[(440 - 70)/3000] = 7^{\circ}$ remained unobservable, hidden behind the hill. For locations closer to the hill, the horizon's elevation at the critical azimuths rose rapidly; at 1 kilometer from the hill the horizon was at 20° ! It happens that the southeastern azimuths are exactly the directions at which the Kreutz sungrazers are computed to have briefly been visible in twilight, just a few degrees above the ideal horizon, more than a week or so before or after the time of the spectacle's anticipated peak performance. It is obvious that Ammianus was prevented by Mount Silpius from seeing the Kreutz sungrazers low in the southeastern sky even if the observing conditions were otherwise favorable. By contrast, the southwestern horizon was essentially unobstructed.

By strange coincidences, Antioch appears to be related, one way or another, to what I consider three generations of the Kreutz sungrazers. Besides the spectacle of AD 363, Antioch is obliquely linked to the comet of 372 BC, known as Aristotle's comet, as the city was founded by Seleucus I. Nicator, a former general in the army of Aristotle's former student, Alexander the Great. There is also an indirect connection between Antioch and the probable Kreutz sungrazer of the third generation, the Great Comet of 1106, by virtue of the city's becoming a Crusader state in 1098. Both the comet and Antioch, especially its conquest, were, side by side, commented on in *Historia Hierosolymitana* (History of Jerusalem) and other Crusader chronicles (e.g., by Fulcher of Chartres; see Ryan 1969).

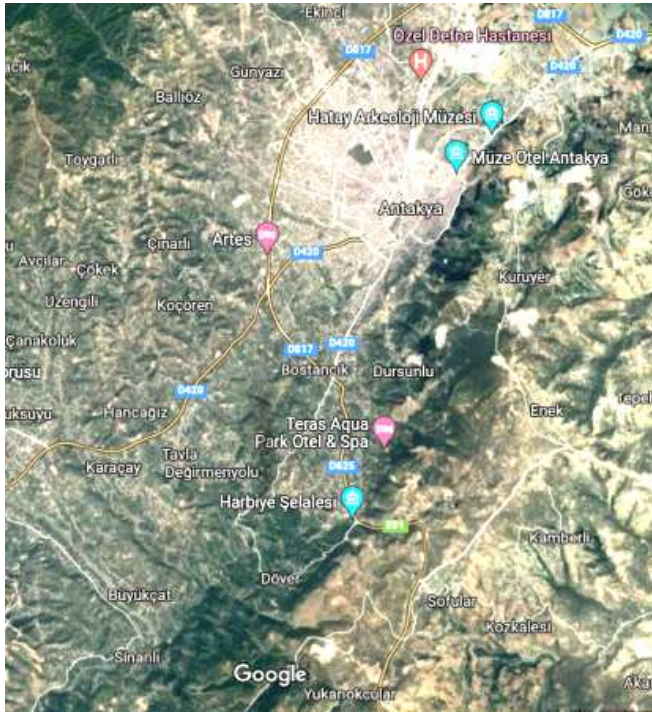


Figure B-1. Satellite image of the city of Antakya and its environs. North is up, east to the left. The diagonal measures about 26 km. The dark green elongated feature just to the city's east and southeast, extending from the north-northeast to the south-southwest is Mount Silpius. The river Orontes, flowing through the city also from the north-northeast to the south-southwest, is too narrow to show on this scale.



Figure B-2 (top). Antioch on the Orontes and Mount Silpius in the early 19th century, seen in a close-up picture made at a location in the city's southwestern suburb. The artist's line of sight subtends a small angle with the direction along which the hill extends, making its main dimension project greatly foreshortened. Note the southern section of the defensive wall on the right, climbing up the slopes of the hill, and the citadel at the summit on the upper left. (W. H. Bartlett 1836; steel engraved print). **Figure**

B-3 (bottom). The modern city of Antakya, with Mount Silpius (Habib-i Neccar) in the background, displayed in a photograph taken from a more distant location to the northwest of downtown. Unlike in Figure B-2, the hill now projects broadside. Note the river Orontes (Asi Nehri) in the foreground.

Appendix C

TABULATION OF POSITIONAL AND VISIBILITY MODELS FOR SWARM OF KREUTZ SUNGRAZERS SIMULATING AMMIANUS' DAYLIGHT COMETS IN AD 363

Below is a series of six tables, C-1 through C-6, showing the positional and brightness predictions for the ten Kreutz sungrazers in a swarm, used to simulate Ammi-*anus' comets seen in broad daylight*. The positions are compared with that of the Sun. Each of Tables C-1 through C-5 consists of six sections, Table C-6 of five sections. Each section provides computed data for a particular time of appearance on a particular date, arranged into 12 columns, which offer:

- (1) date of appearance in local solar time (LST);
- (2) hour and minute LST;
- (3) object identification — the Sun or a sungrazer;
- (4) difference — time of appearance minus perihelion time (days);
- (5) azimuth, reckoned positive from the south to the west (deg);
- (6) elevation, reckoned positive from the flat local horizon toward the zenith (deg);
- (7) solar elongation (deg);
- (8) zenithal position angle, reckoned positive clockwise from the direction to zenith (deg);
- (9) phase angle, Sun-comet-Earth (deg);
- (10) apparent magnitude, computed from the light-curve parameters in Table 7;
- (11) Schaefer's (1998) limiting magnitude, derived as described in the text;
- (12) visibility index, defined by Eq. (17) as a difference of columns 11 and 10 (mag).

For the Sun, only columns 1–3 and 5–6 are relevant. For the sungrazers, columns 5, 6, 8, and 11 refer to the latitude of Antioch, but to an arbitrary longitude. The sidereal time is defined by Eq. (20), an approximation.

Table C-1 provides the data on the swarm appearance for six times on November 15. The first time is 6:36 (civil twilight), when five sungrazers were above the horizon (none visible to the naked eye) and five below it. The average solar elongation, $\langle\epsilon\rangle$, of the five comets above the horizon is $8^\circ.3$, their average visibility index, $\langle\mathfrak{S}\rangle$, is -8.5 mag. The second time is 7:12 (daylight from now on), when all ten sungrazers were above the horizon, one visible with the naked eye ($\mathfrak{S} > +0.5$ mag); $\langle\epsilon\rangle = 6^\circ.4$ and $\langle\mathfrak{S}\rangle = -3.4$ mag. By the next time, 7:48, four sungrazers were visible with the naked eye, $\langle\epsilon\rangle = 6^\circ.5$, $\langle\mathfrak{S}\rangle = 0.0$ mag. At noon, the fourth time, six sungrazers could be seen, $\langle\epsilon\rangle = 6^\circ.8$ and $\langle\mathfrak{S}\rangle = +0.8$ mag. By 15:36 only two sungrazers remained visible, $\langle\epsilon\rangle = 7^\circ.1$ and $\langle\mathfrak{S}\rangle = -1.6$ mag. At the last tabulated time, 16:48, minutes before sunset, only a single sungrazer was just barely above horizon.

Table C-2 lists the data for three particular times on November 13 and 14 each. The first time on both dates is 7:12. On the 13th all comets as well as the Sun were at this time at elevations between $2^\circ.4$ and $4^\circ.2$ and only one sungrazer was visible with the naked eye. Average solar elongation and visibility index were $6^\circ.3$ and -3.9 mag.

Six sungrazers were visible at noon, when $\langle\epsilon\rangle = 5^\circ.8$ and $\langle\mathfrak{S}\rangle = +2.0$ mag. At 15:36 the numbers were five comets, $5^\circ.5$, and -1.0 mag.

The next day, November 14, at 7:12 the number of visible sungrazers equaled three, while the two averages were $\langle\epsilon\rangle = 5^\circ.7$ and $\langle\mathfrak{S}\rangle = -3.5$ mag. At 12:00 the number of visible comets peaked at seven, with $\langle\epsilon\rangle = 5^\circ.8$ and $\langle\mathfrak{S}\rangle = +1.4$ mag. By 15:36 the number of visible sungrazers dropped to four, the average solar elongation continued to climb to $5^\circ.9$ and the average visibility index was down to -0.6 mag.

Table C-3 covers the dates November 16 and 17. The number of displayed sungrazers was clearly on a downturn. On the 16th, no comet was visible at 7:12, four at 12:00, and one at 15:36. The average solar elongations at the three times were, respectively, $8^\circ.2$, $8^\circ.6$, and $9^\circ.0$, indicating that most sungrazers were clearly receding from the Sun; the visibility index equaled, respectively, -3.1 mag, $+0.4$ mag, and -3.8 mag.

The trend continued on November 17. Although one comet was visible at 7:12, the average visibility index declined by 0.5 mag to -3.6 mag and $\langle\epsilon\rangle = 10^\circ.8$. At noon and 15:36 one could see the same two sungrazers (II and IIa, which were close to their perihelia). At 12:00 the averages $\langle\epsilon\rangle$ and $\langle\mathfrak{S}\rangle$ were, respectively, $11^\circ.4$ and -0.7 mag. Even though the Sun was still about 15° above the horizon at 15:36, one sungrazer already set and three others were about to set. This strongly affected the visibility index, whose average for the nine comets was -9.2 mag, while $\langle\epsilon\rangle = 11^\circ.2$.

Table C-4 provides data for a pair of dates long before the spectacle reached its peak. The comets were too faint to be visible in broad daylight, but they had risen before the Sun over the southeastern horizon. For November 1 I list the swarm appearance at 5:24 in astronomical twilight, at 6:00 in nautical twilight, and at 6:36 in civil twilight. Two sungrazers were visible to the naked eye in astronomical twilight, three in nautical twilight, but none in civil twilight, the changes being due to the interplay between atmospheric extinction (peaking in the first case) and increasing interference from sunlight (peaking in the last case). The average solar elongations varied insignificantly, equaling $38^\circ.3$, $38^\circ.2$, and $38^\circ.1$. On the other hand, the average visibility index showed a peak in nautical twilight, the numbers at the three times being -1.8 , -0.3 , and -4.2 mag, respectively.

By November 7, much of the edge relative to the Sun in elevation, enjoyed by the sungrazers six days earlier, was lost. This is seen clearly in their positions on the two dates at 6:36, both in civil twilight. The outcome of this difference is that, even though closer to the time of the best display, no sungrazer was visible on November 7. The average visibility index was then -4.6 mag at 6:36, -5.8 mag at 7:12, and -4.3 mag at 10:48. The average solar elongations at the three times were, respectively, $24^\circ.5$, $24^\circ.4$, and $24^\circ.0$.

Table C-5 describes the appearance of the swarm at selected times on November 11 and 19. On the first date two sungrazers were visible at noon, but none at 7:12, 9:00, and again at 15:00. The average solar elongations and visibility indices were $12^\circ.9$ and -5.4 mag at 7:12; $12^\circ.7$ and -1.9 mag at 9:00; $12^\circ.4$ and -1.5 mag at 12:00; and $12^\circ.0$ and -4.5 mag at 15:00.

Table C-1

Swarm of Daylight Kreutz Sungrazers at First Perihelion in AD 363, Viewed from Latitude of Antioch: Appearance on November 15

Time of appearance		Sun or sun- grazer	Time from perihelion (days)	Azimuth \mathcal{A}	Elevation \mathcal{E}	Solar elonga- tion, ϵ	Zenithal position angle, P_Z	Phase angle, ψ	Apparent magnitude, H (mag)	Limiting magnitude, H_{lim} (mag)	Visibility index, \mathfrak{S} (mag)
Date	LST hr:min										
Nov 15.275	6:36	Sun	-69°87	-3°86
		Ia	+0.27	-68.43	-2.07	2°30	38°8	79°24	(-9.9)
		I	+1.59	-63.16	+1.12	8.35	53.5	93.84	-8.1	-16.9	-8.8
		II	-1.28	-64.86	-4.27	5.01	94.9	135.37	(-9.2)
		Pre-I	+1.93	-61.93	+1.56	9.60	55.8	93.75	-6.2	-13.7	-7.5
		Pe	+1.71	-62.65	+1.22	8.82	54.9	94.19	-5.4	-16.1	-10.7
		Ia	-2.66	-60.26	-3.88	9.59	90.4	125.74	(-6.1)
		Ia*	+0.10	-69.67	-2.96	0.93	12.1	64.37	(-14.9)
		III	+1.48	-64.38	+1.74	7.84	44.5	88.52	-7.5	-13.4	-5.9
		IIIa	+1.19	-65.68	+1.29	6.63	39.2	103.63	-6.3	-15.7	-9.4
		IV	-0.84	-65.23	-4.97	4.75	103.6	116.41	(-6.8)
Nov 15.300	7:12	Sun	-64.56	+2.83
		Ia	+0.30	-62.90	+4.65	2.46	42.4	80.49	-9.6	-10.7	-1.1
		I	+1.61	-57.48	+7.47	8.44	56.4	93.88	-8.0	-8.6	-0.6
		II	-1.26	-59.69	+2.13	4.92	98.1	135.57	-9.3	-15.7	-6.4
		Pre-I	+1.96	-56.22	+7.82	9.69	58.7	93.77	-6.2	-8.5	-2.3
		Pe	+1.74	-56.97	+7.54	8.91	57.8	94.21	-5.4	-8.6	-3.2
		Ia	-2.64	-55.07	+2.23	9.51	93.4	125.86	-6.1	-15.3	-9.2
		Ia*	+0.12	-64.16	+3.91	1.15	20.4	69.66	-14.2	-11.7	+2.5
		III	+1.50	-58.67	+8.17	7.94	47.4	99.54	-7.4	-8.3	-0.9
		IIIa	+1.21	-60.01	+7.80	6.73	42.2	103.65	-6.3	-8.5	-2.2
		IV	-0.81	-60.12	+1.47	4.65	106.9	116.45	-7.5	-18.3	-10.8
Nov 15.325	7:48	Sun	-58.87	+9.22
		Ia	+0.32	-56.93	+11.02	2.62	46.6	81.58	-9.3	-8.3	+1.0
		I	+1.64	-51.29	+13.41	8.53	59.9	93.92	-8.0	-7.1	+0.9
		II	-1.23	-54.09	+8.20	4.84	101.9	135.76	-9.4	-8.7	+0.7
		Pre-I	+1.98	-49.99	+13.66	9.77	62.2	93.79	-6.2	-7.0	-0.8
		Pe	+1.76	-50.76	+13.43	9.00	61.3	94.24	-5.3	-7.1	-1.8
		Ia	-2.61	-49.42	+7.96	9.43	97.0	125.98	-6.2	-8.6	-2.4
		Ia*	+0.15	-58.23	+10.43	1.37	27.7	73.52	-13.6	-9.4	+4.2
		III	+1.53	-52.45	+14.21	8.03	51.0	99.57	-7.3	-7.0	+0.3
		IIIa	+1.24	-53.84	+13.94	6.82	45.8	103.68	-6.2	-7.1	-0.9
		IV	-0.79	-54.59	+7.58	4.54	110.8	116.48	-7.6	-9.0	-1.4
Nov 15.500	12:00	Sun	0.00	+35.26
		Ia	+0.50	+4.40	+34.75	3.64	96.9	86.57	-8.0	-7.2	+0.8
		I	+1.81	+10.35	+32.13	9.16	107.1	94.13	-7.7	-6.3	+1.4
		II	-1.06	+2.39	+31.53	4.23	151.2	137.18	-9.9	-7.2	+2.7
		Pre-I	+2.16	+11.47	+31.30	10.36	109.2	93.88	-5.9	-6.2	-0.3
		Pe	+1.94	+10.73	+31.74	9.61	108.5	94.39	-5.0	-6.3	-1.3
		Ia	-2.44	+5.79	+27.87	8.88	144.7	126.84	-6.4	-6.5	-0.1
		Ia*	+0.32	+3.19	+35.41	2.61	85.9	85.83	-11.3	-7.8	+3.5
		III	+1.70	+10.29	+33.55	8.66	98.5	99.67	-7.1	-6.3	+0.8
		IIIa	+1.41	+9.07	+34.44	7.48	93.7	103.78	-5.8	-6.4	-0.6
		IV	-0.61	+1.42	+31.65	3.80	161.4	116.52	-8.4	-7.3	+1.1
Nov 15.650	15:36	Sun	+52.61	+15.16
		Ia	+0.65	+55.43	+11.71	4.41	141.2	88.97	-7.2	-8.3	-1.1
		I	+1.96	+57.47	+6.74	9.68	150.0	94.26	-7.5	-9.5	-2.0
		II	-0.91	+51.53	+11.61	3.70	196.6	138.50	-10.5	-8.8	+1.7
		Pre-I	+2.31	+57.70	+5.52	10.86	152.0	93.92	-5.8	-10.3	-4.5
		Pe	+2.09	+57.48	+6.24	10.12	151.3	94.47	-4.8	-9.8	-5.0
		Ia	-2.29	+51.40	+6.83	8.41	188.2	127.60	-6.6	-9.6	-3.0
		Ia*	+0.47	+55.24	+12.80	3.48	132.5	89.93	-10.3	-8.3	+2.0
		III	+1.85	+58.35	+7.90	9.18	141.6	99.70	-6.8	-9.0	-2.2
		IIIa	+1.56	+58.14	+9.22	8.03	137.1	103.81	-5.5	-8.5	-3.0
		IV	-0.46	+51.08	+12.42	3.12	208.7	116.15	-9.2	-8.6	+0.6
Nov 15.700	16:48	Sun	+64.49	+2.76
		Ia	+0.70	+66.86	-1.24	4.65	149.4	89.56	(-7.0)
		I	+2.01	+68.23	-6.35	9.85	157.7	94.30	(-7.5)
		II	-0.86	+62.98	-0.42	3.53	205.4	138.96	(-10.7)
		Pre-I	+2.36	+68.31	-7.58	11.02	159.8	93.93	(-5.7)
		Pe	+2.14	+68.18	-6.84	10.29	159.0	94.49	(-4.8)
		Ia	-2.24	+62.18	-5.16	8.26	196.2	127.85	(-6.7)
		Ia*	+0.52	+66.84	-0.15	3.75	141.1	90.84	(-10.0)
		III	+1.90	+69.24	-5.29	9.35	149.5	99.71	(-6.8)
		IIIa	+1.61	+69.20	-3.96	8.21	145.0	103.81	(-5.4)
		IV	-0.41	+62.70	+0.51	2.88	218.4	115.87	-9.5	-26.8	-17.3

Table C-2

Swarm of Daylight Kreutz Sungrazers at First Perihelion in AD 363, Viewed from Latitude of Antioch: Appearance on November 13–14

Time of appearance		Sun or sun- grazer	Time from perihelion (days)	Azimuth \mathcal{A}	Elevation \mathcal{E}	Solar elonga- tion, ϵ	Zenithal position angle, P_Z	Phase angle, ψ	Apparent magnitude, H (mag)	Limiting magnitude, H_{lim} (mag)	Visibility index, \mathfrak{S} (mag)		
Date	LST											hr:min	
Nov 13.300	7:12	Sun	-64°97	+3°16		
		Ia	-1.70	-58.45	+3.50	6°51	86°9	131°91	-6.7	-12.3	-5.6		
		I	-0.39	-63.29	+2.82	1.71	101.4	147.03	-13.6	-13.7	-0.1		
		II	-3.26	-53.60	+4.08	11.38	85.0	123.64	-5.9	-11.3	-5.4		
		Pre-I	-0.04	-65.08	+2.80	0.38	197.2	145.35	-19.6	-14.5	+5.1		
		Pe	-0.26	-63.85	+2.83	1.16	106.5	151.04	-14.1	-13.8	+0.3		
		IIa	-4.64	-49.43	+4.20	15.54	85.7	116.89	-4.1	-11.2	-7.1		
		IIa*	-1.88	-57.44	+3.15	7.52	89.9	126.69	-7.1	-12.8	-5.7		
		III	-0.50	-62.24	+2.40	2.83	105.6	130.92	-10.6	-14.7	-4.1		
		IIIa	-0.79	-60.68	+2.33	4.36	100.8	122.04	-8.3	-15.0	-6.7		
		IV	-2.81	-53.34	+2.87	11.61	91.2	110.32	-3.6	-13.4	-9.8		
		Nov 13.500	12:00	Sun	0.00	+35.78
				Ia	-1.50	+4.51	+31.33	5.83	138.6	133.39	-7.1	-6.8	+0.3
				I	-0.19	+0.12	+34.93	0.86	173.6	152.81	-16.4	-10.0	+6.4
II	-3.06			+8.43	+27.75	10.76	136.0	124.65	-6.1	-6.0	+0.1		
Pre-I	+0.16			+1.83	+35.61	1.49	96.2	71.34	-13.2	-8.8	+4.4		
Pe	-0.06			-0.35	+35.49	0.41	224.1	152.55	-18.6	-11.5	+7.1		
IIa	-4.44			+11.25	+24.40	14.95	136.5	117.74	-4.3	-6.4	-2.1		
IIa*	-1.68			+4.93	+30.32	6.84	141.5	127.89	-7.5	-6.7	+0.8		
III	-0.30			+0.57	+33.92	1.92	165.8	132.66	-12.3	-8.4	+3.9		
IIIa	-0.59			+1.74	+32.58	3.51	155.4	122.97	-9.2	-7.4	+1.8		
IV	-2.61			+7.52	+26.87	10.98	142.2	111.01	-3.9	-6.4	-2.5		
Nov 13.650	15:36			Sun	+52.97	+15.54
				Ia	-1.35	+52.73	+10.24	5.31	182.6	134.59	-7.5	-8.5	-1.0
				I	-0.04	+52.56	+15.69	0.42	290.0	138.43	-19.7	-11.9	+7.8
		II	-2.91	+53.11	+5.26	10.29	179.3	125.43	-6.3	-10.5	-4.2		
		Pre-I	+0.31	+54.55	+13.47	2.58	143.5	81.56	-11.3	-8.7	+2.6		
		Pe	+0.09	+53.63	+15.00	0.84	130.5	59.24	-14.4	-10.5	+3.9		
		IIa	-4.29	+53.07	+1.03	14.51	179.6	118.38	-4.4	-21.8	-17.4		
		IIa*	-1.53	+52.37	+9.24	6.33	185.4	128.83	-7.8	-8.7	-0.9		
		III	-0.15	+52.11	+14.73	1.16	226.0	132.71	-14.4	-9.9	+4.5		
		IIIa	-0.44	+51.85	+12.93	2.83	202.8	123.54	-10.1	-8.6	+1.5		
		IV	-2.46	+51.96	+5.09	10.50	185.5	111.52	-4.0	-10.7	-6.7		
		Nov 14.300	7:12	Sun	-64.77	+2.99
				Ia	-0.70	-61.86	+2.49	2.95	99.8	141.19	-9.9	-14.4	-4.5
				I	+0.61	-61.39	+5.62	4.27	51.9	88.87	-10.5	-9.8	+0.7
II	-2.26			-56.52	+3.03	8.23	89.6	128.98	-7.2	-13.2	-6.0		
Pre-I	+0.96			-59.86	+6.28	5.89	56.0	91.38	-8.2	-9.3	-1.1		
Pe	+0.74			-60.77	+5.84	4.89	54.3	90.59	-7.8	-9.7	-1.9		
IIa	-3.64			-52.18	+3.16	12.57	88.9	121.22	-5.0	-12.8	-7.8		
IIa*	-0.88			-60.83	+2.25	4.00	100.6	133.57	-9.7	-15.2	-5.5		
III	+0.50			-62.46	+5.87	3.68	38.6	95.21	-10.3	-9.6	+0.7		
IIIa	+0.21			-64.04	+4.80	1.95	21.9	94.25	-11.4	-10.6	+0.8		
IV	-1.81			-56.46	+2.05	8.35	96.3	113.72	-5.0	-15.8	-10.8		
Nov 14.400	12:00			Sun	0.00	+35.52
				Ia	-0.50	+1.02	+33.52	2.17	157.0	144.06	-11.1	-8.2	+2.9
				I	+0.81	+6.14	+34.15	5.22	103.4	90.88	-9.8	-6.8	+3.0
		II	-2.06	+5.48	+29.50	7.58	141.0	130.16	-7.6	-6.6	+1.0		
		Pre-I	+1.16	+7.71	+33.32	6.73	106.9	92.28	-7.6	-6.5	+1.1		
		Pe	+0.94	+6.72	+33.78	5.80	105.5	92.00	-7.1	-6.7	+0.4		
		IIa	-3.44	+8.54	+26.06	11.96	139.9	122.11	-5.2	-6.4	-1.2		
		IIa*	-0.68	+1.60	+32.57	3.23	155.4	135.34	-10.6	-7.5	+3.1		
		III	+0.70	+5.71	+35.24	4.67	91.8	97.18	-9.4	-6.9	+2.5		
		IIIa	+0.41	+3.85	+35.94	3.16	81.3	99.72	-9.4	-7.4	+2.0		
		IV	-1.61	+4.64	+28.95	7.65	147.9	114.37	-5.4	-6.6	-1.2		
		Nov 14.650	15:36	Sun	+52.79	+15.35
				Ia	-0.35	+52.00	+13.97	1.58	209.0	146.63	-12.4	-9.4	+3.0
				I	+0.96	+56.05	+10.40	5.89	146.9	91.86	-9.4	-8.4	+1.0
II	-1.91			+52.21	+8.28	7.10	184.6	131.08	-7.8	-8.9	-1.1		
Pre-I	+1.31			+56.49	+8.99	7.32	150.0	92.76	-7.3	-8.7	-1.4		
Pe	+1.09			+56.17	+9.83	6.43	148.8	92.72	-6.7	-8.5	-1.8		
IIa	-3.29			+52.16	+3.86	11.51	183.1	122.80	-5.4	-12.0	-6.6		
IIa*	-0.53			+51.73	+12.92	2.64	202.9	136.80	-11.4	-8.7	+2.7		
III	+0.85			+56.57	+11.48	5.35	136.0	98.05	-8.9	-8.2	+0.7		
IIIa	+0.56			+55.99	+12.94	3.93	127.5	101.42	-8.5	-8.2	+0.3		
IV	-1.46			+51.33	+8.38	7.12	191.7	114.85	-5.7	-8.9	-3.2		

Table C-3

Swarm of Daylight Kreutz Sungrazers at First Perihelion in AD 363, Viewed from Latitude of Antioch: Appearance on November 16–17

Time of appearance		Sun or sun- grazer	Time from perihelion (days)	Azimuth \mathcal{A}	Elevation \mathcal{E}	Solar elonga- tion, ϵ	Zenithal position angle, P_Z	Phase angle, ψ	Apparent magnitude, H (mag)	Limiting magnitude, H_{lim} (mag)	Visibility index, \mathfrak{S} (mag)		
Date	LST hr:min												
Nov 16.300	7:12	Sun	-64°37	+2°67		
		Ia	+1.30	-58.59	+7.03	7°22	52°7	93°25	-5.1	-8.9	-3.8		
		I	+2.61	-54.21	+8.77	11.81	58.5	94.43	-6.8	-8.1	-1.3		
		II	-0.26	-63.50	+1.68	1.32	138.8	144.28	-14.8	-17.3	-2.5		
		Pre-I	+2.96	-53.05	+8.97	12.90	60.3	93.86	-5.1	-8.0	-2.9		
		Pe	+2.74	-53.72	+8.76	12.22	59.7	94.51	-4.0	-8.1	-4.1		
		IIa	-1.64	-58.15	+1.48	6.33	100.7	131.06	-7.8	-18.3	-10.5		
		IIa*	+1.12	-59.61	+7.07	6.47	46.9	95.73	-7.9	-8.8	-0.9		
		III	+2.50	-55.47	+9.75	11.33	50.9	99.54	-6.1	-7.8	-1.7		
		IIIa	+2.21	-56.77	+9.59	10.25	47.1	103.54	-4.5	-7.8	-3.3		
		IV	+0.19	-64.13	+4.35	1.70	8.3	97.21	-11.2	-11.1	+0.1		
		Nov 16.500	12:00	Sun	0.00	+35.01
				Ia	+1.50	+9.23	+32.78	7.98	103.6	93.79	-4.6	-6.4	-1.8
I	+2.81			+13.62	+30.20	12.43	109.0	94.40	-6.6	-6.2	+0.4		
II	-0.06			-0.74	+34.73	0.68	245.1	123.82	-17.8	-10.5	+7.3		
Pre-I	+3.16			+14.51	+29.35	13.50	110.7	93.77	-4.9	-6.2	-1.3		
Pe	+2.94			+13.90	+29.79	12.83	110.1	94.45	-3.8	-6.2	-2.4		
IIa	-1.44			+2.96	+29.92	5.67	153.1	132.21	-8.2	-6.9	+1.3		
IIa*	+1.32			+8.64	+33.66	7.26	98.3	96.35	-7.4	-6.4	+1.0		
III	+2.70			+13.81	+31.81	11.95	101.6	99.42	-5.9	-6.1	-0.2		
IIIa	+2.41			+12.86	+32.81	10.89	98.0	103.38	-4.2	-6.1	-1.9		
IV	+0.39			+3.39	+35.85	2.89	72.1	104.20	-8.9	-7.6	+1.3		
Nov 16.650	15:36			Sun	+52.43	+14.98
				Ia	+1.65	+57.15	+7.81	8.53	146.7	94.09	-4.4	-9.0	-4.6
		I	+2.96	+58.51	+3.56	12.89	151.7	94.36	-6.5	-12.5	-6.0		
		II	+0.09	+53.22	+14.75	0.80	106.9	54.03	-15.8	-10.6	+5.2		
		Pre-I	+3.31	+58.62	+2.44	13.95	153.4	93.70	-4.8	-14.9	-10.1		
		Pe	+3.09	+58.46	+3.10	13.28	152.9	94.38	-3.7	-13.3	-9.6		
		IIa	-1.29	+50.85	+10.04	5.17	197.6	133.10	-8.6	-8.6	0.0		
		IIa*	+1.47	+57.35	+8.81	7.82	141.5	96.68	-7.1	-8.7	-1.6		
		III	+2.85	+59.63	+4.78	12.41	144.5	99.32	-5.7	-10.9	-5.2		
		IIIa	+2.56	+59.59	+6.06	11.36	141.0	103.24	-4.1	-9.9	-5.8		
		IV	+0.54	+55.69	+13.15	3.65	119.6	106.13	-7.9	-8.1	-0.2		
		Nov 17.300	7:12	Sun	-64.18	+2.52
				Ia	+2.30	-55.21	+8.51	10.75	55.7	94.70	-3.3	-8.2	-4.9
I	+3.61			-51.20	+9.80	14.80	60.0	94.03	-5.9	-7.8	-1.9		
II	+0.74			-60.72	+5.84	4.79	46.0	89.96	-10.5	-9.6	+0.9		
Pre-I	+3.96			-50.10	+9.90	15.81	61.5	93.29	-4.3	-7.7	-3.4		
Pe	+3.74			-50.74	+9.73	15.18	61.0	94.00	-3.1	-7.8	-4.7		
IIa	-0.64			-61.65	+1.06	2.92	119.9	137.12	-11.0	-21.1	-10.1		
IIa*	+2.12			-56.22	+8.79	10.10	51.3	97.32	-6.1	-8.1	-2.0		
III	+3.50			-52.52	+11.00	14.35	53.2	98.77	-5.2	-7.4	-2.2		
IIIa	+3.21			-53.80	+10.98	13.33	50.1	102.57	-3.4	-7.4	-4.0		
IV	+1.19			-60.31	+7.61	6.39	36.9	108.42	-5.4	-8.6	-3.2		
Nov 17.500	12:00			Sun	0.00	+34.77
				Ia	+2.50	+12.77	+30.88	11.40	106.4	94.76	-3.1	-6.2	-3.1
		I	+3.81	+16.39	+28.28	15.38	110.4	93.90	-5.8	-6.1	-0.3		
		II	+0.94	+6.79	+33.79	5.69	98.0	91.73	-9.9	-6.7	+3.2		
		Pre-I	+4.16	+17.13	+27.42	16.37	112.0	93.13	-4.1	-6.1	-2.0		
		Pe	+3.94	+16.61	+27.86	15.75	111.5	93.85	-3.0	-6.1	-3.1		
		IIa	-0.44	0.00	+32.59	2.18	180.0	137.93	-12.2	-8.2	+4.0		
		IIa*	+2.32	+12.42	+31.88	10.76	102.1	97.36	-5.9	-6.2	-0.3		
		III	+3.70	+16.80	+30.05	14.92	103.8	98.58	-5.1	-6.1	-1.0		
		IIIa	+3.41	+16.03	+31.11	13.92	100.7	102.34	-3.2	-6.0	-2.8		
		IV	+1.39	+8.68	+34.61	7.13	88.8	108.52	-4.9	-6.4	-1.5		
		Nov 17.650	15:36	Sun	+52.26	+14.80
				Ia	+2.65	+58.34	+4.54	11.87	149.1	94.77	-2.9	-11.2	-8.3
I	+3.96			+59.35	+0.63	15.80	153.1	93.79	-5.7	-25.7	-20.0		
II	+1.09			+56.26	+9.82	6.32	141.5	92.65	-9.5	-8.5	+1.0		
Pre-I	+4.31			+59.38	-0.44	16.78	154.6	93.01	(-4.0)		
Pe	+4.09			+59.25	+0.18	16.17	154.1	93.74	-2.9	-32.0	-29.1		
IIa	-0.29			+50.88	+13.88	1.62	235.7	137.24	-13.5	-9.3	+4.2		
IIa*	+2.47			+58.72	+5.53	11.24	144.9	97.36	-5.7	-10.3	-4.6		
III	+3.85			+60.67	+1.88	15.35	146.5	98.43	-5.0	-16.7	-11.7		
IIIa	+3.56			+60.75	+3.13	14.35	143.5	102.16	-3.1	-13.3	-10.2		
IV	+1.54			+58.00	+9.57	7.67	132.4	108.52	-4.6	-8.4	-3.8		

Table C-4

Swarm of Daylight Kreutz Sungrazers at First Perihelion in AD 363, Viewed from Latitude of Antioch: Appearance on November 1 & 7

Time of appearance		Sun or sun- grazer	Time from perihelion (days)	Azimuth \mathcal{A}	Elevation \mathcal{E}	Solar elonga- tion, ϵ	Zenithal position angle, P_Z	Phase angle, ψ	Apparent magnitude, H (mag)	Limiting magnitude, H_{lim} (mag)	Visibility index, \mathfrak{S} (mag)		
Date	LST hr:min												
Nov 1.225	5:24	Sun	-83°37	-15°61		
		Ia	-13.77	-50.58	+5.40	38°67	59°6	82°63	+1.2	+0.6	-0.6		
		I	-12.46	-53.23	+4.58	36.03	58.3	85.33	-0.6	-0.2	+0.4		
		II	-15.33	-47.61	+6.33	41.66	60.9	79.54	+0.1	+1.3	+1.2		
		Pre-I	-12.12	-54.15	+4.63	35.31	57.3	86.11	-0.2	-0.3	-0.1		
		Pe	-12.34	-53.65	+4.74	35.78	57.7	85.39	+0.4	-0.1	-0.5		
		IIa	-16.71	-44.95	+6.64	44.08	62.5	76.61	+0.9	+1.5	+0.6		
		IIa*	-13.95	-49.70	+4.41	38.88	61.7	81.03	+0.3	-0.4	-0.7		
		III	-12.57	-51.90	+2.50	36.02	62.5	82.14	+0.6	-3.9	-4.5		
		IIIa	-12.86	-51.08	+1.78	36.35	64.3	79.73	+1.2	-6.3	-7.5		
		IV	-14.89	-47.59	+2.53	39.76	66.0	74.70	+2.3	-3.8	-6.1		
		Nov 1.250	6:00	Sun	-78.29	-8.45
				Ia	-13.75	-44.59	+10.72	38.63	60.8	82.70	+1.2	+0.6	-0.6
I	-12.44			-47.34	+10.13	35.98	59.5	85.40	-0.6	+0.4	+1.0		
II	-15.31			-41.50	+11.39	41.62	62.1	79.61	+0.1	+0.8	+0.7		
Pre-I	-12.09			-48.26	+10.25	35.26	58.5	86.18	-0.2	+0.5	+0.7		
Pe	-12.31			-47.75	+10.32	35.73	58.9	85.47	+0.4	+0.5	+0.1		
IIa	-16.69			-38.78	+11.45	44.04	63.7	76.68	+0.9	+0.9	0.0		
IIa*	-13.93			-43.79	+9.66	38.84	62.9	81.10	+0.3	+0.3	0.0		
III	-12.55			-46.17	+7.95	35.97	63.7	82.21	+0.5	-0.3	-0.8		
IIIa	-12.84			-45.40	+7.16	36.31	65.5	70.80	+1.2	-0.7	-1.9		
IV	-14.86			-41.84	+7.60	39.72	67.2	74.75	+2.3	-0.4	-2.7		
Nov 1.275	6:36			Sun	-73.11	-1.42
				Ia	-13.73	-38.03	+15.48	38.58	62.6	82.77	+1.2	-3.4	-4.6
		I	-12.41	-40.88	+15.15	35.93	61.3	85.48	-0.6	-3.5	-2.9		
		II	-15.28	-34.83	+15.84	41.57	63.9	79.68	+0.1	-3.3	-3.4		
		Pre-I	-12.07	-41.81	+15.35	35.20	60.4	86.26	-0.2	-3.5	-3.3		
		Pe	-12.29	-41.28	+15.37	35.67	60.7	85.54	+0.3	-3.5	-3.8		
		IIa	-16.66	-32.06	+15.63	44.00	65.6	76.74	+0.9	-3.2	-4.1		
		IIa*	-13.90	-37.32	+14.35	38.79	64.7	81.17	+0.3	-3.6	-3.9		
		III	-12.52	-39.90	+12.87	35.92	65.5	82.28	+0.5	-3.9	-4.4		
		IIIa	-12.81	-39.20	+12.02	36.26	67.3	79.86	+1.2	-4.1	-5.3		
		IV	-14.84	-35.56	+12.12	39.68	69.0	74.81	+2.3	-4.0	-6.3		
		Nov 7.275	6:36	Sun	-71.64	-2.54
				Ia	-7.73	-48.65	+6.32	24.60	68.8	103.03	-1.1	-5.6	-4.5
I	-6.41			-52.06	+5.63	21.19	67.3	106.97	-3.2	-6.2	-3.0		
II	-9.28			-44.75	+7.06	28.49	70.1	98.62	-2.0	-5.0	-3.0		
Pre-I	-6.07			-53.11	+5.66	20.24	66.1	108.22	-2.9	-6.3	-3.4		
Pe	-6.29			-52.45	+5.80	20.89	66.4	107.14	-2.3	-6.1	-3.8		
IIa	-10.66			-41.29	+7.24	31.82	71.9	94.32	-0.9	-4.8	-3.9		
IIa*	-7.90			-47.68	+5.55	25.26	71.3	100.43	-1.9	-6.1	-4.2		
III	-6.52			-50.68	+4.12	21.97	72.4	101.74	-1.9	-7.8	-5.9		
IIIa	-6.81			-49.58	+3.73	22.91	74.2	97.99	-1.2	-8.3	-7.1		
IV	-8.84			-44.67	+4.47	27.85	75.5	90.74	+0.3	-7.0	-7.3		
Nov 7.300	7:12			Sun	-66.27	+4.23
				Ia	-7.70	-42.59	+11.48	24.53	71.4	103.13	-1.1	-7.3	-6.2
		I	-6.39	-46.10	+11.08	21.11	69.9	107.07	-3.3	-7.4	-4.1		
		II	-9.26	-38.58	+11.85	28.43	72.8	98.71	-2.0	-7.2	-5.2		
		Pre-I	-6.04	-47.16	+11.19	20.16	68.7	108.33	-3.0	-7.4	-4.4		
		Pe	-6.26	-46.48	+11.28	20.82	69.1	107.24	-2.3	-7.3	-5.0		
		IIa	-10.64	-35.07	+11.69	31.76	74.5	94.40	-0.9	-7.3	-6.4		
		IIa*	-7.88	-41.68	+10.62	25.19	73.9	100.53	-1.9	-7.5	-5.6		
		III	-6.50	-44.84	+9.47	21.90	75.1	101.84	-2.0	-7.9	-5.9		
		IIIa	-6.79	-43.76	+8.98	22.85	76.9	98.07	-1.2	-8.0	-6.8		
		IV	-8.81	-38.74	+9.27	27.79	78.1	90.82	+0.3	-7.9	-8.2		
		Nov 7.450	10:48	Sun	-21.17	+34.79
				Ia	-7.55	+4.97	+25.97	24.13	104.3	103.71	-1.2	-6.0	-4.8
I	-6.24			+1.80	+28.01	20.69	102.8	107.70	-3.3	-6.0	-2.7		
II	-9.11			+8.43	+23.55	28.04	105.6	99.25	-2.0	-6.1	-4.1		
Pre-I	-5.89			+1.01	+28.79	19.73	101.5	108.97	-3.1	-5.9	-2.8		
Pe	-6.11			+1.64	+28.41	20.40	101.9	107.87	-2.4	-5.9	-3.5		
IIa	-10.49			+11.02	+21.05	31.39	107.4	94.90	-1.0	-6.2	-5.2		
IIa*	-7.73			+5.07	+24.74	24.80	106.8	101.08	-2.0	-6.1	-4.1		
III	-6.35			+1.65	+25.99	21.50	107.9	102.39	-2.0	-6.1	-4.1		
IIIa	-6.64			+2.19	+24.92	22.46	109.7	98.59	-1.3	-6.1	-4.8		
IV	-8.66			+6.44	+21.78	27.44	110.9	91.26	+0.2	-6.2	-6.4		

Table C-5

Swarm of Daylight Kreutz Sungrazers at First Perihelion in AD 363, Viewed from Latitude of Antioch: Appearance on November 11 & 19

Time of appearance		Sun or sun- grazer	Time from perihelion (days)	Azimuth \mathcal{A}	Elevation \mathcal{E}	Solar elonga- tion, ϵ	Zenithal position angle, P_Z	Phase angle, ψ	Apparent magnitude, H (mag)	Limiting magnitude, H_{lim} (mag)	Visibility index, \mathfrak{S} (mag)		
Date	LST hr:min												
Nov 11.300	7:12	Sun	-65°39	+3°51		
		Ia	-3.70	-52.63	+5.94	12°94	78°7	120°40	-3.9	-9.5	-5.6		
		I	-2.39	-56.59	+5.33	8.95	77.9	126.46	-6.9	-10.1	-3.2		
		II	-5.26	-48.18	+6.49	17.40	79.4	114.45	-4.1	-9.2	-5.1		
		Pre-I	-2.04	-57.77	+5.27	7.80	76.6	128.80	-6.9	-10.1	-3.2		
		Pe	-2.26	-56.99	+5.43	8.59	76.7	126.96	-6.0	-10.0	-4.0		
		IIa	-6.64	-44.23	+6.54	21.29	81.0	108.84	-2.8	-9.1	-6.3		
		IIa*	-3.88	-51.61	+5.41	13.86	81.6	116.63	-4.5	-10.0	-5.5		
		III	-2.50	-55.30	+4.41	10.10	84.6	118.46	-5.3	-11.0	-5.7		
		IIIa	-2.79	-53.99	+4.23	11.39	86.0	112.98	-4.2	-11.2	-7.0		
		IV	-4.81	-47.86	+4.81	17.52	85.1	103.51	-1.8	-10.5	-8.7		
		Nov 11.375	9:00	Sun	-46.49	+21.56
				Ia	-3.63	-32.89	+20.72	12.70	91.3	120.77	-3.9	-6.6	-2.7
I	-2.31			-37.15	+21.20	8.70	90.6	126.93	-7.0	-6.7	+0.3		
II	-5.18			-28.19	+19.96	17.18	92.0	114.77	-4.2	-6.5	-2.3		
Pre-I	-1.97			-38.39	+21.45	7.54	89.3	129.32	-7.1	-6.8	+0.3		
Pe	-2.19			-37.53	+21.40	8.34	89.4	127.44	-6.2	-6.7	-0.5		
IIa	-6.56			-24.21	+18.80	21.08	93.5	109.13	-2.8	-6.5	-3.7		
IIa*	-3.80			-32.01	+19.92	13.63	94.3	116.97	-4.6	-6.6	-2.0		
III	-2.42			-36.08	+19.98	9.85	97.3	118.83	-5.4	-6.8	-1.4		
IIIa	-2.71			-34.79	+19.47	11.16	98.7	113.29	-4.3	-6.7	-2.4		
IV	-4.74			-28.40	+18.27	17.31	97.7	103.76	-1.9	-6.6	-4.7		
Nov 11.500	12:00			Sun	0.00	+36.32
				Ia	-3.50	+10.75	+28.00	12.32	129.5	121.40	-4.1	-6.3	-2.2
		I	-2.19	+7.51	+30.87	8.29	128.9	127.72	-7.2	-6.5	+0.7		
		II	-5.06	+14.08	+24.63	16.81	130.1	115.31	-4.3	-6.3	-2.0		
		Pre-I	-1.84	+6.62	+31.79	7.11	127.7	130.22	-7.3	-6.5	+0.8		
		Pe	-2.06	+7.33	+31.25	7.92	127.7	128.27	-6.4	-6.5	-0.1		
		IIa	-6.44	+16.51	+21.38	20.73	131.6	109.61	-2.9	-6.4	-3.5		
		IIa*	-3.68	+10.93	+26.87	13.25	132.5	117.54	-4.7	-6.3	-1.6		
		III	-2.30	+7.56	+29.32	9.44	135.7	119.45	-5.6	-6.4	-0.8		
		IIIa	-2.59	+8.30	+28.16	10.75	137.0	113.82	-4.5	-6.4	-1.9		
		IV	-4.61	+12.79	+23.45	16.96	135.9	104.18	-2.0	-6.4	-4.4		
		Nov 11.625	15:00	Sun	+46.45	+21.50
				Ia	-3.38	+49.02	+9.83	11.93	167.7	122.03	-4.2	-8.3	-4.1
I	-2.06			+48.23	+13.81	7.87	167.3	128.54	-7.4	-7.7	-0.3		
II	-4.93			+49.77	+5.38	16.44	168.2	115.86	-4.4	-10.4	-6.0		
Pre-I	-1.72			+48.11	+15.00	6.68	166.0	131.16	-7.6	-7.6	0.0		
Pe	-1.94			+48.31	+14.22	7.49	166.0	129.12	-6.6	-7.7	-1.1		
IIa	-6.31			+50.02	+1.42	20.37	169.7	110.10	-3.0	-19.0	-16.0		
IIa*	-3.55			+48.55	+8.79	12.87	170.6	118.11	-4.9	-8.6	-3.7		
III	-2.17			+47.40	+12.51	9.03	174.1	120.08	-5.8	-7.8	-2.0		
IIIa	-2.46			+47.30	+11.18	10.35	175.3	114.34	-4.6	-8.0	-3.4		
IV	-4.49			+48.17	+4.98	16.60	174.0	104.60	-2.1	-10.8	-8.7		
Nov 19.375	9:00			Sun	-45.16	+19.94
				Ia	+4.37	-27.62	+24.22	16.88	72.1	93.97	-1.4	-6.1	-4.7
		I	+5.69	-23.55	+23.78	20.40	75.2	92.26	-4.8	-6.0	-1.2		
		II	+2.82	-32.67	+24.14	12.31	67.8	95.41	-7.2	-6.2	+1.0		
		Pre-I	+6.03	-22.51	+23.41	21.30	76.5	91.40	-3.1	-6.0	-2.9		
		Pe	+5.81	-23.14	+23.50	20.74	76.1	92.13	-1.9	-6.1	-4.2		
		IIa	+1.44	-37.99	+23.63	7.61	59.8	96.05	-6.6	-6.6	0.0		
		IIa*	+4.20	-28.38	+25.07	16.31	68.6	96.42	-6.1	-6.0	+0.1		
		III	+5.58	-24.35	+25.70	19.99	69.4	96.52	-4.2	-5.9	-1.7		
		IIIa	+5.29	-25.57	+26.28	19.07	66.9	99.99	-1.9	-5.9	-4.0		
		IV	+3.26	-32.53	+26.04	13.12	60.0	106.95	-2.3	-6.1	-3.8		
		Nov 19.500	12:00	Sun	0.00
				Ia	+4.50	+18.25	+27.12	17.22	109.7	93.88	-1.3	-6.1	-4.8
I	+5.81			+21.01	+24.46	20.71	112.7	92.14	-4.7	-6.2	-1.5		
II	+2.94			+14.17	+30.09	12.69	105.4	95.40	-7.1	-6.1	+1.0		
Pre-I	+6.16			+21.54	+23.57	21.62	114.0	91.27	-3.0	-6.2	-3.2		
Pe	+5.94			+21.12	+24.00	21.06	113.6	92.00	-1.8	-6.2	-4.4		
IIa	+1.56			+9.53	+32.83	8.07	97.8	96.38	-6.3	-6.3	0.0		
IIa*	+4.32			+18.22	+28.28	16.66	106.2	96.32	-6.0	-6.1	-0.1		
III	+5.70			+21.77	+26.41	20.32	106.9	96.37	-4.1	-6.0	-1.9		
IIIa	+5.41			+21.27	+27.56	19.40	104.5	99.82	-1.9	-6.0	-4.1		
IV	+3.39			+15.72	+31.47	13.48	97.7	106.79	-2.2	-6.0	-3.8		

Table C-6

Swarm of Daylight Kreutz Sungrazers at First Perihelion in AD 363, Viewed from Latitude of Antioch: Appearance on November 25

Time of appearance		Sun or sun-grazer	Time from perihelion (days)	Azimuth \mathcal{A}	Elevation \mathcal{E}	Solar elongation, ϵ	Zenithal position angle, P_Z	Phase angle, ψ	Apparent magnitude, H (mag)	Limiting magnitude, H_{lim} (mag)	Visibility index, \mathfrak{S} (mag)		
Date	LST hr:min												
Nov 25.250	6:00	Sun	-73°01	-12°06		
		Ia	+10.25	-45.11	+4.08	31°24	60°5	87°97	+1.2	-2.4	-3.6		
		I	+11.56	-42.90	+4.52	34.21	62.8	85.74	-2.9	-1.9	+1.0		
		II	+8.69	-49.86	+3.15	27.58	58.0	90.67	-4.5	-3.9	+0.6		
		Pre-I	+11.91	-41.96	+4.37	34.97	63.8	84.83	-1.2	-2.0	-0.8		
		Pe	+11.69	-42.44	+4.29	34.51	63.5	85.51	+0.2	-2.1	-2.3		
		IIa	+7.31	-53.50	+2.41	24.18	54.5	94.19	-1.9	-5.8	-3.9		
		IIa*	+10.07	-47.18	+5.01	30.84	57.9	90.08	-1.8	-1.4	+0.4		
		III	+11.45	-44.39	+6.66	34.06	58.1	89.27	-2.1	-0.2	+1.9		
		IIIa	+11.16	-45.49	+7.05	33.37	56.5	92.14	+0.3	+0.1	-0.2		
		IV	+9.14	-50.80	+5.59	28.27	52.6	98.84	+0.9	-0.9	-1.8		
		Nov 25.275	6:36	Sun	-68.05	-5.21
				Ia	+10.27	-40.11	+9.06	31.29	63.0	87.95	+1.2	-1.8	-3.0
I	+11.59			-36.85	+9.18	34.27	65.3	85.72	-2.9	-1.7	+1.2		
II	+8.72			-43.98	+8.48	27.63	60.4	90.65	-4.4	-2.1	+2.3		
Pre-I	+11.93			-35.92	+8.94	35.02	66.3	84.80	-1.2	-1.7	-0.5		
Pe	+11.71			-36.41	+8.91	34.56	66.0	85.48	+0.2	-1.8	-2.0		
IIa	+7.34			-47.70	+8.04	24.24	57.0	94.16	-1.9	-2.4	-0.5		
IIa*	+10.10			-41.10	+10.08	30.89	60.3	90.05	-1.8	-1.5	+0.3		
III	+11.48			-38.14	+11.47	34.12	60.6	89.23	-2.0	-1.0	+1.0		
IIIa	+11.19			-39.21	+11.96	33.42	58.9	92.11	+0.3	-0.9	-1.2		
IV	+9.16			-44.70	+10.98	28.33	55.1	98.81	+0.9	-1.3	-2.2		
Nov 25.300	7:12			Sun	-62.83	+1.39
				Ia	+10.30	-33.57	+13.42	31.35	66.0	87.92	+1.2	-6.7	-7.9
		I	+11.61	-30.27	+13.20	34.32	68.3	85.69	-2.9	-6.6	-3.7		
		II	+8.74	-37.54	+13.23	27.69	63.5	90.62	-4.4	-6.8	-2.4		
		Pre-I	+11.96	-29.35	+12.86	35.08	69.3	84.77	-1.2	-6.6	-5.4		
		Pe	+11.74	-29.85	+12.88	34.62	69.1	85.45	+0.2	-6.6	-6.8		
		IIa	+7.36	-41.34	+13.15	24.31	60.1	94.13	-1.8	-7.0	-5.2		
		IIa*	+10.12	-34.46	+14.54	30.95	63.4	90.02	-1.8	-6.5	-4.7		
		III	+11.50	-31.31	+15.61	34.17	63.7	89.20	-2.0	-6.2	-4.2		
		IIIa	+11.21	-32.34	+16.21	33.48	62.0	92.07	+0.3	-6.1	-6.4		
		IV	+9.19	-38.02	+15.80	28.39	58.1	98.77	+0.9	-6.4	-7.3		
		Nov 25.425	10:12	Sun	-28.61	+27.27
				Ia	+10.42	+5.89	+22.27	31.63	91.9	87.78	+1.3	-6.1	-7.4
I	+11.74			+8.50	+20.16	34.60	94.1	85.54	-2.8	-6.2	-3.4		
II	+8.87			+2.41	+24.42	27.99	89.4	90.48	-4.4	-6.0	-1.6		
Pre-I	+12.08			+9.03	+19.35	35.35	95.2	84.63	-1.1	-6.3	-5.2		
Pe	+11.86			+8.64	+19.65	34.89	94.9	85.30	+0.3	-6.2	-6.5		
IIa	+7.49			-0.94	+26.54	24.61	85.9	94.00	-1.8	-5.9	-4.1		
IIa*	+10.25			+5.88	+24.69	31.24	89.2	89.87	-1.8	-5.9	-4.1		
III	+11.63			+9.22	+22.69	34.46	89.5	89.04	-2.0	-6.0	-4.0		
IIIa	+11.34			+8.76	+23.77	33.77	87.9	91.91	+0.3	-5.9	-6.2		
IV	+9.31			+3.71	+26.76	28.69	84.0	98.59	+1.0	-5.8	-6.8		
Nov 25.500	12:00			Sun	0.00	+33.01
				Ia	+10.50	+29.34	+15.48	31.80	116.4	87.69	+1.3	-6.8	-8.1
		I	+11.81	+30.86	+12.62	34.77	118.6	85.45	-2.8	-7.2	-4.4		
		II	+8.94	+27.11	+18.69	28.16	113.8	90.40	-4.4	-6.5	-2.1		
		Pre-I	+12.16	+31.03	+11.69	35.51	119.6	84.54	-1.1	-7.4	-6.3		
		Pe	+11.94	+30.79	+12.11	35.06	119.4	84.22	+0.3	-7.3	-7.6		
		IIa	+7.56	+25.04	+21.83	24.79	110.5	93.93	-1.8	-6.2	-4.4		
		IIa*	+10.32	+29.89	+16.80	31.41	113.7	89.78	-3.5	-6.6	-3.1		
		III	+11.70	+32.46	+14.74	34.63	114.0	88.95	-2.1	-6.8	-4.7		
		IIIa	+11.41	+32.47	+15.89	33.95	112.4	91.80	+0.3	-6.7	-7.0		
		IV	+9.39	+29.23	+20.39	28.87	108.5	98.49	+1.0	-6.3	-7.3		

The conditions on November 19 are compared with those on November 11 employing the display data at 9:00 and 12:00. On the 19th one sungrazer, Fragment II, was visible at either time. However, while $\langle \epsilon \rangle = 16^\circ.8$ and $\langle \mathfrak{S} \rangle = -2.1$ mag at 9:00, the respective numbers were $17^\circ.1$ and -2.3 mag at 12:00, so that the conditions at noon were, surprisingly, slightly inferior to those three hours earlier.

Table C-6 presents the data for the final date, November 25. The visibility conditions appear to have been more favorable than expected that long after the peak display. They may in fact be compared with those on November 1 examined in Table C-4. The data are shown for the end of astronomical twilight at 6:00, early civil twilight at 6:36, just after sunrise at 7:12, mid-morning at 10:12, and noon. During this period of

time the visibility conditions are seen to have suddenly deteriorated at sunrise. Three comets were visible at the two twilight times, but none later on. As expected, the average solar elongation was very slowly increasing from $31^{\circ}.3$ at 6:00 to $31^{\circ}.9$ at 12:00, but the visibility index dropped abruptly at sunrise, its values equaling -0.9 and -0.5 mag at the two twilight times, but -5.4 , -4.9 , and -5.5 mag for the three daylight times. As noted in the text, the conditions could at these times be more favorable for any sungrazer, whose brightness was substantially enhanced by a contribution from the post-perihelion dust tail.

REFERENCES

- Bartlett, W. H. 1836, *Syria, the Holy Land, Asia Minor, etc. Illustrations*. London: Fisher, Son, & Co.
- Broughton, R. P. 1979, *J. Roy. Astron. Soc. Canada*, 73, 24
- Close, M. 1843, *Mon. Not. Roy. Astron. Soc.*, 5, 293
- Drijvers, J. W. 2011, *J. Late Antiqu.*, 4, 280
- Drijvers, J. W. 2022, *The Forgotten Reign of the Emperor Jovian (363–364): History and Fiction*. New York: Oxford University Press, 264 pp
- Eddie, L. A. 1883, *Mon. Not. Roy. Astron. Soc.*, 43, 289
- Elkin, W. L. 1882, *Mon. Not. Roy. Astron. Soc.*, 43, 22
- Encke, J. F. 1843, *Astron. Nachr.*, 20, 349
- Ernst, M. 1911, *Astron. Nachr.*, 187, 303
- Ferrin, I., & Gil, C. 1988, *A&A*, 194, 288
- Finlay, W. H. 1883, *Mon. Not. Roy. Astron. Soc.*, 43, 319
- Galle, J. G. 1894, *Verzeichniss der Elemente der bisher berechneten Cometenbahnen nebst Anmerkungen und Literatur-Nachweisen (neu bearbeitet, ergänzt und fortgesetzt bis zum Jahre 1894)*. Leipzig: W. Engelmann, 315pp
- Gill, D. 1882, *Mon. Not. Roy. Astron. Soc.*, 43, 19
- Gould, B. A. 1883a, *Astron. Nachr.*, 104, 129
- Gould, B. A. 1883b, *Astron. Nachr.*, 106, 273
- Green, D. W. E. 2012, *CBET* 2967
- Green, D. W. E., & Morris, C. S. 1987, *A&A*, 187, 560
- Hamid, S. E., & Whipple, F. L. 1953, *AJ*, 58, 100
- Hasegawa, I., & Nakano, S. 2001, *PASJ*, 53, 931
- Herrick, E. C. 1843a, *Amer. J. Sci. Arts*, 43, 412
- Herrick, E. C. 1843b, *Amer. J. Sci. Arts*, 45, 188
- Ho, P.-Y. 1962, *Vistas Astron.*, 5, 127
- Holetschek, J. 1896, *Denk. Akad. Wiss. Wien (Math.-Naturwiss. Kl.)*, 63, 317
- Kendall, E. O. 1843, *Astron. Nachr.*, 20, 387
- Kiang, T. 1972, *Mem. Roy. Astron. Soc.*, 76, 27
- Kreutz, H. 1888, *Publ. Sternw. Kiel*, 3
- Kreutz, H. 1891, *Publ. Sternw. Kiel*, 6
- Kreutz, H. 1901, *Astron. Abhandl.*, 1, 1
- Kronk, G. W. 1999, *Cometography: Volume 1 (Ancient–1799)*. Cambridge, UK: Cambridge University Press, 580 pp
- Kronk, G. W. 2004, *Cometography: Volume 2 (1800–1899)*. Cambridge, UK: Cambridge University Press, 852 pp
- Lynn, W. T. 1903, *Observatory*, 26, 326
- Maclear, T. 1851, *Mem. Roy. Astron. Soc.*, 20, 62
- Marcus, J. N. 2007, *Internat. Comet Quart.*, 29, 39
- Marsden, B. G. 1967, *AJ*, 72, 1170
- Marsden, B. G. 1989, *AJ*, 98, 2306
- Milon, D. 1966, *Stroll. Astron.*, 19, 206
- Milon, D., Solberg, G., & Minton, R. B. 1967, *Stroll. Astron.*, 20, 165
- Morris, C. S., & Green, D. W. E. 1982, *AJ*, 87, 918
- Öpik, E. 1966, *Ir. AJ*, 7, 141
- Orchiston, W., Drummond, J., & Kronk, G. 2020, *J. Astron. Hist. Herit.*, 23, 628
- Peirce, B. 1844, *American Almanac*. Boston: J. Munroe, 94
- Plummer, W. E. 1889, *Observatory*, 12, 140
- Roemer, E. 1966, *PASP*, 78, 83
- Rolfe, J. C. 1940, *The Roman History of Ammianus Marcellinus, Res Gestae*, Book 25, Section 10.2 (Online Translation from Latin), https://penelope.uchicago.edu/Thayer/E/Roman/Texts/Ammian/25*.html
- Ryan, F. R. 1969, *A History of the Expedition to Jerusalem, 1095–1127*; by Fulcher of Chartres (Translation from Latin), ed. H. S. Fink. Knoxville, TN: University of Tennessee Press, 348 pp.
- Schaefer, B. E. 1993, *Vistas Astron.*, 36, 311
- Schaefer, B. E. 1998, *Sky Tel.*, 95, 57; code version by L. Bogan at <https://www.bogan.ca/astro/optics/vislimit.html>
- Seargent, D. 2009, *The Greatest Comets in History: Broom Stars and Celestial Scimitars*. New York: Springer Science+Business Media, LLC, 260pp
- Sekanina, Z. 1982, in *Comets*, ed. L. L. Wilkening (Tucson, AZ: University of Arizona), 251
- Sekanina, Z. 2000, *ApJ*, 542, L147
- Sekanina, Z. 2002, *ApJ*, 566, 577
- Sekanina, Z. 2021, eprint arXiv:2109.01297
- Sekanina, Z., & Chodas, P. W. 2004, *ApJ*, 607, 620
- Sekanina, Z., & Kracht, R. 2015, *ApJ*, 801, 135
- Simms, W. 1845, *Mon. Not. Roy. Astron. Soc.*, 6, 22
- Stephenson, F. G., Yau, K. K., & Hunger, H. 1985, *Nature*, 314, 587
- Strom, R. 2002, *A&A*, 387, L17
- Tebbutt, J. 1882, *Observatory*, 5, 367
- Warner, B. 1980, *Mon. Not. Roy. Astron. Soc. South Africa*, 39, 69
- Weinberg, J. L., & Beeson, D. E. 1976, in *Study of Comets*, NASA SP-393, ed. B. Donn, M. Mumma, W. Jackson, M. A'Hearn, & R. Harrington. Washington, DC: U.S. GPO, 92
- Yau, K., Yeomans, D., & Weissman, P. 1994, *Mon. Not. Roy. Astron. Soc.*, 266, 305
- Ye, Q.-Z., Hui, M.-T., Kracht, R., & Wiegert, P. A. 2014, *ApJ*, 796, 83 (8 pp)
- Yeomans, D. K., & Kiang, T. 1981, *Mon. Not. Roy. Astron. Soc.*, 197, 633